PONTIFICIA UNIVERSIDAD CATOLICA DE CHILE

SCHOOL OF ENGINEERING

DEVELOPMENT OF ALTERNATIVES THAT AVOID CAKING OF MICROALGAE POWDER DURING SUPERCRITICAL CO_2 EXTRACTION

FABIÁN ALBERTO REYES MADRID

Thesis submitted to the Office of Graduate Studies in partial fulfillment of the requirements for the Degree of Doctor in Engineering Sciences.

Advisor:
JOSE MANUEL DEL VALLE

Santiago de Chile, November 2015

PONTIFICIA UNIVERSIDAD CATOLICA DE CHILE
SCHOOL OF ENGINEERING

DEVELOPMENT OF ALTERNATIVES THAT AVOID CAKING OF MICROALGAE POWDER DURING SUPERCRITICAL CO_2 EXTRACTION

FABIAN ALBERTO REYES MADRID

Members of the Committee:

JOSE MANUEL DEL VALLE

PEDRO BOUCHON

JUAN DE LA FUENTE

JULIO ROMERO FIGUEROA

ELENA IBAÑEZ

Thesis submitted to the Office of Research and Graduate Studies in partial fulfillment of the requirements for the Degree of Master of Science in Engineering (o Doctor in Engineering Sciences)

Santiago de Chile, November 2015

Dedicated to my parents, Luis and Andrea, and Caroline for all their love and support along all these years.

ACKNOWLEDGEMENTS

First I would like to thank my parents Luis, Andrea and my family for their constant support and encouragement throughout these years. I would especially thank Caroline for all her love, support, understanding, good times, and friendship during these years. You were a warm light that illuminated me every day.

I thank my advisor Dr. Jose Manuel del Valle for the experience and opportunity of doing research in the *Laboratorio de Extracción de Materiales Biológicos* (LEMaB). Your tutelage had great impact in my professional and personal life from which I am grateful. I would also like to thank Dr. Elena Ibañez (CIAL-CSIC) for the wonderful experience of working together during my doctoral internship in Spain. Your invaluable advices changed my way of approaching problems in research and in my personal life.

For all those great moments during my doctoral internship I want to thank my colleagues in the *Instituto de Investigación en Ciencias de la Alimentación* (CIAL): Lydia Montero, Andrea Sánchez, Mariagiovanna Sarò, Sabrina Sansanelli, Marta Arias Raquel Leonardo, Marcelo Fabiano, David Villanueva, Natalia Casado, Maria Rodríguez and especially José Mendiola for your help and dedication.

I am very grateful for having shared great experiences both in science and in our personal lives with my colleagues and friends from LEMaB: Gonzalo Nuñez, Freddy Urrego, Julia Arango, Soledad Murias, Eduardo Richter, Arturo Bejarano, Andrea Reveco, Sofia Andrighetti, Natalia Carathanassis and Victor Casado. Gonzalo and Freddy, without your support and discussion this thesis would not have been possible.

To my longtime friends that never cease in cheering me up and supporting my path: Nicolas Pizarro, Camila Berner, Valentina Silva, Ricardo Morales, Orlando Contreras, Rafael Contreras and Sebastian Gutierrez, Thank you all.

I thank the people that worked at the *Departamento de Ingeniería Química y Bioprocesos* that made this place a great place to be: Francisco Palma, Loreto Muñoz, Rosa Araya, Jakeline Salvatierra, Ricardo Cayupe, Ulises Lazo, and particularly María Inés Valdebenito. Last but not least I want to thank CONICYT and its scholarships that allowed me to study and work throughout these years.

GENERAL INDEX

Pág.

TABLE INDEX

Pág.

FIGURE INDEX

PONTIFICIA UNIVERSIDAD CATOLICA DE CHILE

ESCUELA DE INGENIERIA

DESARROLLO DE DOS ALTERNATIVAS TECNOLÓGICAS QUE EVITAN EL APELMAZAMIENTO DEL POLVO DE MICROALGAS DURANTE LA EXTRACCIÓN CON CO_2 SUPERCRÍTICO

Tesis enviada a la Dirección de Postgrado en cumplimiento parcial de los requisitos para el grado de Doctor en Ciencias de la Ingeniería

FABIÁN ALBERTO REYES MADRID

RESUMEN

Las microalgas representan una rama diversa de microorganismos capaces de producir una amplio rango de ingredientes funcionales (*i.e* carotenoides) que pueden ser ocupados en la industria de alimentos, cosméticos, farmacéuticos, y de energía. El CO_2 supercrítico (CO_2-SC) emerge como una alternativa a los solventes orgánicos tradicionales debido a su alta selectividad y cualidad de no dañar compuestos bioactivos. Bajo un punto de vista industrial, existe un riesgo importante de apelmazamiento del polvo de microalgas, como de *Haematococcus pluvialis* (polvo fino e higroscópico), durante la extracción con CO_2-SC. Esto provoca la canalización del CO_2 a través del lecho empacado, disminuyendo así el rendimiento de la extracción de carotenoides. Esta tesis propone dos alternativas que evitan el fenómeno de apelmazamiento de polvos finos de microalga destinados a la extracción comercial con CO_2-SC. Estas alternativas consisten en el uso de Compactación de Alta Presión (CAP) del polvo de microalgas como un tratamiento previo a la extracción con CO_2-SC, y la extracción directa del la pasta de microalga. Para entender el efecto del apelmazamiento en CAP, esta tesis desarrolló un método simple y rápido para caracterizar polvos higroscópicos que toma ventaja del comportamiento de escurrimiento inducido por

presión que se observa durante la compactación. Los resultados mostraron que este comportamiento está fuertemente relacionado con la temperatura de transición vítrea. Este estudio permitió el diseño de una metodología CAP basado en la compresión uniaxial del polvo, similar al proceso de tableteo. La investigación demostró que al ajustar cuidadosamente la presión de compresión y el tamaño del dado de compactación es posible fabricar comprimidos reproducibles que poseen una microestructura favorable para la extracción de carotenoides con CO_2-SC. Por otro lado, al evaluar el uso de la extracción directa de la pasta de microalga, esta tesis propone un sistema batch a escala pequeña en el cual la pasta de microalga es estáticamente colocada dentro del extractor mediante el uso de adsorbentes. El agua demostró ser una fuerte barrera para la extracción de carotenoides aun cuando se utilizó etanol como co-solvente. Con todo, ambas alternativas evitan el fenómeno del apelmazamiento, sin embargo solamente CAP es una mejora con respecto a la extracción de polvo seco. Esta tesis valida el uso de CAP con prometedoras aplicaciones industriales en la producción de carotenoides de *H. pluvialis*.

Miembros de la Comisión de Tesis Doctoral:

José Manuel del Valle

Pedro Bouchon

Juan de la Fuente

Julio Romero Figueroa

Elena Ibañez

Cristian Vial Edwards

Santiago, Noviembre 2015

PONTIFICIA UNIVERSIDAD CATOLICA DE CHILE

SCHOOL OF ENGINEERING

DEVELOPMENT OF TWO TECHNOLOGICAL ALTERNATIVES THAT AVOID CAKING OF MICROALGAE POWDER DURING SUPERCRITICAL CO_2 EXTRACTION

Thesis submitted to the Office of Research and Graduate Studies in partial fulfillment of the requirements for the Degree of Doctor in Engineering Sciences by

FABIÁN ALBERTO REYES MADRID

ABSTRACT

Microalgae represent diverse branch of microorganism that can produce a wide range of unique functional ingredients, such as carotenoids, that can be used in food, cosmetics, pharmaceuticals, and energy. Supercritical CO_2 ($scCO_2$) emerges as an alternative to organic solvents because of its high selectivity and bioactivity-preserving qualities. Under an industrial point of view, there is an important risk of caking of microalgae such as *Haematococcus pluvialis* (fine hygroscopic powder) during $scCO_2$ extraction. This results in CO_2 channeling through the packed bed, lowering carotenoid's yield. This thesis proposes two alternatives that avoid caking phenomenon of microalgae powders destined for a commercial $scCO_2$ extraction. These alternatives consist in the use High Pressure Compaction (HPC) of the microalgae powder as a pretreatment before $scCO_2$ extraction and direct-extraction of the microalgae paste. To understand the effect of caking in HPC, this thesis developed a simple and easy method to characterize hygroscopic powders by taking advantage of the pressure-induce squeeze flow behavior during compaction. Results showed that this phenomenon was strongly related to the glass transition temperature. This study led to the design of an HPC methodology based on uniaxial compaction of the

powder in a process similar to tableting. Findings showed that by carefully adjusting the compression pressure and size of the die it is possible fabricate reproducible compacts that have favorable microstructure for the $scCO_2$ extraction of carotenoids. When evaluating the use of direct-extraction of microalgae paste this thesis proposed a scale-down batch-wise extraction system were the microalgae paste is statically placed within the extractor by the use of adsorbents. Water proved to be a strong barrier to the extraction of carotenoids even when using ethanol as a co-solvent. This thesis showed that although both alternatives avoid caking phenomenon, only HPC is an improvement over the powder extraction with promising industrial applications for the production of carotenoids from *H. pluvialis*.

Members of the Doctoral Thesis Committee:

Jose Manuel del Valle

Pedro Bouchon

Juan de la Fuente

Julio Romero Figueroa

Elena Ibañez

Cristian Vial Edwards

Santiago, November 2015

LIST OF PAPERS

This thesis is based on the following scientific papers published in ISI journals and pending patent application process (PCT):

1. Reyes, F.A., Muñoz, L.A., Hansen, A., & del Valle, J.M. (2015). Water relationships in *Haematoccoccus pluvialis* and their effect in high-pressure agglomeration for supercritical CO_2 extraction. *Journal of Food Engineering*,*162*, 18-24

2. Reyes, F.A., Sielfeld, C.S., & del Valle, J. M. (2015). Effect of high-pressure compaction on supercritical CO_2 extraction of astaxanthin from *Haematococcus pluvialis*. Journal of Food Engineering (submitted).

3. Reyes, F.A., Mendiola, J.A., Ibanez, E., & del Valle, J. M. (2015). Adsorbent-assisted supercritical CO_2 extraction of carotenoids from aqueous suspension of *Neochloris oleoabundans*. The Journal of Supercritical Fluids (submitted)

4. Reyes, F.A., Núñez G.A., del Valle J.M., (2013). Métodos para la obtención de bioactivos a partir de derivados de organismos unicelulares. Chilean Patent Application 2013-03813.

1. INTRODUCTION

The energy crisis in the 1970s was responsible for sustained research aimed at alternatives to fossil fuels such as the Aquatic Species Program in the United States for the production of microalgae-derived energy (Dunahay et al, 1998). Microalgae are photosynthetic prokaryote or eukaryote microorganisms that can be found in both marine and fresh water environments. Although their photosynthetic mechanisms resemble those of terrestrial plants, microalgae convert solar energy into biomass more proficiently due to their simple cellular structure and efficient access to basic nutrients in aquatic environments (Carlsson & Bowles, 2007; Guedes et al, 2011). Several promising species have been isolated that can produce biofuels such as biodiesel, and there have been great advances in cultivation, harvesting, and downstream bioprocessing of microalgae, but microalgae-derived biofuels are still not competitive with fossil fuels (Brennan & Owende, 2010; H. Chen et al, 2015; Halim et al, 2012; Mercer & Armenta, 2011; Satyanarayana & Mariano, 2011).

Microalgae can also synthesize a wide range of unique, environment-dependent high-value substances that can be used in pharmaceuticals, cosmetics, and foods, among others. Research has recently shifted towards a more profitable and sustainable production of high-value bioactives as functional foods for humans and related applications (Chacón Lee & González Mariño, 2010; Harun et al, 2010). The health benefits associated to functional foods depend on low concentrations of added ingredients that are not usually present in conventional foods. These so-called functional ingredients are bioactive molecules that can act as antioxidant, antiviral, and antihypertensive agents, among others (Plaza et al, 2008). The ever-increasing demand of food, and healthcare cost, likewise the desire of elderly to improve their quality of life and its expectancy have supported the need to identify and purify functional ingredients from microalgae (Plaza et al, 2009).

Within the functional ingredients, carotenoids have traditionally been used for food coloring because of their natural color enhancement. However, they have attracted considerable interest in recent years because of their antioxidant properties and the reduction of the incidence of some chronic diseases where free radicals are involved

(cancer, cardiovascular diseases, osteoporosis and diabetes) (Christaki et al, 2012). Carotenoids are a family of yellow to orange-red terpenoids pigments synthesized by a wide range of photosynthetic organisms being microalgae one of its prominent sources (Barredo, 2012). Some of the most studied carotenoids synthesized by microalgae include β-carotene from *Dunaliela salina*, astaxanthin from *Haematococcus pluvialis* and canthaxanthin from *Coalestrella striolata*. Other less know yet effective is fucoxanthin from *Phaeodactylum tricornutum* and *Isochrysis galbana* (Raposo et al, 2015). Over more than 600 identified carotenoids are produced industrially with new sources been discover continuously such as *Neochloris oleoabundans* for the production of lutein, canthaxanthin and astaxanthin (Castro-Puyana et al., 2013).

1.1. Production of high-value compounds from microalgae

Although hundreds of microalgae have been identified and studied as potential source of biofuels or bioactives compounds, relatively few have progress towards mass cultivation and industrial applications (Richmond, 2008). The main reasons are the limited growth performance of microalgae in industrial photobioreactors (Spolaore et al, 2006a) and high-energy intensive processes (*i.e* harvesting or drying) that lead to high production costs (Lam & Lee, 2012). Successful mass cultivation of microalgae has only been done in open-air systems such as open-ponds. These relatively unsophisticated systems take advantage of natural sunlight, however they are expose to changing weather and contamination risks, restricting cultivation to a few resistant species (Borowitzka, 1999). Closed photobioreactors solve these issues by allowing fine control over the operation conditions, making reproducible and productive cultures (Fernández et al, 2013). While many types of closed photobioreactors (*i.e* tubular, flat-plate, vertical-column) have been design and proposed, with good results at laboratory scale, only few can be successfully scaled-up (Ugwu et al, 2008). High-cost is a mayor limitation for these types of photobioreactors, for instance, current application of artificial light increases the production costs by $ 25.3 dollars per kilogram of dry-weight biomass (Blanken et al, 2013). Blanken et al. (2013) concluded that artificial light may only be acceptable when producing high-value compounds, other applications should focus in using sunlight.

Once the cultivation phase is finished, the microalgae is harvested and concentrated to reduce the excess water and dissolved contaminants. This process is usually done by centrifugation followed by pressing or filtration. The result is a pasty fluid that has around 25% of dry biomass (Crampon et al, 2011). Since most of the products of interest are found intracellularly, a cell disruption step is generally recommended to increase the bioactive's availability after harvesting (Yen et al, 2015). Traditional methods involve milling and using high pressure homogenizers, but new developments based on enzymatic treatments, ultrasound or microwave-assisted processes have shown promise (Ibáñez & Cifuentes, 2013; Kadam et al, 2013). To stabilize the biomass and avoid water-induce degradation a drying step is followed producing a fine powder that can be commercialized of further purified by an extraction process.

Relevant technological innovations are needed in areas of culturing and downstream processing to drive production costs down and allow large-scale production of a wider range of microalgae species with potential high-value substances. Commercial production of bioactives compounds from microalgae has been proven for species such as *Chlorella sp.* (lutein), *Arthrospira* (*Spirulina*) *platensis* (phycobilins and polyunsaturated fatty acids), *Dunaliella sp*. (β-carotene), *Haematococcus pluvialis* (astaxanthin), *Porphyridium sp*. (polysacharides), and *Nostoc* (polysacharides) (Borowitzka, 1999; 2013; Richmond, 2008). Particularly, *H. Pluvialis* is of interest in this thesis because it is the main microalgae commercially produce in Chile, being cultivated by Atacama BioNatural Products and Pigmentos Naturales in the north of Chile. Their product is mainly marketed as a feed additive for farmed salmon and trout, however recent trends have encouraged the interest in producing premium products for human consumption.

H. pluvialis is known to accumulate large amounts of astaxanthin (Figure 1-1), a potent natural antioxidant (Lorenz & Cysewski, 2000). This carotenoid can be used as a food coloring agent in aquaculture (Dufossé et al, 2005) and as an antioxidant in human nutrition (Goswami et al, 2011). Astaxanthin has an antioxidant activity ten times higher than other carotenoids such as zeaxanthin, lutein, and β-carotene, and over 500 times greater than tocopherol (Higuera-Ciapara et al, 2006; Lorenz & Cysewski, 2000; Sarada et

al, 2006). There is growing evidence gathered by both *in vitro* and *in vivo* studies, that astaxanthin has the potential to be a health-promoting agent in the prevention and treatment of free-radical associated diseases such as oral, skin, liver, and gastrointestinal cancers; degenerative ailments such as Parkinson's and Alzheimer's diseases; chronic inflammatory diseases; metabolic disorders such as diabetes; and cardiovascular diseases (Christaki et al., 2012; Guerin et al, 2003; Han et al, 2013; Yuan et al., 2011).

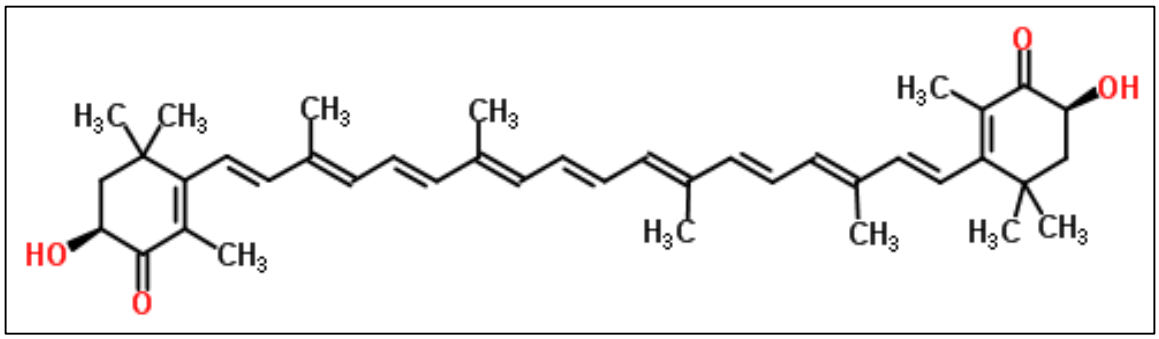

Figure 1-1: Molecular structure of astaxanthin

On one hand synthetic astaxanthin has typically occupied most of the global market, being predominantly used in the aquaculture sector. The demand for natural astaxanthin on the other hand, has increased significantly because of the rise in consumer awareness and health benefits (Industry-Experts, 2015). A growing trend for natural ingredients has raise concerns for consumer safety and regulatory issues over synthetic chemicals for human consumption. For this reason, natural astaxanthin derived from *H. pluvialis* has been preferred for human applications.

1.2. Supercritical CO_2 extraction of natural compounds

Traditionally high-value compounds have been extracted by conventional organic solvents (*i.e* hexane, acetone), which are usually toxic to humans. The increasing legislative restrictions on the presence of organic solvents in food products (Mendes et al, 2003) coupled with their negative effects on the nutritional and functional properties of compounds such as carotenoids (Crampon et al., 2011; Jaren-Galan et al, 1999) have driven the search of "greener" alternatives. High-pressure extractions using supercritical

and pressurized fluids have emerged as an alternative to normal pressure extractions using conventional organic solvents. These high-pressure processes can reduce the demand of food grade solvents, increase the selectively towards valuable bioactive compounds, and preserve their bioactivity (Herrero et al, 2013). An important advantage of supercritical fluids over conventional liquid solvents is that its density varies considerably with the operation conditions, particularly near the critical point the fluid is markedly compressible, thus granting it variable solvent power (Aguilera, 1999). In addition, supercritical fluids exhibit intermediate properties between a liquid and a gas; at high pressures the density is like-liquid increasing its solvent power, at lower pressures mass transfer properties are like-gas (low viscosity and high diffusivity) facilitating overall mass transfer and reducing process time (la Fuente & Cardarelli, 2005). This allows the development and design of simple separation processes in which the solute is dissolved at high pressures and subsequently precipitated when lowering the pressure. It does not resort to phase changes that usually are energy intensive when using liquid solvents (Aguilera, 1999).

The most interesting region from the perspective of a supercritical separation process is a temperature slightly above the critical temperature (T_c) and pressures between one to ten times de critical pressure (P_c) of the fluid. In this sense fluids with T_c's close to normal ambient temperatures and low P_c's values of, such as the case of carbon dioxide (T_c = 31.0ºC, P_c = 7.39 MPa or 73.9 bar), are particularly interesting because they can reduce the risk of thermal degradation of bioactives. Moreover, carbon dioxide (CO_2) is relatively cheap, inert, non-toxic and non-flammable. It doesn't damage the bioactives and can be very selective depending on the operation conditions. The shaded area of Figure 1-2 indicates the operation conditions that are generally used for the extraction of bioactives with supercritical (sc) CO_2. Using scCO_2 for extraction has some disadvantages, for instance, scCO_2 has a poor solvent power thus requiring equipment able to operate at high-pressures (30-100 MPa).

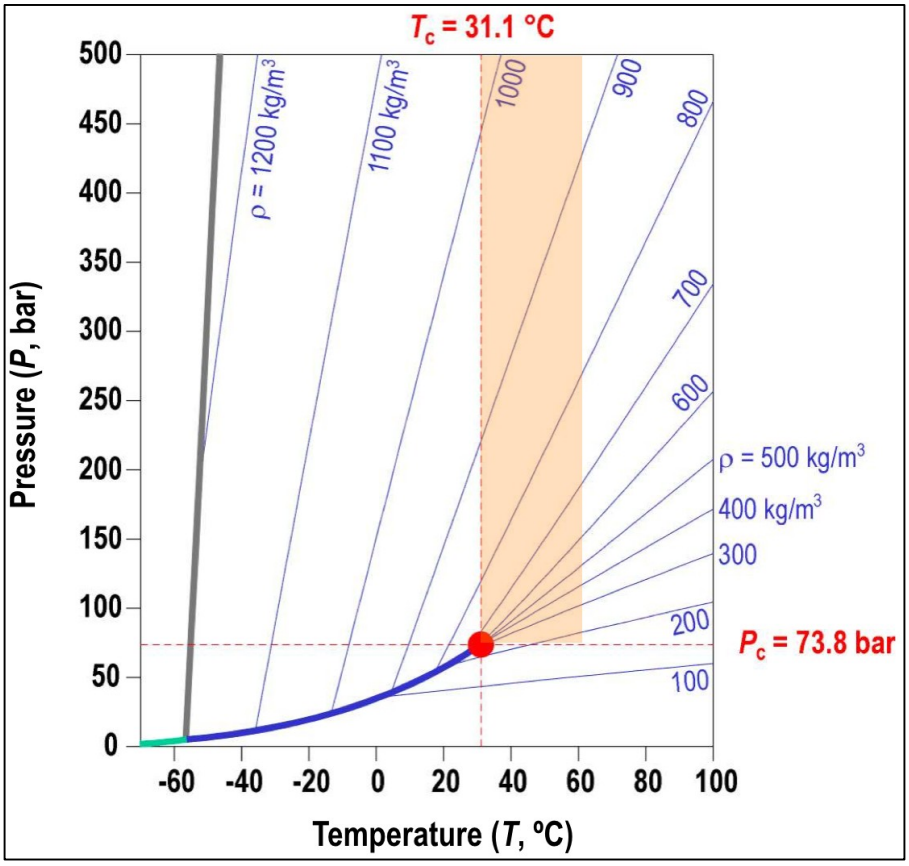

Figure 1-2: Pressure-temperature diagram for CO_2. Shaded area indicate the operation condition region which is normally used for bioactive separation.

High-pressure batch-wise extraction systems are difficult to load and unload, and the CO_2 solvent cycle in some cases are energy intensive. Also, high-pressure associated hazards have hindered a wider adoption urging the need of important safety measures, specially during scale-up (Díaz-Reinoso et al, 2006). Nevertheless, extensive R&D has been systematically tackling these disadvantages increasing both the number and capacity of industrial plants. Today over 200 industrial plants operate all over the world (Perrut, 2000; Sovová & Stateva, 2011).

1.2.1. Supercritical CO_2 extraction of astaxanthin from *Haematococcus pluvialis*

Previous studies of $scCO_2$ extraction of astaxanthin from *H. pluvialis* are summarize in Table 1. *H. pluvialis* cells synthetizes most of the astaxanthin when forming a cyst, which has a tough cell wall, under growth-limiting conditions (Mendes-Pinto et al, 2001). Nowadays there is a general agreement that to increase astaxanthin availability during the extraction a cell disruption step is essential, thus most of the studies in Table 1 experiment with disrupted cysts (Nobre et al., 2006; Valderrama & Perrut, 2003). Typically, extraction of astaxanthin has been investigated as a function of extraction pressure, temperature, and/or time but few authors (Thana et al., 2008; Wang et al, 2012a) studied the effect of these variables on the antioxidant activity of the $scCO_2$ extracts, which is in fact one of its main attributes. Astaxanthin recovery generally improved as pressure and extraction time increased. Temperature generally enhances astaxanthin recovery at high pressures, but this not always resulted in an increase in antioxidant activity (Thana et al, 2008). A closer look, it appeared that above 50 ºC there is a reduction in the net gain of the antioxidant recovery (Krichnavaruk et al, 2008; Pan et al, 2012) this could be explained by thermal degradation of astaxanthin, which could imply a reduction in the antioxidant activity.

The supercritical extraction of *H. pluvialis* is limited because of the low solubility of astaxanthin (a heavy and polar solute) in $scCO_2$ (Dandge et al, 1985). This has led to recommend increasing extraction pressures (above 50 MPa) to improve extraction rate and/or yield with a foreseeable increase in processing costs. This drawback can be overcome by increasing astaxanthin solubility by using a polar co-solvent such as ethanol (Machmudah et al, 2006; Nobre et al., 2006; Pan et al., 2012; Valderrama & Perrut, 2003; Wang et al., 2012a). Ethanol has also been used in pressurized liquid extractions (PLEs) leading to extracts with a high yield of astaxanthin and antioxidant activity (Jaime et al., 2010; Santoyo et al., 2009).

Table 1-1: Summary of studies on H. pluvialis using scCO2 for the extraction of astaxanthin (Reyes et al, 2014).

Research Groups	Co-solvents	Pressure (MPa)	Temperature (ºC)	Extraction time (min)	Astaxanthin Recovery (%)
Valderrama *et al.* {Valderrama:2003is}	0, 9.4% (w/w) Ethanol	30	60	*n.d**	97
Nobre *et al.* {Nobre:2006em}	0, 10% (v/v) Ethanol	20-30	40-60	*n.d**	90
Machmudah *et al.* {Machmudah:2006de}	1.67-7.5% (v/v) Ethanol	20-55	40-80	240	80
Thana, *et al.* {Thana:2008cz}	-	30-50	40-80	60-240	84
Krichnavaruk, *et al.* {Krichnavaruk:2008fu}	0-12% (v/v) Vegetable oils	30-50	50-80	300	51
Wang *et al.* {Wang:2012gc}	1.25-8.75% (v/v) Ethanol	30-50	35-75	210	87
Pan *et al.* {Pan:2012el}	0.154-1% (v/v) Ethanol	7-34	30-80	0-100	74

1.3. Importance of caking of fine powders during supercritical CO_2 extraction

Studies involving $scCO_2$ extraction of *H. pluvialis* (Table 1), as with other species of microalgae such as *Chlorella sp.* (Kitada et al, 2009; Mendes et al., 1995; Ruen ngam et al, 2012), *Spirulina sp.* (Mendes et al, 2006; Mendiola et al, 2007; Sajilata et al, 2008) and *D. salina* (Macías-Sánchez et al., 2008; 2009), are mostly done at laboratory scale. Because dry microalgae is a fine hygroscopic powder, loading the extractor usually involves adding extracting aids such as silica particles or glass beads to avoid caking of the powder during the extraction. This is impractical at an industrial scale, these aids reduce the extractor's load lowering the volumetric productivity (extraction yield per time and volume) of the industrial plant. This phenomenon has been observed in our laboratory when extracting garlic powder with $scCO_2$ (Glatzel & Martínez, 2012a). Caking was also confirmed with *H. pluvialis* powder in preliminary extraction experiments with $scCO_2$ (Figure 1-3).

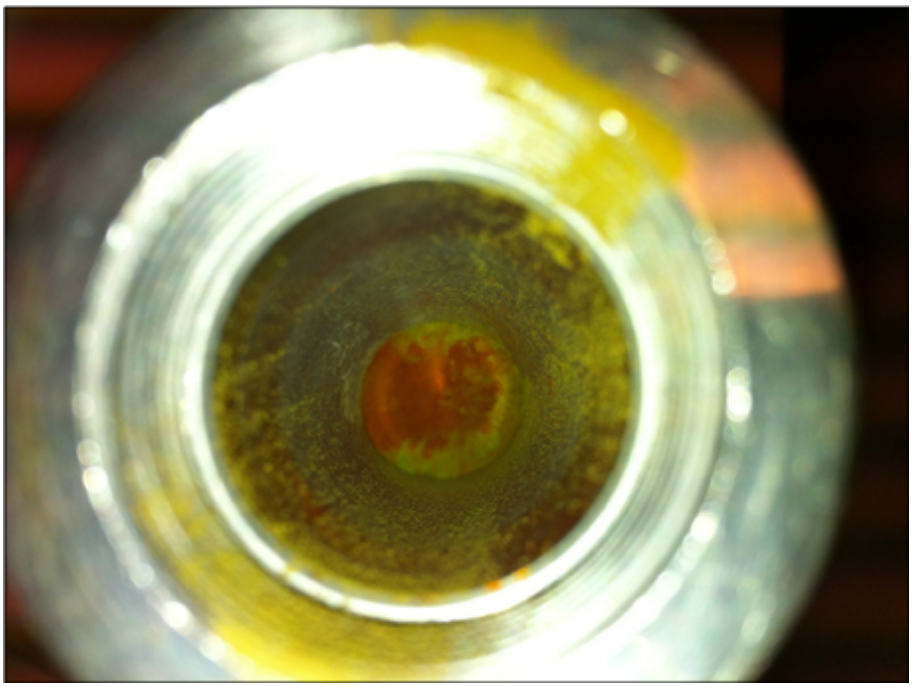

Figure 1-3: Evidence of caking of *H. pluvialis* powder after $scCO_2$ extraction. Green color areas of the powder indicate the preferential pathways of CO_2.

When caking occurs particles get consolidated within the packed bed extractor opposing the passage of fluids and resulting in CO_2 channeling through preferential pathways (green zones in Figure 1-3). Dead zones, characterize by very slow extraction, are formed where CO_2 does not pass, and are the main reason for low extraction yields (red zones in Figure 1-3). Caking of fine powders is a continuous and complex, time-dependent phenomenon in food and related biomaterials (Aguilera et al, 1995). Its been recognized that undesirable caking or stickiness can have a negative impact on product's handling, transportation, storage, and quality (Aguilera et al., 1995; X. D. Chen & Özkan, 2007; Wahl et al., 2008). This phenomenon is strongly influenced by moisture, substrate particle size, temperature and extraction time. Smaller particles, which have a large specific surface, favor caking by exposing more contact areas to the sticky surfaces of neighboring particles (Glatzel & Martínez, 2012a; Peleg, 1993). For this reason, pretreatment of microalgae substrate becomes necessary, particularly at large scale extractions, to avoid caking without the use of extracting aids.

This thesis proposes two alternatives to avoid caking of *H. pluvialis* powder during the $scCO_2$ extraction of astaxanthin. These alternatives are the use of high-pressure compaction (HPC) as a pretreatment of the microalgae powder before $scCO_2$ extraction and the direct extraction of the microalgae paste before the production of the fine powder. Both of these alternatives, which are going to be introduced separately, avoid the use of the fine powder by pretreating it (HPC) or by extracting its precursor which is the wet biomass (microalgae paste).

Since caking phenomenon is related with glass-rubber transitions of the material, particularly with the glass transition temperature, *Paper 1* focused in understanding the relationship of water and glass rubber transitions in *H. pluvialis*. The study also evaluates the effect of water content in the production of compacts using HPC and gives practical recommendations for the $scCO_2$ extraction of the *H. pluvialis* powder.

1.3.1. High-pressure compaction as a pretreatment for supercritical CO_2 extraction of fine powders

A mayor risk of caking comes from having a large specific surface because of small particle size. This risk is significantly reduced when increasing the particle size of the substrate, however this new particle must have certain conditions to facilitate $scCO_2$ extraction. First, a matrix of interconnected pores where the solute is accessible, second, that these pores are open to the exterior of the particle to allow $scCO_2$ penetration and extraction, and third, that the whole particle structure does not collapse by the high pressures of a supercritical extraction process. This thesis proposes the use of HPC, such as pelletization or tableting, to produce uniform and stable compacts that do not cake during $scCO_2$ extraction. Although increasing the particle size hinders mass transfer of the solute to the solvent (because of the increase dependencies on the internal diffusion) it also allows an increase bulk density of the extractor. By carefully studying these phenomena it is possible to balance the negative effect of lower mass transfer by maximizing the volumetric productivity of a supercritical extraction process. Previous work in “Extraction Laboratory of Biological Material” (LEMaB acronym from the Spanish name) have corroborated this hypothesis by extracting prepress or pelletized Jalapeño (del Valle et al,

2003a; del Valle et al, 2003b; Uquiche et al., 2006) or red pepper (Uquiche & Ortiz, 2004). Moreover, they are patents that proposes the pelletization of hops (Hallberg et al, 1989) and prepress oil seeds (Chordia & Martínez, 2006) before a $scCO_2$ extraction, nevertheless there is no evidence of any type of compaction study that analyses the challenges of using fine powders, such as microalgae powder, for a subsequent $scCO_2$ extraction process. There has been increase evidence that one side effect of using HPC is the subsequent collapse and rupture of cellular microstructure produced by the high shearing forces (Uquiche et al., 2006; Uquiche & Ortiz, 2004). Since many microalgae (such as *H. pluvialis*) need a cell disruption step, advancement in HPC could lead to design efficient downstream processing in which the cell disruption step is done during the controlled compaction of the substrate. Challenges remained on how the HPC must be done, what are the conditions that the substrate must have for successful production of compacts, and how can we control the HPC step to produced compacts that have reproducible physical parameters (porosity, specific surface, size, weight) that favor $scCO_2$ extraction of bioactives. These question are answered in *Paper 2* for the extraction of astaxanthin from *H. pluvialis*. One important aspect of the study was to analyzed how the HPC influenced the microstructure of the compact and consequently its extraction. We estimated the microstructural factor, which quantifies the effect of the microstructure on the diffusion of a solute within a solid matrix, by Sovová's broken-and-intact cell model (Sovová & Stateva, 2011). Sovová's cell model has become a standard in the supercritical fluid extraction community. Although the versatility of the model is an advantage because it can be applied to various types of extractions, it includes several additional parameters. However, these parameters have physical meaning and most of them, can be independently calculated, as exemplified in our work.

1.3.2. Direct-extraction of microalgae paste

Current extraction processes from microalgae are carried out by drying the paste to increase overall efficiency of oil extraction. However, this process is energy intensive and in in areas, such as biodiesel production, drying can be responsible for up to 59% of the total energy consumption (Im et al, 2014; Yanfen et al, 2012). Furthermore, drying can

also have a negative impact in some themolabile bioactives. Therefore, the direct-extraction of the microalgae paste is a promising alternative that can reduce the cost of downstream processing and caking related problems during the extraction process. The advantages of using a fluid mixture (microalgae paste and $scCO_2$) is that the process can be adapted to be continuous avoiding issues related to depressurizing, loading and cleaning typically associated with batch-wise systems. Multiple equilibrium stages can be achieved by selecting a countercurrent configuration, allowing the separation of solutes that have small separation factors. Thus, $scCO_2$ extraction of liquids can sometime be the only alternative to obtain high purity products when extracting under poor selective conditions.

Table 1-2: Comparison between a supercritical CO_2 extraction of solids and liquids.

Criteria	$scCO_2$ extraction solids	$scCO_2$ extraction Liquids
Solvent consumption	High	Low
Equilibrium stages	Few, depends on the number of separators	Many, depends on the height of the column
Fouling	Not relevant	Critical
Required separation factor	High	Low
Type of process	Batch	Continuous

One mayor problem, assuming pumping of the paste is resolved, is fouling of the pipelines. Roney et al. (2008) patent describes a process of transforming carrot feedstock into pumpable carrot paste, but did not give details on how to avoid potential fouling of the column packing. A summary of the comparison between liquid and solid $scCO_2$ extraction are described in table 1-2.

The first step towards the development of this technology is to understand the effect that water has over the extraction of bioactives (*i.e* carotenoids) during $scCO_2$ extraction. To facilitate experimentation one can adapt existing solid extraction equipment to test the extraction of the paste while $scCO_2$ flows through the extractor. Aravena (2011) investigated this configuration in LEMaB by extracting astaxanthin from a *H. pluvialis* paste. Results showed that water was an important impediment for the extraction reducing

significantly the astaxanthin yield. The author also noticed that water was co-extracted during the extraction, which eventually dried the paste, becoming a solid type extraction. This undesirable water co-extraction was address in this thesis, because to simulate the continuous extraction of microalgae paste it is necessary to keep the water within the extractor. To achieve this, the thesis proposes the use of adsorbents that can bind water and positively influence the extraction of bioactives. This work analyzed 6 different low cost and easily available adsorbent: sea sand, active carbon, two types of silica gel and two types of chitosan derivatives, and evaluate its effect when extracting carotenoids from *N. oleoabundans*. This adsorbent-assisted extraction opens a new branch of sustainable low cost extraction methods of liquid substrate using supercritical fluids.

1.4. Hypothesis

In comparison with powder extraction of *H. pluvialis*, adsorbent-assisted $scCO_2$ extraction of microalgae paste (fluid mixture) or compacts from *H. pluvialis* (densified material with greater particle size) avoid caking of the material and improve the extraction of carotenoids from microalgae such as *H. pluvialis*.

1.5. Objectives

The main objective of this thesis is to validate the use of compacts produced by HPC from *H. pluvialis* and the direct-extraction of microalgae paste assisted by adsorbents as alternatives that avoid caking of *H. pluvialis* powder during the $scCO_2$ recovery of carotenoids, such as astaxanthin. This thesis describes the relationships between the pretreated material and the extraction yield and purity.

The specific objectives of this thesis are:

1. Understand the caking phenomenon in *H. pluvialis* and evaluate the effect of water content in high pressure compaction (***Paper 1***).
2. Study the effect of high pressure compaction on $scCO_2$ extraction of carotenoids, such as astaxanthin, from *H. pluvialis* (***Paper 2***).

3. Study the $scCO_2$ extraction of microalgae paste and evaluate the the use of adsorbents to reduce the negative effect of water content on the carotenoid extraction yield and purity from *N. oleoabundans* (***Paper 3***).

2. WATER RELATIONSHIPS IN *HAEMATOCCOCCUS PLUVIALIS* AND THEIR EFFECT IN HIGH-PRESSURE COMPACTION FOR SUPERCRITICAL CO_2 EXTRACTION

Abstract

Stickiness and caking of fine powders such as in dry disrupted microalgae should be avoided in supercritical (sc) CO_2 extraction, because they negatively impact extraction rate and yield. To establish limits in water content of *H. pluvialis* cysts and extraction temperature, this work studied water-state diagrams of the powder. The powder's squeeze flow behavior as a function of water content was useful to characterize the transition between glassy and rubbery states as water content increased. Water sorption (W *versus* a_w) at 20 ºC was represented using the Guggenheim-Anderson-de Boer equation, with a monolayer water content of 3.67 % (d.b.). The glass transition diagram (T_g *versus* W_w) was represented using the Gordon-Taylor equation, with T_{gs} = 88.3 ºC (glass transition temperature of the anhydrous solids) and k = 3.49. The compression pressure necessary for squeeze flow behavior decreased 2.5 to 3 times at ambient temperature (*ca.* 23 ºC) as a result of an increase in water content from 3.8% (d.b.) to 10-15% (d.b.) at which level glass-rubber transitions manifested, and then kept relatively constant when the water content increased even further. Alternatives to prevent caking of *H. pluvialis* during scCO_2 extract include reducing the initial water content of the powder, increasing particle size by high-pressure agglomeration, and/or reducing the extraction temperature so as to prevent the glass-rubber transition that is responsible for sample stickiness. Taking into account that the scCO_2 extractions are carried out above ambient temperature ($40 \leq T \leq 60$ ºC), we recommend reducing the water content of *H. pluvialis* powder to $W \leq 5\%$ (d.b.).

2.1. Introduction

Microalgae comprises an extremely diverse group of organisms capable of synthesizing a broad range of biomolecules ranging from biofuels to pharmaceuticals (Chacón Lee & González Mariño, 2010; Harun et al., 2010; Spolaore et al, 2006b). Among them, astaxanthin (3,3'-dihydroxy-β-carotene-4,4'-dione) is a high-value carotenoid that is achieving commercial success (Lorenz & Cysewski, 2000). Although astaxanthin is widely distributed in nature, the microalgae *Haematococcus pluvialis* has been identified as the richest natural source of astaxanthin. This red ketocarotenoid is a more potent antioxidant than β-carotene, zeaxanthin, canthaxanthin, vitamin C, and vitamin E, and has many potential applications related mainly to human health and nutrition (Goswami et al., 2010; Guerin et al., 2003; Lorenz & Cysewski, 2000; Yuan et al., 2011). Human supplementation of bioactive compounds faces strong demands for quality (high purity and antioxidant activity) and absence of traces of organic solvents (Mendes et al., 2003; C. G. Pereira & Meireles, 2009). These concerns have prompted the use of supercritical (sc) carbon dioxide (CO_2) as an alternative to organic solvents because of its nontoxic and bioactivity-preserving qualities (Valderrama & Perrut, 2003).

Dry *H. pluvialis*, as with other types of microalgae, is a fine hygroscopic powder that may cake inside an extraction vessel, thus causing CO_2 channeling within the packed bed extractor and a decreasing extraction yield (Glatzel & Martínez, 2012b; C. G. Pereira & Meireles, 2009; Reverchon & De Marco, 2006). Small amorphous particles favor caking because of their stickiness and large specific surface, which allows exposing a large contact area to the neighboring particles (Glatzel & Martínez, 2012b; Peleg, 1993). Caking has been extensively studied in the food and pharmaceutical industry because of its negative impact on product handling, transportation, and (Boonyai et al, 2004; Hartmann & Palzer, 2011; Palzer, 2011). Furthermore, caking results in loss of functionality and decreases quality of food products (Aguilera et al., 1995).

Caking is a moisture-dependent physical process that may result from glass-rubber transitions when process temperature increases above the so-called glass transition temperature (T_g) of the material (Aguilera et al, 1993; Glatzel & Martínez, 2012b; Peleg,

1993). The glass-rubber transition temperature is an important physicochemical property of amorphous solids that governs functional characteristics and plasticization of organic as well as inorganic glasses (Roos, 2010). As long as the temperature is below T_g, the glassy material behaves like a solid, whereas above T_g, the material becomes rubbery and its viscosity decreases markedly with increasing temperature leading to particle bridging and a decrease in powder flowability (Descamps et al, 2013). The water plasticizing effect on foods is usually described by the dependence of T_g on the weight fraction of water.

To avoid caking phenomena during $scCO_2$ extraction of a powdery material, the Extraction Laboratory of Biological Materials (LEMaB acronym from the Spanish name) proposes increasing the particle size by compacting the powder using high-pressure compaction (e.g., tableting or pelletization). Pelletization of capsicums produced new microstructures due to the fracture, rearrangement, and/or plastic deformation of constituent tissue particles which progressively occupied void spaces (Uquiche & Ortiz, 2004). Additionally, high shearing forces destroyed cell walls and other barriers to mass transfer within the substrate (Uquiche et al., 2006). Although mass transfer rates may decrease as a result of high-pressure agglomeration, this reduction would be partially overcome by the excellent transport properties of $scCO_2$, thus increasing the "volumetric" yield of the extraction process (del Valle et al, 2003a).

Compacts production depends strongly on the material composition, its conditioning (e.g., water content), manufacturing parameters (e.g., compression pressure), and compact shape (Nagy & Simándi, 2008; Rhén et al, 2005). In particular, water acts as a binder during compaction (Palzer, 2005); as the water content increases an initially brittle powdery material becomes softer and more susceptible to undergo plastic deformation under stress. Plastic deformation during high-pressure compaction (HPC) generates areas of intimate and permanent contact between particles giving cohesiveness to the pellets. However, as water content increases, T_g decreases and the powder may become sticky, thus hindering its loading into the die and the overall compaction process (Descamps et al., 2013).

The aim of this work was to study water relationships in *H. pluvialis* powder and its

effect on compaction by HPC. These water relationships include the effect of ambient relative humidity on equilibrium water content (sorption characteristics), and of water content on T_g (glass transition characteristics) of *H. pluvialis* powder. The manuscript thoroughly discusses the implications of these water relationships on the preparation of *H. pluvialis* samples for $scCO_2$ extraction processes.

2.2. Materials and methods

2.2.1. Samples

Dried and disrupted cell cysts of *H. pluvialis* with a maximum of 1.5% weight astaxanthin (feed grade powder corresponding to Supreme Asta Powder 1.5% ®) was kindly provided by Atacama Bio Natural Products S.A. (Iquique, Chile). To avoid degradation, the powder was placed in vacuum-sealed aluminum bags and stored at -20 ºC until use.

2.2.2. Sorption isotherm

The water sorption isotherm of *H. pluvialis* powder was measured at 20 °C (± 1 ºC) by using a static gravimetric method and oversaturated salt solutions to maintain constant water activity (a_w) values at equilibrium. Triplicate samples (0.5 g) were weighted in small aluminum wells and placed inside hermetically sealed desiccators containing oversaturated solutions (Greenspan, 1977) of LiCl ($a_w = 0.11$), $MgCl_2$ ($a_w = 0.34$), K_2CO_3 ($a_w = 0.43$), $Mg(NO_3)_2$ ($a_w = 0.60$), NH_4NO_3 ($a_w = 0.67$), NaCl ($a_w = 0.75$), KCl ($a_w = 0.85$), and $BaCl_2$ ($a_w = 0.90$) as recommended by Labuza (2000). Samples were periodically weighed until a constant weight (± 0.001 g) was reached. The water content (W) was calculated on a dry basis (d.b.) after correction for the initial water content determined gravimetrically by drying in a WTB Binder (Tutlingen, Germany) oven (105 ºC) to a constant final weight (24 h approximately).

2.2.3. Differential scanning calorimetry

The thermal characteristics of each conditioned sample from 2.2.2 were measured in a Differential Scanning Calorimeter (DSC) Mettler Toledo Star System 821e (Greifensee,

Switzerland). For each measurement, 10-15 mg samples taken from the desiccators were weighted and immediately hermetically sealed in a 40-µL-capacity aluminum pan. Each pan was cooled down to -100 ºC using liquid N_2 and scanned in the DSC up to 150 °C at a heating rate of 10 °C/min to determine the thermal transitions, using an empty aluminum pan as the reference. The T_g of each conditioned sample was taken as the inflection point of the change in specific heat observed at the endothermal shift in the base line on the thermogram from the dynamic scan, which was determined by using the data analysis system software Stare.

2.2.4. Pressure-induced squeeze flow

The pressure necessary to initiate squeezing flow was used to characterize the relationship between water content and HPC of *H. pluvialis*. The powder material was uniaxially compressed in a semiautomatic laboratory tablet press Natoli NP-RD10A (St. Charles, MO). All experiments were done in quintuplet at 23 ºC using a die diameter of 5 mm and the minimum allowable fill depth of 2 mm. After setting the compression parameters (depth fill of the die, compression force), conditioned powder samples from 2.2.2 were loaded completely into the die fill (Figure 2-1A), and then manually compressed until achieving squeeze flow (Figure 2-1B-D). Compaction pressure was recorded when the material started protruding between the punch tool and die (Figure 2- 1B). The selected die diameter was determined by the experimental compression pressure range defined by the minimum that allowed detection (20 MPa) and the maximum permitted by the punch tooling element (400 MPa) of the equipment. All experiments were done by the same experienced operator, which had an estimated ram speed of 30 ± 6 MPa/s.

2.2.5. Statistical analysis

A non-linear least square regression analysis was used to determine the parameters of equations describing the effect of W on a_w or T_g. The goodness of fit of each model was evaluated by calculating the correlation coefficient (R^2) statistics, and the Mean Relative Error (MRE) using Eq. (2.1) (Goula et al, 2008; Palou et al, 1997):

$$\text{MRE}\ (\%) = \frac{100}{N}\sum_{i=1}^{N}\left|\frac{m_{\text{ei}} - m_{\text{pi}}}{m_{\text{ei}}}\right|, \tag{2.1}$$

where N is the number of individual observations (i), m_{ei} is the experimental value, and m_{pi} the predicted value of the model.

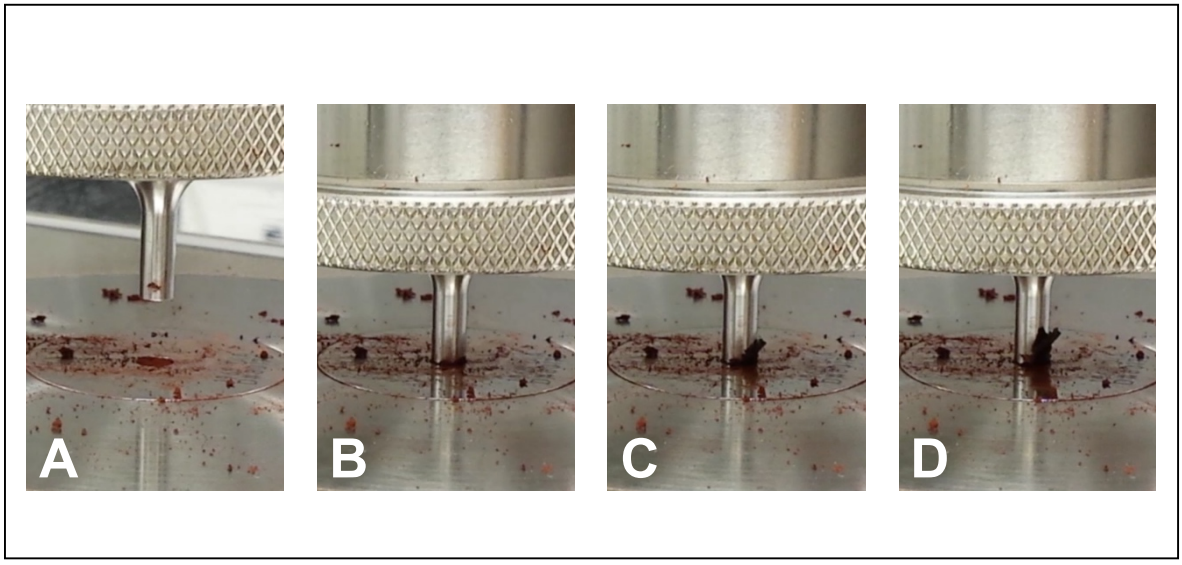

Figure 2-1: Pressure-induce squeeze flow behavior in *H. pluvialis* powder. In the test, after filling the die completely with powder sample (A), this is uniaxially compressed in the laboratory tablet press. In the example the powder was equilibrated to $a_w = 0.85$ using a oversaturated aqueous solution of KCl ($W = 28.9\%$ d.b.). The sequence of consecutive frames (B)-(D) shows the start of squeeze flow that is back-extruded between the punch and die (*cf.* extrudate protuding from the front right). The compaction pressure was recorded when the squeeze flow started (B).

The package "segmented" from R software was used to describe the segmented relationship between compression pressure and $\otimes T$. The function "segmented" identifies as many linear portions as the data has. The function also returns the slope and intercept of each linear portion and it was used to construct the graphical lineal segments that described the data.

2.3. Results

2.3.1. Sorption isotherm

Figure 2-2 shows the experimental water sorption data for *H. pluvialis* at 20 ºC. The isotherm exhibits the sigmoid shape typically observed in food products. A Guggenheim-Anderson-de Boer (GAB) sorption model, Eq. (2.2), was fitted to the experimental data of water content in a dry basis (W) (Dutcher et al, 2011; Van den Berg, 1984):

$$W = \frac{W_m \cdot C \cdot K \cdot a_w}{\left(1 - K\ a_w\right)\left[1 - K\left(1 - C\right)a_w\right]}, \tag{2.2}$$

where W_m, C, and K are best-fitted to the water sorption data; being W_m the monolayer water content (% d.b.), C a term related to the energy of water molecules bound to the solid substrate (contained in the monolayer), a $C\,K$ a term related to the energy of water molecules in the multilayer (all bound water molecules but those in the monolayer) (Dutcher et al., 2011). Because the GAB equation usually holds for $a_w < 0.90$ (Timmermann et al, 2001; Van den Berg, 1984), parameters of Eq. (2.2) were best-fitted for all experimental data. The experimental data fitted with GAB model (Eq. 2.1) resulted in the following parameters: $W_m = 3.67 \pm 0.084$ % (d.b.), $C = 25.6 \pm 1.5$, and $K = 0.995 \pm 0.005$.

Our model parameters lie within the expected boundaries for BET class II isotherm (Blahovec & Yanniotis, 2008; Brunauer et al, 1940): $C \geq 2$; and $0 < K \leq 1$. As the value of K approaches 1 the energy of water molecules in the multilayer approaches that of pure liquid (condensed) water molecules, and GAB's model approaches the classical Brunauer Emmett-Teller sorption model (Dutcher et al., 2011). The model showed a high R^2 (0.99) and a low MRE (5.93%) which is considered a good fit (Lomauro & Bakshi, 1985).

To the best of our knowledge, there has been a single previous study of water sorption in microalgae done on *Spirulina platensis* by Oliveira et al. (2009). *S. platensis* is one of the richest protein sources in nature that, the same as *H. pluvialis*, has great potential as functional food and animal feed. As with our regression, the GAB model fitted experimental data at 20 ºC properly ($R^2 \approx 99\%$ and MRE < 10%), but the fitted GAB

parameters (W_m = 7.30 ± 0.10 % (d.b), C = 44.7 ± 13.5, and K = 0.970 ± 0.004) differed from ours. For instance, *S. platensis* showed to be more hygroscopic than *H. pluvialis* (its monolayer water content was approximately twice larger than ours) due possibly to compositional differences between the microalgae. Indeed, the reported protein content of *S. platensis* is between 60 – 70% weight (de Oliveira et al, 1999), whereas our *H. pluvialis* strain has approximately half (~33%; Atacama Bio Natural Products S.A, 2010).

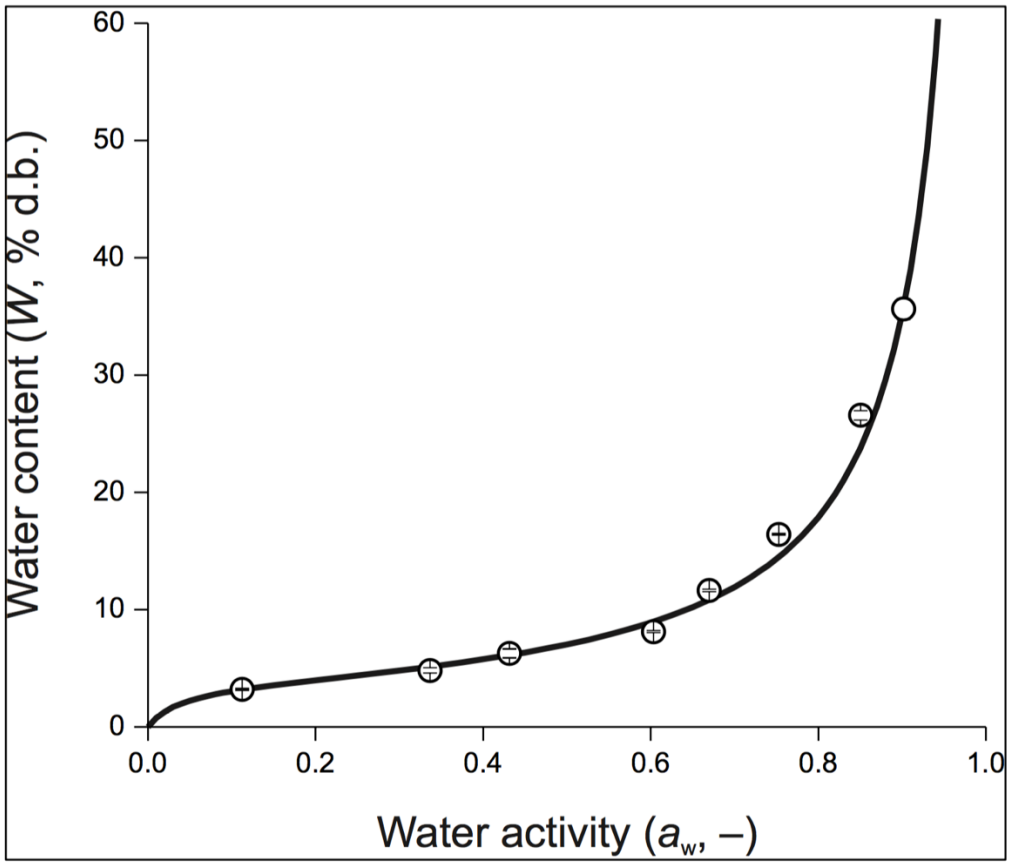

Figure 2-2: Water sorption isotherm of *H. pluvialis* powder at 20 °C (±1 ºC). Symbols and error bars (standard deviation of triplicates) represent experimental data points and the line is the best-fitting Guggenheim-Anderson-de Boer model. Water plasticizing effect on glass transition temperature

The glass-rubber transition is not instantaneous; it occurs within a temperature interval bracketed by the onset and endset temperatures. In our experiments, this interval ranged

from 7 to 27 ºC, with an average of 19 ºC, which is similar to the observation of Aguilera et al. (1993) for fish protein hydrolyzates. Although the onset temperature is usually reported because many changes in food materials are initiated when this temperature is exceeded (Roos & Karel, 1991), we preferred using the inflection point, which usually lied near the midpoint, because it was more consistent in our measurements.

The Gordon-Taylor (GT) equation, Eq. (2.3), that relates T_g of a miscible blend to the weight fraction and T_g values of the blend constituents (water and anhydrous solids in our case), was used to model the changes in T_g (ºC) (Gordon & Taylor, 1952):

$$T_g = \frac{T_{gs} - W_w\left(T_{gs} + 135\,k\right)}{1 - W_w\left(1 - k\right)}, \tag{2.3}$$

where T_{gs} is the glass transition temperature of the anhydrous solid mixtures, k is a fitting parameter, and:

$$W_w = \frac{W}{100 + W}, \tag{2.4}$$

is the weight fraction of water in the material. Parameter k relates to the curvature of the relationship describing T_g as a function of the binary composition of the mixture, that may relate also to the strength of the interaction between water and the anhydrous solids in the material (Aguilera et al., 1995; Gordon & Taylor, 1952). In Eq. (2.3), a value T_{gw} = -135 ºC was adopted for the glass transition temperature of pure water, as informed by Johari et al. (1987) for hyperquenched water. Experimental results fitted the GT equation well, with a high R^2 (0.98) and low MRE (7.54%). Best-fitted values were T_{gs} = 88.3 ºC and k = 3.49. The effect of water as a plasticizing agent can be observed in Figure 2-3, where the inflection T_g is plotted against the weight fraction of water; as the weight fraction of water increases, T_g decreases until it reaches the value of pure water, which is implicit in Eq. (2.3). The GT equation is the most frequently and successfully used to predict the water plasticization effects on food materials (Foster et al, 2006). The equation has been proved to be a reliable predictor of T_g for polysaccharides, proteins, and derivatives and has been applied to several fruit (Goula et al., 2008) and animal (Aguilera et al., 1993) tissues.

To the best of the authors' knowledge, there is no information on glass transitions for microalgae samples and the plasticizing effect of water on them.

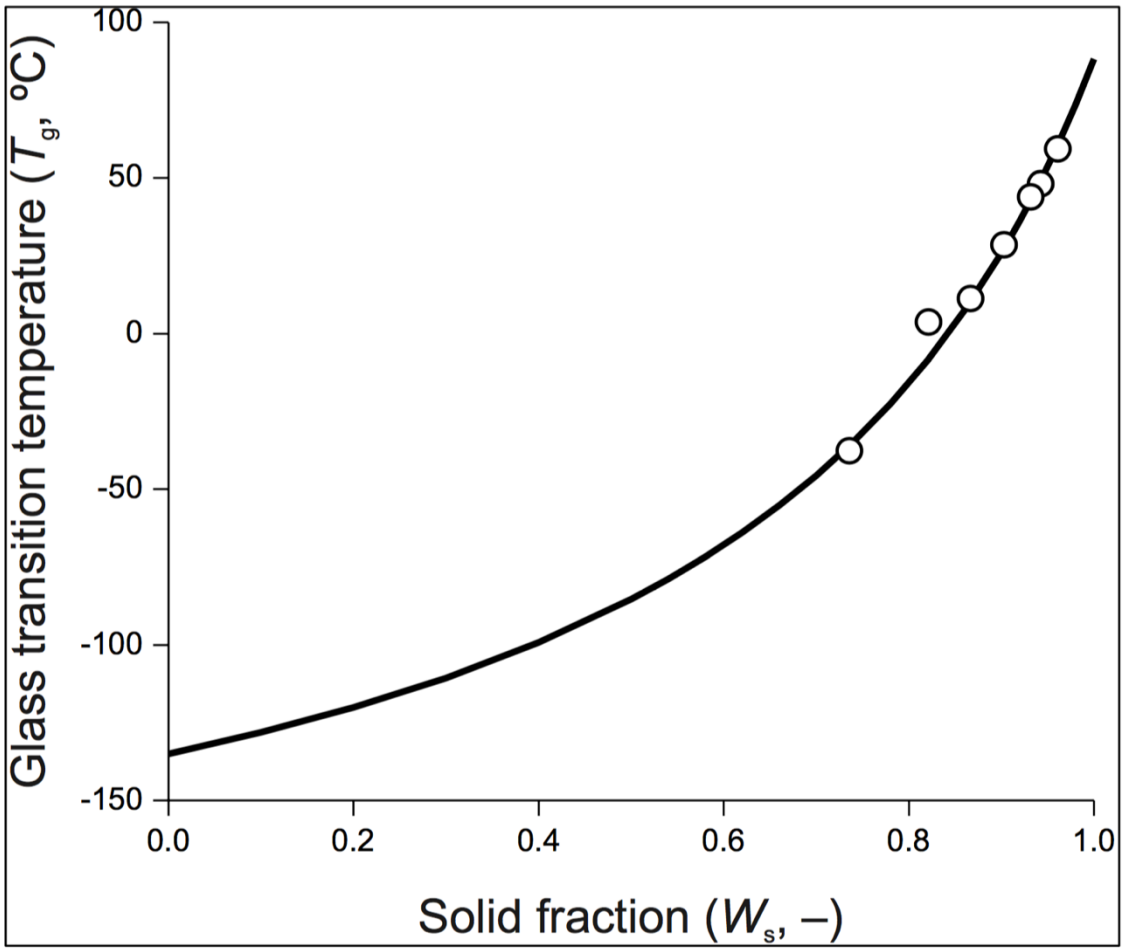

Figure 2-3: Water plasticization effect on the glass transition temperature of *H. pluvialis* powder. Symbols represent experimental data points and the line the best-fitting Gordon-Taylor model using T_{gw} = -135 ºC as the glass transition temperature for

2.3.2. Water plasticizing effect on pressure-induced squeeze flow

Preliminary experiments on *H. pluvialis* uniaxial compaction showed that the microalgae powder protruded from the die at high pressures and different water content. An example of this phenomenon can be observed in Figure 2-1 parts C to D when compressing *H. pluvialis* powder conditioned to a water content of 28.9% d.b. This phenomenon is analogous to yield stress determination of viscous liquids and viscoelastic solids through squeezing flow between two parallel plates (Campanella & Peleg, 2002; Sun &

Gunasekaran, 2009). Squeeze flow set an upper limit to the applied compression pressure in terms of compacts' quality and hardness; its manifestation resulted in deformed low-density pellets. The liquid-like flow was observed at decreasing compaction pressures when increasing the water content of the powder (Figure 2-4). At first the compaction pressures decreased sharply up to 9.3 % water (d.b.). Then, the slope flattened suggesting a change in powder properties closer to that of rubber-like solids typically observed when $T \geq T_g$. When evaluating the difference $\otimes T$ between ambient temperature (T) and T_g values estimated using the GT equation for this water content, a negative difference of 10.8 ºC was observed. Although positive values of the difference $\otimes T$ are expected for phenomena dependent on the glass-rubber transition, we believe that the negative value is due to methodological issues in our experiments (temperature fluctuations, water pick up from the environment, use of inflection instead of onset T_g value). A simple smear test using a palette knife to slide the powder against a flat surface can be used to qualitative assess its stickiness at different water contents. A steep change is confirmed when the water content surpasses the grey shaded area in Figure 2-4.

To the best of the authors' knowledge there are no reports on the use of compression tests in a simple tableting device to ascertain changes is consolidation patterns of pharmaceutical powders as a function of sample water content.

2.4. Discussion

This section discusses the experimental results in section 3 from the standpoint of their implications on the preparation of *H. pluvialis* samples for $scCO_2$ extraction processes. These powder samples can be either high-pressure compacted to increase particle size, or further dried to prevent operational problems caused by stickiness-associated consolidation of the packed bed. As it will be detailed below, the water content of the powder samples affects sample handling during high-pressure agglomeration as well as during $scCO_2$ extraction.

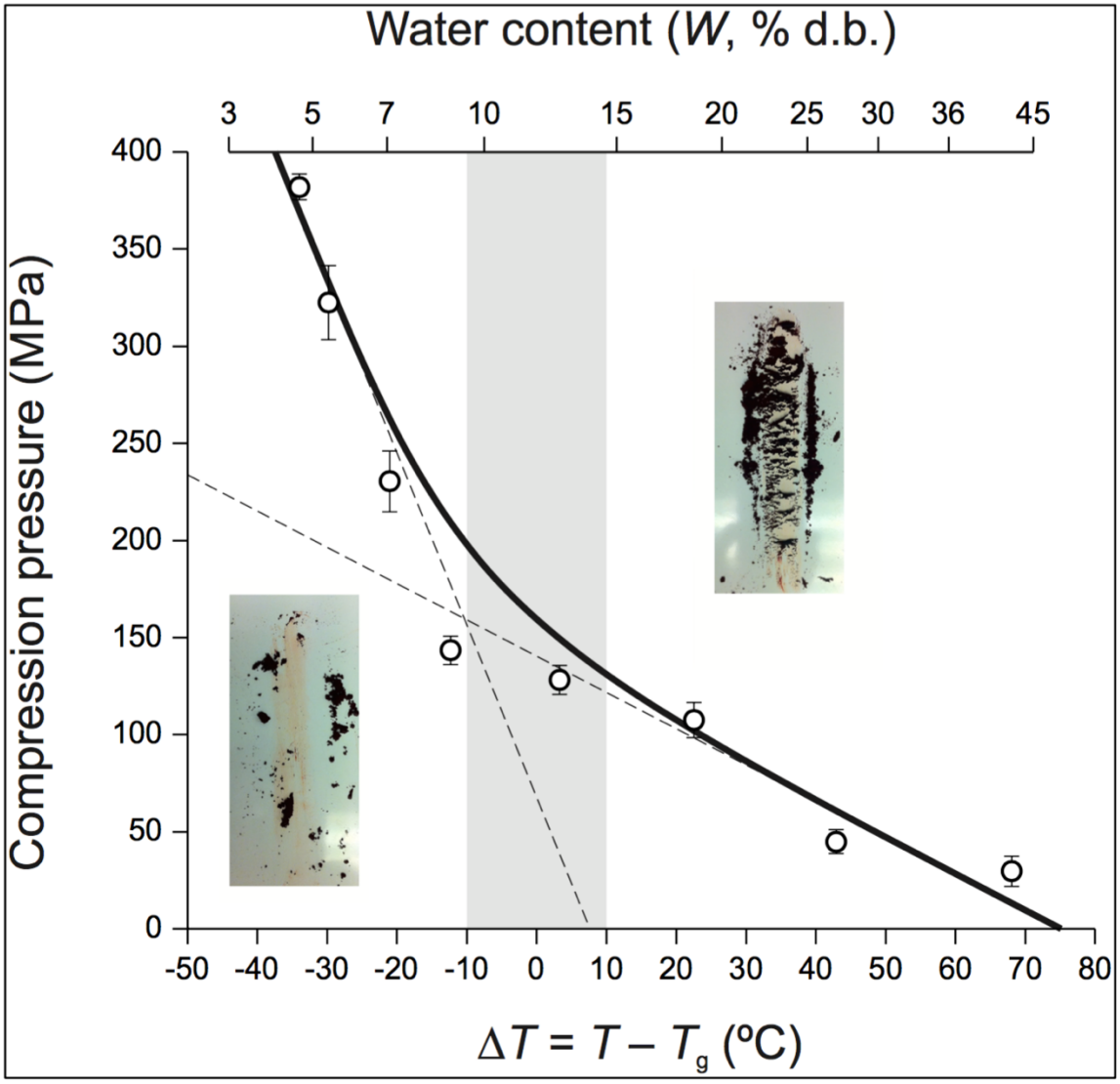

Figure 2-4: Water plasticization effect on the pressure-induced squeeze flow behavior of *H. pluvialis* at ambient temperature ($T \approx 23$ ºC). Symbols and error bars (standard deviation of quintuplets) represent experimental data points and the curve a trend line based on a two-straight line spline (segmented lines) for the data. The shaded area highlights the glass-rubber transition. Pictures above and below the transition visually represent changes in powder stickiness using a simple smear test.

2.4.1. Effect of water content on high-pressure compaction

Biological substrates can be compacted to improve the yield and/or rate of the subsequent $scCO_2$ extraction process. These compaction processes (e.g., pelletization,

tableting) have multiple purposes such as increasing solute availability, increasing extraction vessel load, and facilitating flow of CO_2 through the packed bed (del Valle & la Fuente, 2006). Although compaction solves many of the problems faced by the $scCO_2$ extraction of *H. pluvialis* powder, it also prompts new questions: How does the increase in particle size affect the extraction of astaxanthin? Is it possible to control the inner structure of the compacted substrate to facilitate $scCO_2$ extraction? A significant obstacle when studying and modelling $scCO_2$ extraction of bioactive compounds from biological substrates is describing the mass transfer mechanism within the solid matrix, which depends strongly on its inner structure. The ability to compact substrates while controlling its inner structure remains a challenge. This has been LEMaB's main research effort, focusing on different compaction parameters that can produce reproducible inner structure features such as pore size distribution and connectivity. The materials's water content is an important parameter to consider when compacting powders to fabricate pellets with a pre-determined inner structure. For example, a water content of 6.3% (d.b.) in sawdust from Norway spruce was necessary to increase compression strength and dry density of pellets (Rhén et al., 2005). Because compact's density is inversely related to porosity, improving particle-to-particle contact by adding a binding agent such as water, could produce more homogenous compacts with a lower porosity. Nevertheless, there are limits to water content that depend on the substrate. In wood, pellets cannot be pressed if the water content is above 12-15% (d.b.); pressed pellets will disintegrate if the water content increases above this level (Henriksen et al., 2008). In our case, an increase in water content increases the pressure-induced squeeze flow phenomenon of the material during compaction and the risk of powder caking when manipulating the substrate (Figure 2-4). The effect of water content on the handling of powder samples prior to $scCO_2$ extraction, which affects the stickiness of the sample and the feeding to a HPC device such as a tableting machine, will be discussed in next section.

2.4.2. Effect of water content on sample stickiness and caking

Stickiness and caking can be studied in light of T_g analysis and mechanical tests. The squeeze flow data is an easy, fast, and simple way to characterize hygroscopic powders

destined for HPC techniques such as pelletization or tableting. On the other hand, $\otimes T$ is a relevant measure for caking risk because it is the essential driving force behind the phenomenon. As T_g decreases and approaches the ambient temperature ($\otimes T \approx 0$) there is an increased probability for the solid to behave in a liquid-like fashion, as defined the Williams-Ladel-Ferry (WLF) equation, Eq. (2.5), that describes the pronounced effect of temperature on a mechanical property (Williams et al., 1955) or the time constant of a kinetic phenomenon (Aguilera et al., 1995) (P):

$$\log\left[\frac{P(T)}{P(T_g)}\right] = \frac{C_1 \cdot \Delta T}{C_2 + \Delta T}$$

Williams et al. (1955) proposed the use of universal constants C_1 = -17.44 and C_2 = 51.6 ºC (Peleg, 1992), based on measurements for the viscosity of several polymers, but because individual values for different polymers change slightly, Peleg (1992) proposed best-fitting them to model WLF-type processes in foods above T_g.

The data of sorption isotherm, glass transition temperature, and pressure-induced squeeze flow may be used to prevent stickiness or caking problems during storage and handling of *H. pluvialis* powder. Combining the water plasticization effect on T_g and a_w, it is possible to evaluate T_g at various storage/room conditions (T, RH) (Haque & Roos, 2004; Karel et al., 1994). As a reference, the critical water content and critical water activity of the powder can be determined when $\otimes T$ equal zero. For example, at T = 20 ºC the sample has a critical water content of 13.3% (d.b.) (corresponding to W_w = 0.117 in Figure 2-3) and a critical a_w of 0.69 (corresponding to W = 13.3% in Figure 2-2). Since stickiness was problematic when handling and compacting *H. pluvialis* powder, this data signals the relative humidity of the storage room (RH = 69%) and the water content that should not be exceeded to facilitate high-pressure agglomeration. Our mechanical test showed that a change in the pressure-induced squeeze flow behavior occurs for $\otimes T$ = -10.8 ºC (or about 0 ºC considering the average difference between the onset and inflection temperature observed in our experiments). It is relevant to stress that only a relative importance should be given to this value because of the pronounced effect in this region of

sample water content on T_g, that increases from 15 to 25 ºC as W decreases from 14.8 to 11.9% (d.b.), respectively. Based on these results, we recommend that the water content of *H. pluvialis* powder be kept at 3.67 % (d.b.) (monolayer water content ensuring maximal stability against chemical during storage) to 11.9% (d.b.) (the value of T_g at a near-environment temperature of 25 ºC) to avoid stickiness problems preventing proper loading of HPC devices. Further research will be required to precisely characterize and validate the stickiness or caking temperature of *H. pluvialis* powder under different temperatures and relative humidity. This characterization could involve not only DSC measurements but also thermal mechanical analysis (TMA) or more novel techniques such as the thermal mechanical compression test (TMCT), which is more closely related to what was done in this work (Boonyai et al 2007; Sablani et al, 2010).

When considering a subsequent $scCO_2$ extraction process for *H. pluvialis* powder, it is possible to evaluate the caking phenomenon using the same criteria that for storage. Because the extraction temperature is known beforehand, it is possible to estimate if the powder will cake inside the extractor at a given initial water content. For example, $scCO_2$ extraction temperature for *H. pluvialis* typically ranges from 40 to 60 ºC (Reyes et al., 2014). A critical water content of 4.1-7.9 % (d.b.) can be calculated considering these temperatures instead of 23 ºC as the reference temperatures, and under the assumption that stickiness and caking depend solely on glass transition phenomena of food polymers such as carbohydrates and proteins. Nevertheless, this critical water content is not conservative enough because typical extraction processes take longer than thermal and mechanical tests performed in this work. Furthermore, the high fat content of disrupted cyst of *H. pluvialis* (26.2 %; Atacama Bio Natural Products S.A, 2010) may contribute to stickiness and caking under $scCO_2$ extraction conditions, because of its eventual melting and contribution to interparticle bridging (X. D. Chen & Özkan, 2007). This was noted by Nijdam and Langrish (2006) who observed an increase in the caking of milk powder samples when the fat content increased above 5% fat (the level that warranted a maximal content of surface fat). Preliminary experiments in LEMaB showed the need of complementary drying to ca. 5% water (d.b.) Supreme Asta Powder samples to avoid caking of the packed substrate during $scCO_2$ extraction experiments (Aravena, 2011).

2.4.3. Recommendations for the $scCO_2$ extraction of H. pluvialis samples

Being caking a time-dependent phenomenon that depends greatly in the ability to form bridges between particles, it is possible avoiding the consolidation of the material inside a packed bed during the $scCO_2$ extraction process by reducing its specific surface. LEMaB has attempted this by subjecting the substrate to a high-pressure agglomeration process such as pelletization or tableting (Reyes et al, 2013). Water content also influences compaction of the powder by causing manipulation-hindering stickiness, and by promoting squeeze flow during compression. When investigating compaction and its effect in the compact's inner structure by varying its water content, we recommend performing this process always below the T_g of the sample, within the range described by the first slope of Figure 2-4 in case of *H. pluvialis*.

In case that high-pressure agglomeration is not possible, to avoid the risks of caking inside the extraction vessel during $scCO_2$ extraction and undesirable chemical changes during storage, we recommend a complimentary drying of *H. pluvialis* down to 5% (d.b.), if needed (typical water contents of *H. pluvialis* after drying are 4-9% weight; (Lorenz, 1999).

3. EFFECT OF HIGH-PRESSURE COMPACTION ON SUPERCRITICAL CO_2 EXTRACTION OF ASTAXANTHIN FROM *HAEMATOCOCCUS PLUVIALIS*

Abstract

Supercritical (sc) carbon dioxide (CO_2) has the potential of extracting high-value compounds such as astaxanthin from *Haematococcus pluvialis* microalgae. However, there is a significant risk of caking of *H. pluvialis* (a fine hygroscopic powder) during scCO_2 extraction that may lead to a decrease in extraction rate and/or yield. We propose pretreating *H. pluvialis* by High-Pressure Compaction (HPC) to increase the bulk density and prevent caking during extraction. The resulting microestructure may depend strongly on the conditioning of the material and compaction parameters. The objective of this work was to determine de effects HPC on the formation *H. pluvialis* compacts and scCO_2 extraction of astaxanthin from them. A goal of this study was to produce reproducible and defined microstructures by varying the die and compression parameters during uniaxial compression of *H. pluvialis* powder. We fabricated 42 types of compacts in a semiautomatic tableting machine by varying the compression pressure (15-400 MPa), die diameter (3, 5, and 7 mm), and depth fill (2, 5, and 8 mm). Statistical analysis identified three distinguishable clusters depending on the porosity (microstructural feature) and specific surface (macrostructural feature) of the compacts. Supercritical CO_2 extraction showed that clusters with low specific surface had lower extraction yield than clusters with higher specific surface. The effect of compact microstructure on kinetics of scCO_2 extraction was ascertained by computing a microstructural factor (*MF*) from the best-fitted inner mass transfer coefficient of Sovová's broken-and-intact cell model. Because *MF* depended on the shape of the compacts, this work explored their assimilation to infinity slabs or infinite cylinders. Resulting *MF* values were significantly larger in clusters with high porosity than clusters with low porosity. Finally, the fraction of broken cells in Sovová's model was higher in clusters subjected to higher compression pressures that may have favored cell disruption.

3.1. Introduction

Haematococcus pluvialis, a green microalga, has been identified as the prime natural source of astaxanthin; a valuable ketocarotenoid and powerful biological antioxidant. Astaxanthin has ten times higher antioxidant activity than other carotenoids such as zeaxanthin, lutein, and ß-carotene, and 500 times higher antioxidant activity than tocopherol (Higuera-Ciapara et al., 2006; Lorenz & Cysewski, 2000). The effects of astaxanthin consumption on human health has been described previously by several authors (Ambati et al, 2014; Dhankhar et al, 2012; Guerin et al., 2003; Hussein et al, 2006; Kidd, 2011; Yang et al, 2013; Yuan et al., 2011). The major market for synthetic astaxanthin (95% market share) is aquaculture, as a pigment for salmon and trout (Spolaore et al, 2006b). Human supplementation, on the other hand, faces strict demands both in terms of quality (high purity) and antioxidant activity (Lorenz & Cysewski, 2000). Astaxanthin can be extracted from *H. pluvialis* using organic solvents, but they exhibit limited selectivity and favor astaxanthin degradation, and the extracts contain solvent residues potentially toxic (Crampon et al., 2011). This has motivated the use of supercritical (sc) carbon dioxide (CO_2) as an alternative to organic solvents because of its unique characteristics: it is nontoxic, non-flammable, cost-efficient, readily available, and easy to remove from the treated materials (L. Wang et al, 2012b).

Successful scale-up for the industrial production of concentrated astaxanthin extracts depends on the fine-tuning of substrate pretreatment and extraction parameters (pressure, temperature, and superficial solvent velocity). Most studies on scCO_2 extraction of astaxanthin focused on quantifying the effect of extraction pressure, temperature, time, and/or co-solvents such as ethanol (Krichnavaruk et al., 2008; Machmudah et al., 2006; Pan et al., 2012; Reyes et al., 2014; Thana et al., 2008; L. Wang et al., 2012b), but few authors additionally studied the effect of pretreatments such as milling or crushing (Nobre et al., 2006; Valderrama & Perrut, 2003). Most studies generally agree in the need of a cell disruption step to increase the availability of astaxanthin. However, disrupted *H. pluvialis* is usually a fine hygroscopic powder, which may cake inside the extraction vessel, thus causing CO_2 channeling and a decrease in extraction rate and/or yield (C. G. Pereira &

Meireles, 2009; Reyes, Muñoz, & A, 2015a). Caking phenomena has been described in garlic (Glatzel & Martínez, 2012b) and *Nannochloropsis oculatai* microalgae (Crampon et al, 2013).

To avoid caking phenomena during $scCO_2$ extraction of fine powders, the Extraction Laboratory of Biological Materials (LEMaB acronym from the Spanish name) proposes increasing the particle size by precompacting the powdery material using High-Pressure Compaction (HPC) processes such as tableting or pelletization. In the area of powder technology it is important to understand, quantify, and predict density variations within the compacts during HPC. For pharmaceutical tablets, the internal density distribution is relevant because it affects the local material properties, which in turn can influence the mechanical properties of the tablets and the bioavailability of the drug (Sinka, 2007). Similarly in food matrices, high shearing forces during HPC destruct cells walls and other mass transfer barriers within the solid (Uquiche & Ortiz, 2004). As a result, the solid matrix acquires a new microstructure, which in turn affects the mass transfer coefficient within the solid matrix (Aguilera & Stanley, 1999; Crossley & Aguilera, 2001). Hence, it is expected that the extraction rate and yield will depend strongly on the microstructure and size of the compact.

There have been significant efforts to fabricate predictable and reproducible microstructures in compacts (*e.g.* tablets, pellets) (Lannutti, 1997). The choice of powder composition (*e.g.*, moisture, granulometry) and process parameters (*e.g.*, compression pressure, die geometry, pressing schedule) determine the microstructure and final properties of compacts (Lannutti, 1997; Sinka, 2007). In extraction process, Aguilera and Stanley (1999) proposed a microstructural factor (*MF*) that quantifies the effect of the microstructure on the diffusion of a solute within a solid matrix, which is defined as:

$$MF = \frac{D_e}{D_{12}}, \tag{3.1}$$

where D_e is the effective diffusivity and D_{12} the binary diffusion of the solute in $scCO_2$. For porous solids, they proposed the following relationship to estimate *MF* as a function of the solid particle porosity (ε_p) and tortuosity (τ_p):

$$MF = \frac{\varepsilon_p}{\tau_p}, \tag{3.2}$$

This factor has been successfully used to estimate the effective diffusivity as a function of the binary diffusion coefficient in mathematical models (del Valle et al, 2006; Uquiche et al., 2006). Uquiche et al. (2006) investigated the possibility of fabricating different microstructures by varying the moisture and granulometry of milled Jalapeño pepper flakes before pelletization. Their study showed mix results for moisture, however reducing particle size through milling reduced the porosity and increased the tortuosity of the pellets resulting in a smaller *MF*. The estimated D_e fitted reasonably well the experimental data, but further studies are required to understand this factor and to effectively reproduce these results.

The objective of this work was to determine de effects HPC on the formation of *H. pluvialis* compacts and the recovery of astaxanthin from the compacts by means of $scCO_2$ extraction. An important goal of this study was to produce reproducible and defined microstructures by varying the compression pressure and die geometry during uniaxial compression of *H. pluvialis* powder. *MF* was quantified by mathematical modeling of extraction curves.

3.2. Materials and methods

The objective of this work was to determine de effects HPC on the formation of *H. pluvialis* compacts and the recovery of astaxanthin from the compacts by means of $scCO_2$ extraction. An important goal of this study was to produce reproducible and defined microstructures by varying the compression pressure and die geometry during uniaxial compression of *H. pluvialis* powder. *MF* was quantified by mathematical modeling of extraction curves.

3.2.1. Samples

Disrupted, dried *H. pluvialis* (maximum of 1.5% w/w astaxanthin feed grade powder) was kindly provided by Atacama Bio Natural Products Inc. (Iquique, Chile). The powder

was stored at -18 ºC inside hermetically sealed desiccators containing silica gel to standardize its moisture and avoid stickiness during manipulation. This was also done with the compacts previous to $scCO_2$ extraction. The moisture of the powder and compacts was of 3.27 ± 0.19% in a dry basis.

3.2.2. High-pressure compaction of H. pluvialis

H. pluvialis powder was uniaxially compressed in a semiautomatic laboratory tablet press Natoli NP-RD10A (St. Charles, MO). A wide range of compacts were fabricated by changing the compression parameters such as diameter of the die (3, 5, and 7 mm), depth fill (2, 5, and 8 mm), and compression pressure (15, 25, 50, 100, 200, and 400 MPa). After setting the compression parameters the compaction process consisted in three steps: die filling, compaction until achieving the desire compression pressure, and ejection from the die. The usable compression pressure range was determined by the minimum allowed for detection (15-25 MPa) and the maximum permitted by the punch tooling elements (200-400 MPa) of the equipment. Each compact was labeled by its compression parameters. For example, 3.2.100 means a compact fabricated with a 3 mm die, 2 mm of depth fill, and 100 MPa of compression pressure.

3.2.3. Compacts characterization

The bulk density of the compacts in a packed bed (ρ_b) was determined in triplicate using the gravimetric procedure of Uquiche et al. (2004), whereas the true density (ρ_t) of the substrate was determined by N_2 pycnometry using a Quantachrome Ultrapyc 1200e (Boynton Beach, FL) device. The tablet press produces well defined compacts with small variations in dimensions; each compact consisted of a cylinder with 2 spherical caps. Thus, by measuring its length and diameter it was possible to calculate its volume, superficial area, and specific surface a_p (superficial area-to-volume ratio). Ten random compacts of each type were individually weighted and then photographed with a 13-Mpx camera; their length and diameter were precisely measured using software ImageJ 1.46 (NIH, USA). The compact's density (ρ_s) was calculated as the ratio between its mass and volume.

Porosity of the compact (ε_p) was measured from the calculated densities using Eq. (3.3):

$$\varepsilon_p = 1 - \frac{\rho_s}{\rho_t}, \tag{3.3}$$

then the bed porosity (ε_b) was determined as previously described by del Valle et al. (2006).

3.2.4. Supercritical CO_2 extractions

Extraction experiments were carried using a Thar Technologies' (Pittsburgh, PA) SFE-1L process development unit that was modified for screening purposes. The extraction vessel (20-mm internal diameter, 50-cm^3 capacity) was loaded with approximately 1 g of compacts and the remaining volume was filled with glass beads at the bottom and the top of the cell, then placed in a thermostatic convection oven. All experiments were carried out using 10 g/min of food grade (99.8% pure) CO_2 from Indura (Santiago, Chile) at 40º C, 50 MPa. Six unequally spaced samples were taken in all cases and total extraction times were approximately 4 h. The recovered extract was assessed gravimetrically by difference with cleaned and dried vials and later stored at -18º C until analyses. The vials were placed within a desiccator prior to weighing in order to remove water traces from extract samples and adjust them to room temperature (22 °C).

The astaxanthin content in oleoresin samples was determined using an spectrophotometric method (Wright et al, 2005). The extracted oleoresin was dissolved in acetone (Labtec, Santiago, Chile) and absorbance measurements were performed at 476 nm in a Shimadzu's (Kyoto, Japan) UVmini-1240 spectrophotometer. The absorbance was adjusted by dilution to be between 0.2 and 0.8 OD. Pigment concentration was estimated by using the extinction coefficient in acetone of astaxanthin ($E^{1\%}$ = 2100). Astaxanthin extraction yield was expressed as milligrams of astaxanthin per gram of substrate (microalgae compacts). Moisture content before and after the extraction of the compact samples were determine gravimetrically by drying in an oven (Binder, Tutlingen,

Germany) at 105 ºC overnight to reach constant weight. In all cases, extractions were done in duplicates.

3.2.5. Mathematical model

Extraction kinetics were represented using the model of Sovová (2005) based on the broken-and-intact cells concept. This concept assumes that close to the surface of a vegetable tissue, there is a region of broken cells damaged by mechanical pretreatment, and that the core region contains mostly intact cells. Although this model was developed for vegetable tissue constituted of cells with tough cell walls, we believe it is possible to extend its use to unicellular material. The volumetric fraction of broken cells is represented by *r*.

The solute equilibrium partition curve is divided into four regions depending on solute concentration: A, B, C, and D. The shape of H. pluvialis compacts extraction curves suggested type D (Sovová, 2005), which implies that phase equilibrium is determined by a constant partition coefficient K during all extraction. The solution of the complete model for plug flow considers the extractor divided into a large number of mixers (n); by changing n different degrees of axial dispersion can be simulated. Because of the small extraction bed heights (<10 mm), we assumed that axial dispersion did not affect extraction kinetics. Therefore, we modeled the extraction curves with n = 25 considering that n = 10 is enough to simulate plug flow for type D curves (Sovová, 2005).

Mass balances for the dimensionless solute concentration in the fluid phase is described by Eq. (4), in the broken cells by Eq. (5), and in the intact cells by Eq. (6) as a function of dimensionless time, as described by Sovová (2005). Dimensionless concentrations in broken (X_1) and intact cells (X_2) are defined as the ratios between the actual concentrations (x_1 and x_2) and corresponding initial values (x_{10} and x_{20}) in broken and intact cells, respectively. The dimensionless concentration in the fluid phase (Y) is defined as the ratio between the actual (y) and initial concentration (y_0) of solute in the $scCO_2$ phase. Finally, dimensionless time ( ) is defined as the ratio between extraction time and residence time (t_r) of the solvent in the extractor.

The residence time (t_r) can instead be calculated as the ratio between the extraction bed height (H_b) and the interstitial fluid velocity (U):

$$\frac{dY_j}{d\tau} + n\left(Y_j - Y_{j-1}\right) = \frac{(Y_j^* - Y_j)}{\Theta_e}, \text{ where } Y_j^* = Y^*\left(X_{1j}\right), \tag{3.4}$$

$$\frac{dX_{1j}}{d\tau} = \frac{1}{r\ \Theta_i}\ (X_{2j} - X_{1j}) - \Gamma\ \frac{Y_j^* - Y_j}{\Theta_e}, \text{ and} \tag{3.5}$$

$$\frac{dX_{2j}}{d\tau} = -\frac{1}{(r-1)\ \Theta_i}\ (X_{2j} - X_{1j}). \tag{36}$$

The equations have the following initial and boundary conditions:

$$Y_j = X_{1j} = 1 \text{ and } X_{2j} = 1 + \Gamma \text{ for } \tau = 0, \text{ and} \tag{3.7a}$$

$$Y_{j-1} = 0 \quad \text{for } j = 1. \tag{3.7b}$$

The amount of extract obtained after a dimensionless time (τ) is estimated by integration as indicated in Eq. (8).

$$\Phi = \frac{\Gamma\ r}{1+\Gamma}\int_0^{\tau} Y_n\ d\tau, \text{ for j = 1, 2, … 25.} \tag{3.8}$$

The dimensionless partition (Γ), external mass transfer (Θ_e), and external mass transfer (Θ_i) parameters are calculated as follows:

$$\Gamma = \frac{\rho_f\ \varepsilon\ K}{\rho_s\left(1-\varepsilon\right) r}, \tag{3.9}$$

$$\Theta_e = \frac{\varepsilon}{k_f a_0 t_r}, \text{ and} \tag{3.10}$$

$$\Theta_i = \frac{1-\varepsilon}{k_s a_s t_r}. \tag{3.11}$$

To calculate values of *MF*, we modified the model by expressing the mass transfer coefficient in the solid substrate ks in terms of the effective internal diffusivity (Reverchon, 1996):

$$k_s = \frac{D_e \, a_p}{\nu} \quad , \tag{3.12}$$

where ν is a factor that depends on particle geometry, and is equal to 3/5 for spheres, 1/3 for slabs, and 1/2 for cylinders (Villermaux, 1987). Using Eq. (1) to write MF in terms of the mass transfer coefficient in the solid substrate and the binary diffusion coefficient, we obtained the following expression for MF:

$$MF = \frac{k_s \, \nu}{a_p D_{12}} \quad . \tag{3.13}$$

3.2.6. Model parameters

Density (ρ_f = 991.3 kg/m^3) and viscosity (μ_f = 1.18×10^{-4} Pa·s) of CO_2 at the extraction conditions were calculated using the NIST database for pure CO_2 (Lemmon et al, 2012). The binary diffusion coefficient (D_{12} = 4.78 m^2/s ×10^{-9}) was estimated as a function of the reduced density ($\rho_{r1} = \rho_f/\rho_c$, ρ_c = 467.6 kg/m^3) and reduced temperature ($T_{r1} = T_f/T_c$, T_c = 304.1 K) of CO_2 (component 1), and the critical volume (V_{c2} = 1983.5 cm^3/mol) and molecular weight (MW = 596.84 g/mol) of the solute (component 2, astaxanthin) using the correlation of Catchpole and King (1994). The critical volume of the solute was estimated using Joback's group contribution method with group parameter values informed by the Dortmund Data Bank Software & Separation Technology (Bank, 2011). The value of the external mass transfer coefficient (k_f) was estimated using the correlation of Puiggené et al. (1997) and the diameter of a sphere with the same surface-to-volume ratio of the compact as its characteristic dimension. In case of the initial concentration of the solute in the untreated solid (c_u), we selected one compact of each selected cluster to be extracted until exhaustion (~16 hours) and estimated the parameter value from the horizontal asymptote of the cumulative extraction curve. The solvent residence time (t_r), the specific surface area per unit volume of extraction bed (a_0), the particle specific surface (a_p), and the specific surface area per unit volume of solid (a_s) were calculated as previously described by Sovová (2005).

The adjustable parameters in the model were K (one for all), r (one per cluster), and k_s (one per compact). Ordinary differential equations were solved using MATLAB R2013a (Math Works, Natick, MA) function ode23. We fitted simultaneously all extraction curves by minimizing the absolute average deviation (*AAD*, %) between experimental and modeled extraction curves:

$$AAD = \frac{100}{\text{Number of observations}} \sum \left| \frac{x_{\text{exp}} - x_{\text{cal}}}{x_{\text{exp}}} \right| \tag{3.14}$$

The confidence intervals (95%) of the model parameters was determined by nonlinear regression using the nlparci function in MATLAB.

3.2.7. Clustering and statistical analysis

Hierarchical clustering methodology using R package (Team, 2014) was used to screen the experimental data and classify groups of compacts that would potentially present distinct micro- and macrostructural features. Our classifying criterion for compact microstructure was its porosity and for compact macrostructure its specific surface. All variables were normalized to avoid biasing clustering by the magnitude of the classifying criterions. Clustering methods rely on a measure of dissimilarity between sets of observations; in this case the Euclidean distance was used to build the dissimilarity matrix. Ward's minimum variance method was chosen to produce packed clusters.

The statistical analysis of the compacts characteristics and clusters was done by a one-way ANOVA using RStudio software, version 0.98.953 that uses R package (Boston, MA).

A general tendency for scatter plots for astaxanthin yield *versus* dimensionless extraction time was described by an empirical equation, Eq. (3.15), which was used to fit the data for assumedly spherical, slab, and cylindrical geometries:

$$y = 1 - a \cdot \exp\left(-b \cdot t_{\text{d}}\right) \tag{3.15}$$

where y is astaxanthin recovery (mg extracted/mg extractable astaxanthin); a and b, fitting parameters; and t_{d} the dimensionless extraction time calculated using Eq. (3-16):

$$t_d = \frac{3 \cdot D_e}{S/V}, \tag{3.16}$$

The statistical dispersion of each plot was analyzed by quantifying its residuals or fitting deviation, the R-square statistic, and *AAD*.

3.3. Results

Results of clustering analysis based on the compacts characteristics will be presented first, followed by $scCO_2$ extraction curves and model parameters based on the clusters, and ending with calculations of the microstructural factor and its relationships with compacts' geometry.

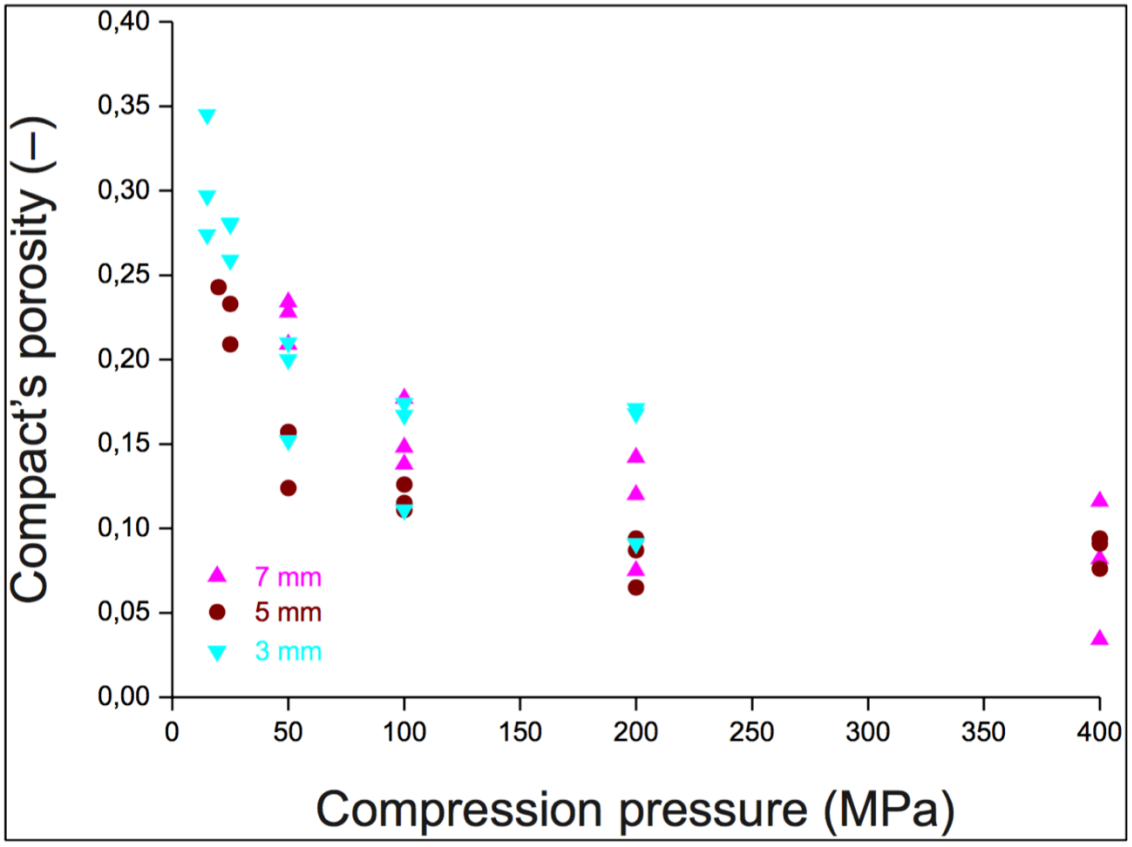

Figure 3-1: Porosity as a function of compression pressure for compacts of 3, 5 and 7 mm of diameter.

3.3.1. Compact clustering

Preliminary studies varying compression pressure and die diameter (3, 5, or 7 mm) showed a strong relationship between compact porosity and compression pressure (Figure 4-1). Porosity decreases sharply up until 100 MPa, then the tendency flattened showing no statistical difference ($p > 0.05$) over 200 MPa. This result allowed us to propose compact's porosity as a measure of inner structure.

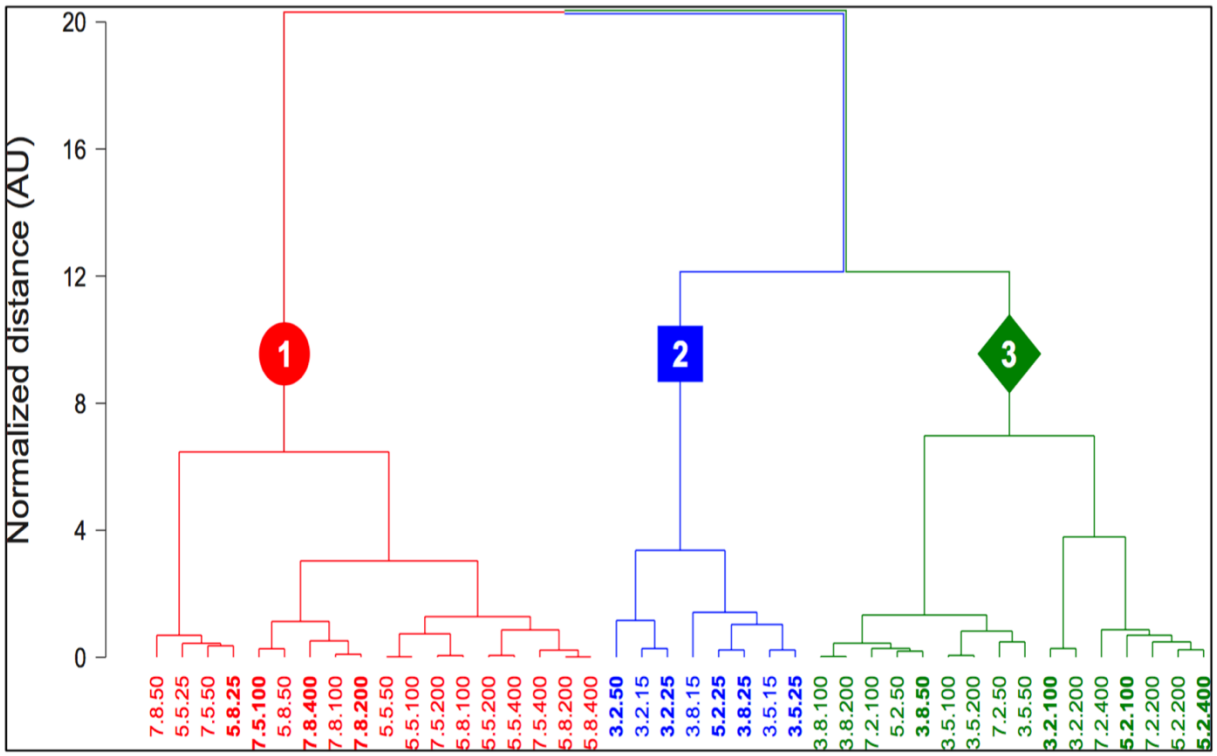

Figure 3-2: Dendrogram of *H. pluvialis* compacts classified by the hierarchical clustering method based on their porosity and specific surface. Compact codes refer to compaction parameters. For example, 7.5.100 stands for 7 mm of die diameter, 5 mm of depth fill, and 100 MPa of compression pressure.

A total of 42 types of compacts were produced by varying the compression parameters. Hierarchical clustering analysis resulted in the dendrogram shown in Figure 3-2. Since our objective was to identify groups of compacts that are very distinguishable from each other, we chose clusters that had distances greater than 10, thus three clusters were selected.

A closer look at each cluster showed that the porosity of compacts in Cluster 1 and Cluster 3 were not significantly ($p > 0.05$) different from each other, whereas compacts in Cluster 2 were significantly ($p < 0.05$) more porous (Figure 3-3A). This result agrees with our compression parameters: the overall compression pressure to produce compacts was higher for Cluster 1 and Cluster 3 than for Cluster 2. On the other hand, compacts in Cluster 1 had significantly ($p < 0.05$) less specific surface than those in Cluster 2 and Cluster 3, which were not significantly ($p > 0.05$) different from each other (Figure 3B). Average values of compact's porosity were 0.161 ± 0.040 for Cluster 1, 0.244
± 0.027 for Cluster 2, and 0.113 ± 0.031 for Cluster 3, whereas the specific surface was 1091.5 ± 127 kg/m^3 for Cluster 1, 1820.3 ± 256 kg/m^3 for Cluster 2, and 1795.4 ± 250 kg/m^3 for Cluster 3.

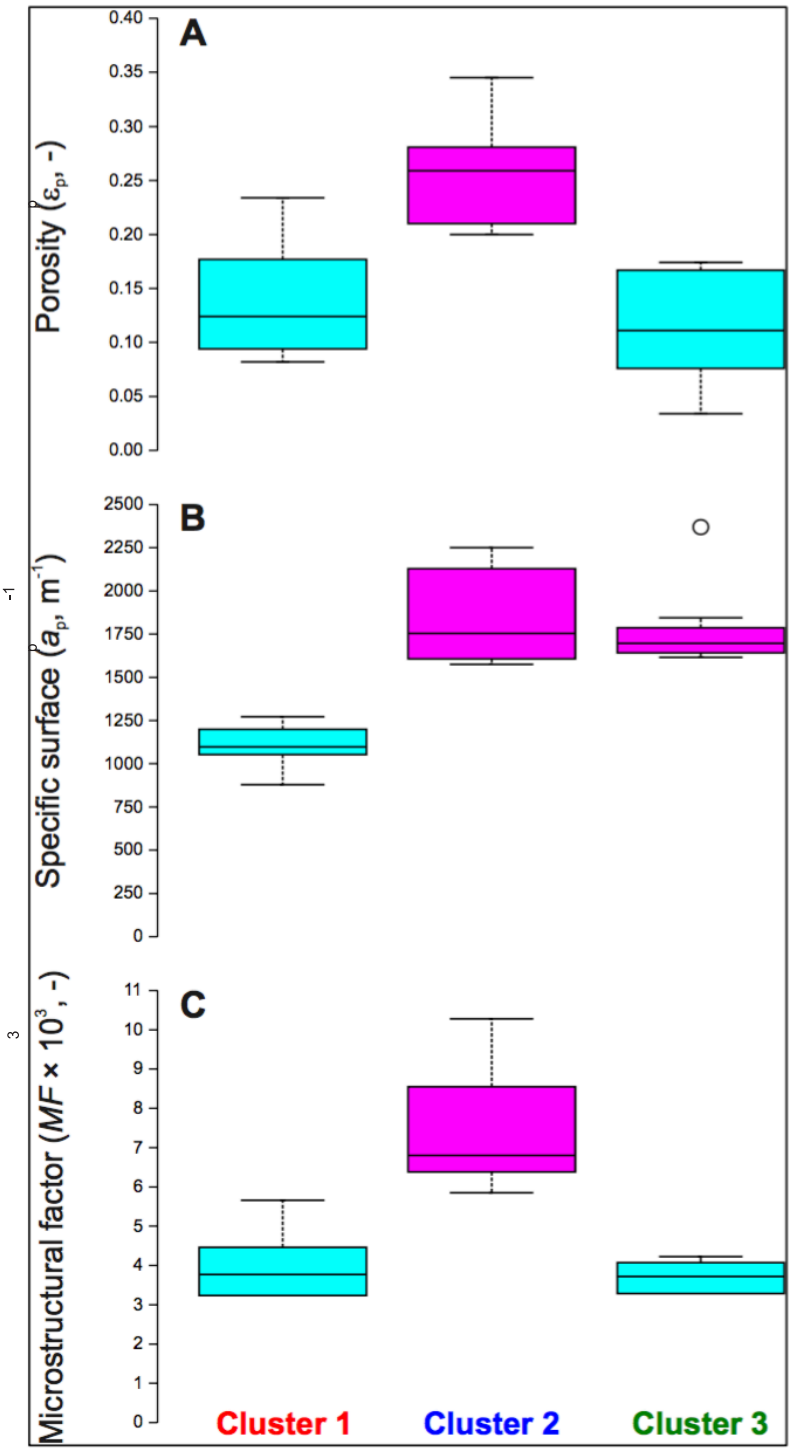

Figure 3-3: Boxplots of density, specific surface, and microstructural factor of compacts based on mixed geometrical factors (slab/cylinder). Differences in color indicate significant ($p < 0.05$) differences between clusters.

3.3.2. Modelling parameters

Samples of 4 to 5 compact types were selected from each cluster to be extracted using $scCO_2$. Table 1 summarizes the physical characteristics and astaxanthin yields following 4 h of extraction of these compacts, whereas Table 2 summarizes geometrical parameters of the same compacts. On average, astaxanthin yield was 3.51 ± 0.21 mg/g for Cluster 1, 6.51 ± 0.72 mg/g for Cluster 2, and 6.57 ± 0.40 mg/g for Cluster 3. ANOVA analysis showed significantly ($p < 0.05$) lower astaxanthin yield for compacts in Cluster 1 than those in Cluster 2 and Cluster 3.

Figure 3-4 shows the experimental and modeled extraction curves. The agreement between the experimental data and the mathematical model was outstanding (*AAD* ranged from 2.3% to 9.6% with an overall average deviation of 5.8%). Particularly, on average Cluster 2 modeling data fitted the experimental data worst (*AAD* = 7.3%). Extractions until exhaustion showed that the amount of extractable astaxanthin varies among clusters; values of c_u for compacts of Cluster 2 (7.85 mg/g) and Cluster 3 (7.83 mg/g) were very close and considerably higher than for those in Cluster 1 (6.00 mg/g).

Table 3-1 summarizes the parameters of the fitted model for all extraction experiments. Statistical analysis of fitted parameters K, r and k_s indicated that they were statistically significant or different from zero (i.e., confidence intervals did not include zero). Indeed, the 95%-confidence interval for parameter K was 0.030 to 0.036 (best fit value = 0.033). On the other hand, the confidence intervals for parameter r were 0.40 to 0.43 for compacts in Cluster 1 (best-fit value = 0.42), 0.21 to 0.23 for those in Cluster 2 (best-fit value = 0.23), and from 0.38 to 0.40 for compacts in Cluster 3 (best-fit value = 0.39). Interestingly, best-fit parameter r for compacts in Cluster 2 was almost half of those in Cluster 1 or Cluster 3, and could be related to a disruptive effect of HPC on *H. pluvialis* cysts. In fact, r parameter correlated well with the clusters' average porosity, hence with the applied compression pressure; low porosity values were associated with high values of parameter r. The internal mass transfer parameters from Sovova's model (k_s) for compacts of Cluster 2 were on average almost in all cases two-to-three times higher than corresponding values for those in Cluster 1 and Cluster 3.

On average the range of the confidence interval of k_s is 4.34×10^8 with low dispersion (0.97×10^8). However, this was not considering the compact 3.2.50 which we consider an outlier because it showed the highest confidence interval range (12.25).

Table 3-1. Physical characteristics of *H. pluvialis* compacts produced and extracted in this study.

Cluster	Compact code	Weight (mg)	Volume ($m^3 \times 10^8$)	Compact density (ρ_s, kg/m^3)	Bulk density (ρ_b, kg/m^3)	Particle porosity (ε_p, -)	Bed porosity (ε, -)	Surface ($m^2 \times 10^5$)	Astaxanthin yield* (mg/g)
1	7.5.100	137	12.4	1101	557	0.177	0.494	13.4	3.76
1	7.8.200	219	19.0	1156	601	0.142	0.480	17.1	3.25
1	7.8.400	217	18.2	1191	599	0.116	0.483	16.7	3.45
1	5.8.25	125	11.5	1087	540	0.209	0.504	12.4	3.58
2	5.2.25	40.4	3.89	1038	516	0.243	0.503	6.25	6.23
2	3.2.25	13.0	1.23	1054	542	0.226	0.486	2.97	6.40
2	3.8.25	38.4	3.87	989	502	0.259	0.493	6.27	6.09
2	3.2.50	10.9	1.20	1074	561	0.210	0.477	2.56	7.78
2	3.5.25	26.0	2.60	963	513	0.280	0.467	4.59	6.06
3	5.2.100	41.7	3.40	1227	590	0.111	0.519	5.83	6.50
3	5.2.400	38.1	2.97	1280	610	0.076	0.523	5.49	6.51
3	3.8.50	41.5	3.84	1132	554	0.152	0.511	6.25	6.16
3	3.2.100	13.0	1.08	1222	574	0.111	0.531	2.55	7.12

* Astaxanthin yield corresponds to the average following 4 h of extraction using 10 g/min of supercritical CO_2 at 40 ºC and 50 MPa.

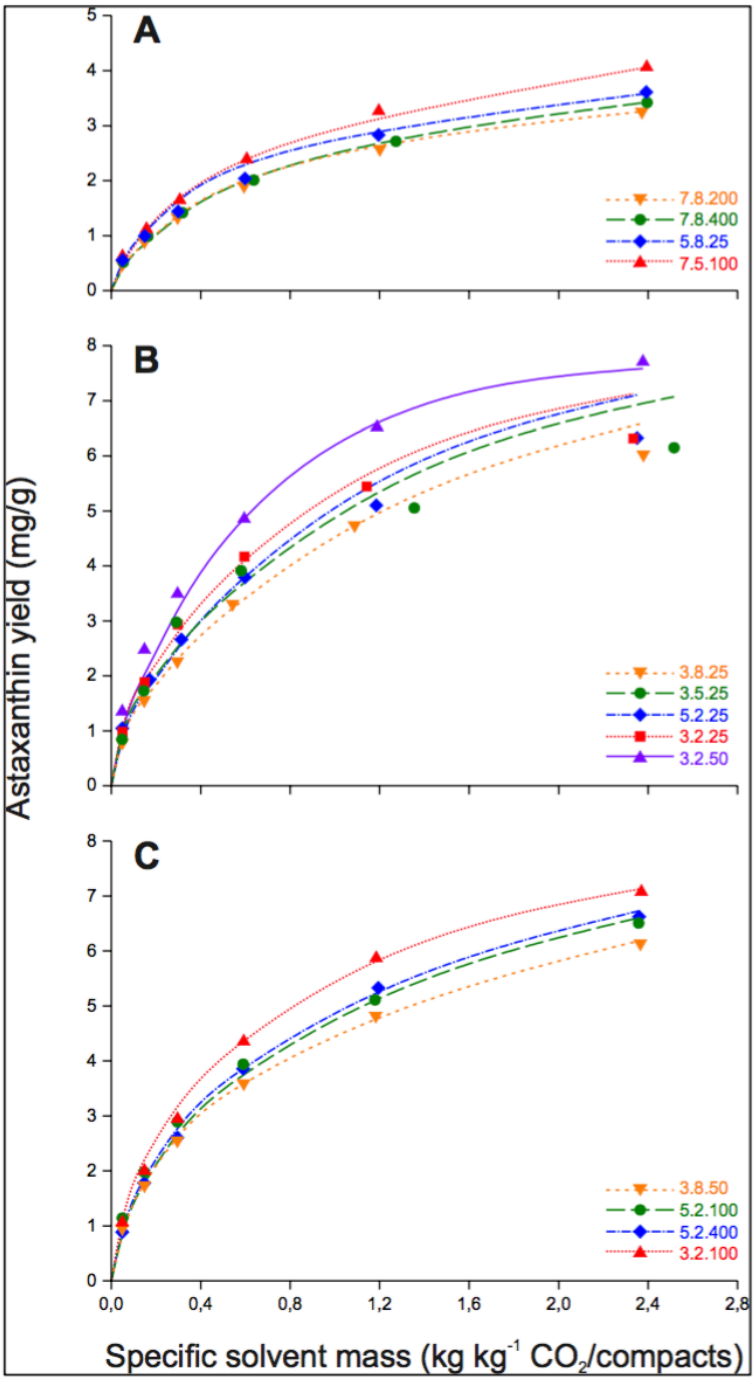

Figure 3-4: Cumulative extraction kinetics of astaxanthin from *H. pluvialis* compacts from (A) Cluster 1, (B) Cluster 2, and (C) Cluster 3 *versus* the specific CO_2 mass. Symbols represent experimental data points and lines model predictions

3.3.3. Microstructural and geometrical factors

The determination of the microstructural factors depends on the selection of a geometrical factor with its corresponding specific surface (Eq. 3.13). Compacts fabricated in this work were highly uniform; in some cases resembled a slab ($D/H >> 1$), and in others a cylinder ($D/H << 1$), as observed in Table 3-2. Hence, instead of arbitrarily selecting a geometrical factor that could lead us to considerable error in the estimation of the effective diffusivity and *MF*, we chose to compare the resulting *MF* when assuming spherical, cylinder, and slab geometry. Instead of using a_p in Eq. (3.13) we decided to substitute a characteristic dimension corresponding to each of these geometries [$(S/V)_{slb}$, $(S/V)_{cyl}$, $(S/V)_{sph}$], which correspond to the specific surface of a sphere, infinite cylinder, and infinite slab (plane), respectively. For the calculation of $(S/V)_{sph}$, an average distance from the center of the compact to the surface (X_{sph}) was used. In case of cylinders, an average distance from the central axis of the compact to the surface (X_{cyl}) was used to compute $(S/V)_{cyl}$. Finally, in the case of slabs, and an average distance from the central plane (perpendicular to the axis) of the compact to the surface (X_{slb}) was used to compute $(S/V)_{slb}$. Appendix A details these computations.

The selection of the most appropriate geometry for the determination of *MF* was made based on the following criteria; under the assumption that the substrate is equal then when astaxanthin recovery is plotted against dimensionless time, then as observed and proposed by Ma and Evans (1968), of experimental data points would converge to a single line of tendency. The plots of all extraction curves for each of the four possible cases (spheres, cylinder, slabs, or a mix of cylinders or slabs), are presented in Figure 4-5 along with the best-fitted empirical tendency lines, Eq. (3.15), residuals, R-square, and *AAD*, which indicates the level of dispersion of the data. As R-square statistic increases, the residuals and *AAD* values decrease, as expected for the correlated variables. The lowest statistical dispersion corresponds to the case in which slab and cylinder geometries are selected based on the *D*/*H* ratio, which indicates that this assumption leads to the most accurate estimation of *MF* values.

Table 3-2: Estimated physical properties and best-fit parameters (95% confidence interval) of the broken- and intact cell model for the supercritical CO_2 extraction of astaxanthin from *H. pluvialis* compacts.

Compact code	D/H (-)	Sphericity (-)	a_p (m^{-1})	a_0 (m^{-1})	a_s (m^{-1})	K (-)	r (-)	k_s ($m/s \times 10^8$)	MF_{sph} ($\times 10^3$)	MF_{cyl} ($\times 10^3$)	MF_{slb} ($\times 10^3$)	$MF_{cyl/slb}$ ($\times 10^3$)
7.5.100	2.18	0.90	1075	544	380	0.033	0.42	3.36 (1.76-4.96)	3.9	4.9	3.8	3.8
7.8.200	1.42	0.93	901	469	327	0.033	0.42	2.60 (0.63-4.57)	4.2	4.0	4.5	4.5
7.8.400	1.48	0.93	915	473	330	0.033	0.42	3.44 (2.58-4.29)	5.4	5.3	5.7	5.7
5.8.25	0.85	0.93	1072	532	371	0.033	0.42	2.78 (1.2-4.36)	4.5	3.2	5.7	3.2
5.2.25	2.54	0.89	1607	799	671	0.033	0.23	12.5 (9.5-15.43)	8.8	13	8.6	8.6
3.2.25	1.54	0.87	2406	1237	1039	0.033	0.23	8.59 (6.8-10.38)	5.8	5.6	5.9	5.9
3.8.25	0.55	0.88	1622	822	691	0.033	0.23	9.1 (7.30-11.53)	13	6.8	18	6.8
3.2.50	1.97	0.99	2129	1113	935	0.033	0.23	19.3 (13.8-26.1)	11	12	10	10
3.5.25	0.82	0.93	1762	939	789	0.033	0.23	9.11 (7.2-11.04)	9.3	6.4	12	6.4
5.2.100	2.94	0.87	1714	825	575	0.033	0.39	7.13 (5.06-9.19)	4.3	7.1	4.2	4.2
5.2.400	3.38	0.85	1845	880	614	0.033	0.39	6.37 (4.61-8.14)	3.2	6.3	3.3	3.3
3.8.50	0.55	0.88	1624	794	554	0.033	0.39	5.64 (4.07-7.21)	7.5	4.1	11	4.1
3.2.100	1.99	0.92	2370	762	532	0.033	0.39	7.07 (5.21-8.93)	3.9	4.5	3.7	3.7

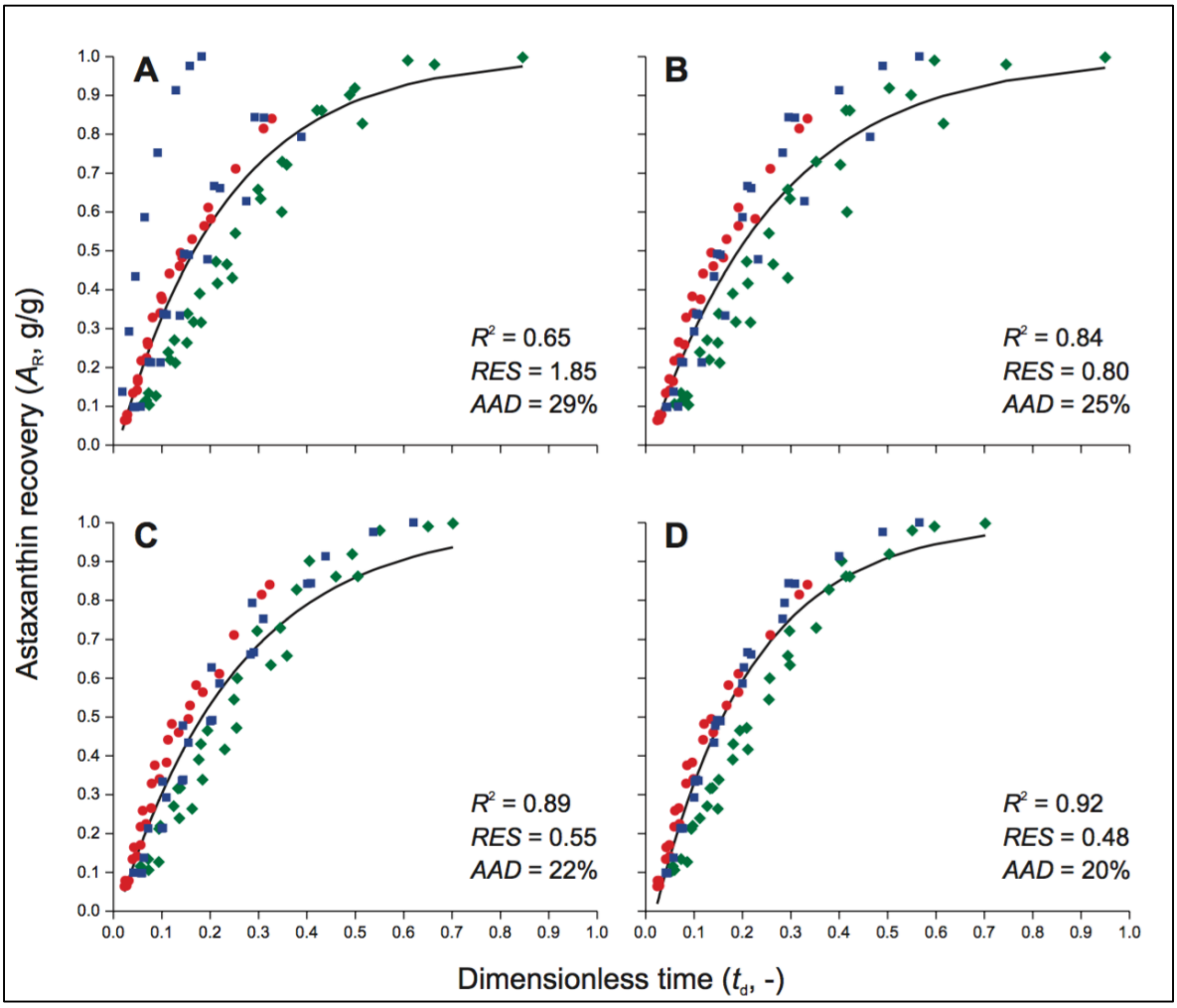

Figure 4-5. Astaxanthin recovery *versus* dimensionless time for assumedly (A) spheres, (B) slabs, (C) cylinders, and (D) cylinder/slab geometries for samples from (●) Cluster 1, (■) Cluster 2, or (◆) Cluster 3. For each data plot the residuals (RES), R-square statistic (R^2), and AAD.

Table 3-2 includes the *MF* determination for sphere, cylinder and slab geometries based on Eq. (3-13). When analyzing the variability between the *MF* of these three geometries it significantly deviates when the compacts *D*/*H* resemble a cylinder (*D*/*H* << 1) such as 5.8.25, 3.8.25, 3.8.50, and 3.5.25 or a slab (*D*/*H* >> 1) such as 5.2.25, 5.2.100, and 5.2.400, whereas when *D*/*H* nears 1 and the sphericity is above 0.9 there is low dispersion and agreement between *MF* values. When assuming spherical geometry, the resulting *MF*

values are in agreement with our initial hypotheses; compacts in Cluster 2 show significantly ($p < 0.01$) higher *MF* factors, consequently higher D_e, than those in Cluster 1 and Cluster 3, which do not significantly ($p > 0.01$) differ between them. An outlier is observed in cluster 2 (3.2.25), which has half the *MF* value of the group average. When assuming cylindrical geometry, *MF* values of compacts in Cluster 2 show a wide dispersion showing no significant difference ($p > 0.01$) with those in Cluster 1 and Cluster 3. Thus, in this scenario there are no microstructural differences between compacts regardless of compression parameters. Similarly, there are not significant differences ($p > 0.01$) in *MF* values between compacts in Cluster 1, Cluster 2, and Cluster 3 when adopting slab geometry. Moreover, two outliers can be observed in Cluster 2 and Cluster 3, which correspond to compacts that are conclusively cylindrical ($D/H << 1$ and sphericity < 0.9), supporting the idea of incorrect assignation of geometric factor. When assigning cylindrical geometry for compacts with $D/H << 1$ and slab geometry for those with $D/H >> 1$, compacts in Cluster 2 are significantly different from those in Cluster 1 or Cluster 3, confirming that it is possible to fabricate distinct microstructures by changing compression parameters, especially the compression pressure (Figure 3-3C).

3.4. Discussion

One objective of this research was to fabricate reproducible distinct microstructures by varying compression parameters of a HPC process. Because of the limited quantities we had of *H. pluvialis* powder we set out to fabricate a wide range of small samples of compacts. We hypothesized that the combination of compression parameters could produce:

1. groups of compacts that would have very similar microstructure but different macrostructural features such as volume, surface, or weight. The extraction kinetics of these compacts would be dependent solely on their size; consequently, as size decreases the overall interfacial area with the $scCO_2$ would increase with the end result of an increase in yield.
2. groups of compacts that would have very similar macrostructure but dissimilar microstructural features. These compacts extraction kinetics would be on average

very similar at the beginning of an extraction, however at longer extraction times when the internal mass transfer turns relevant, differences on the extraction yield would become apparent.

To identify these potential groups, we chose hierarchical clustering methodology because it can screen the characteristics of each compact type fast and efficiently so as to identify their patterns and similarities. This type of methodology requires prior knowledge of uncorrelated independent variables that define the compacts to be screened. We selected the specific surface of the compact as global indicator of its macrostructure, because it indirectly measures particle size and shape. In addition, the specific surface greatly influences the inner mass transfer coefficient of the compacts as attested by Eq. (3.12). On the other hand, a global indicator of the compact's microstructure was complicated due to the fact that it depends on several factors. An alternative is an estimate of *MF* as defined by Eq. (3.2). Because Wakao and Smith (1962) related the tortuosity of catalyst particles to the inverse of their porosity, *MF* can be re written only in terms of compact's porosity. Although a large body of empirical data does not sustain this relationship (Carniglia, 1986), porosity values could shed light on the microstructure of compacts. In compaction this could be particularly relevant since porosity is strongly influenced by compression pressure; as compression pressure increases so does compact's density, with a concomitant decrease in compact's porosity (Figure 3-1).

Figure 3-2 defines three main clusters based on the analysis of compact's porosity and specific surface. Distance between Cluster 2 and Cluster 3 is smaller than between them and Cluster 1; this was expected because most compacts from Cluster 1 come from using a large die with a large fill, whereas compacts in Cluster 1 and Cluster 2 are mostly small. A cut-off distance above 10 was selected given that we were interested in comparing gross differences between groups and the possibility of having a shared characteristic between groups that could facilitate our study. By conveniently selecting three big clusters we discovered that two of them shared on average the same ($p > 0.05$) porosity (Cluster 1 and Cluster 3), but also other two shared the same ($p > 0.05$) specific surface (Cluster 2 and

Cluster 3). Thus, by comparing Cluster 1 and Cluster 3 one can test hypothesis 1, whereas by comparing Cluster 2 and Cluster 3 one can test hypothesis 2.

Supercritical CO_2 extractions of *H. pluvialis* compacts confirmed our hypotheses. Extraction of compacts in Cluster 1 and Cluster 3 were significantly different, being yield higher for those compacts having larger specific surface (belonging to Cluster 3). However, there were not large differences in extraction between compacts in Cluster 2 and Cluster 3. This could mean that 4-h extractions are not long enough to show the effect of substrate microstructure on astaxanthin extraction from axially compressed *H. pluvialis*; instead, macrostructural (specific surface) differences dominate extraction rate and yield for short extractions. Extractions to exhaustion support this idea; 16 h were necessary to recover all astaxanthin in compact samples from either Cluster 1 or Cluster 2, whereas 8 h were enough for a compact sample from Cluster 3. Thus, mathematical modeling was necessary to ascertain the contribution of micro- and macrostructure features of compacts on the $scCO_2$ extraction performance in 4 h extractions.

The mathematical model of Sovová (2005) is very flexible, and this work contributed to its robustness by independent estimation of a large number of parameters. We reduced the number of parameters fitted to experimental data to reduce the degrees of freedom of the model. In addition to k_s, parameters K and r were fitted also to circumvent experimental difficulties to measure them. Nevertheless, because parameter K depends solely on extraction pressure and temperature (Urrego et al, 2015), a single value was fitted to all curves given that extractions were carried out at the same conditions (50 MPa and 40 ºC). On the other hand, although parameter r defines the ratio of broken to intact cells in a cellular tissue, in our case solute diffusion occurs in an interconnected pore matrix; hence, r represents the fraction of the porous matrix that contains easily accessible solute. We believe that, in case of HPC, the amount of easily accessible solute may depend less on the size than the density of compacts that is defined by the compression pressure (del Valle et al, 2003a). As compression pressure increases so does compact density and the extent of the cell disruption. Consequently, because compact density varies markedly between clusters we chose to fit cluster-dependent values of parameter r. Best-fitted values of r

support this claim; compacts in Cluster 2, which had the lowest density thus the lowest cell disruption, exhibited also the lowest value of *r* (Table 3-1 and Table 3-2). Further research should evaluate the extent of cellular disruption as a function of compression pressure or compact density. HPC had also an unpredicted side effect. Extractions to exhaustion showed that extractable solute c_u was considerably less for compacts in Cluster 1 than those in Cluster 2 and Cluster 3. This could suggest that during HPC (specially at high compression pressure) a fraction of the solute gets trapped in sections of the compact that $scCO_2$ cannot access (del Valle & Aguilera, 1989). This phenomenon may be size dependent because it was not observed for small compacts in Cluster 3, which were on average compressed at similar compression pressures.

Rigorous treatment of diffusion on solid particles in a packed bed has shown to depend on the shape or geometry of the particle (Villermaux, 1987). Solutions for well-known geometries such as infinite slabs, infinite cylinders, and spheres have been proposed, but because solid substrate particles do not comply normally with these geometries, many times an equivalent spherical geometry is assumed. Although, this may simplify the problem, it may bias results and produce misleading *MF* estimates. The ability to fabricate reproducible uniform geometries in this work opened the opportunity to test different assumptions about the geometric factor.

In an effort to find correlations for arbitrarily shapes for solutions in transient diffusion, Ma and Evans (1968) plotted extraction yields *versus* dimensionless time independently of the geometric factor and its internal diffusivity. It is expected that extraction curves, *ceteris paribus*, should collapse into one single extraction curve. This tendency is observed in general for all of our assumptions being the cylinder/slab scenario extraction curve that had the lowest statistical dispersion. Therefore, it was selected to estimate a geometrical factor. Interestingly, in all the cases compacts from Cluster 2 tended to be slightly separated from those from Cluster 1 and Cluster 3 (Figure 3-5). This difference could be attributed to the cell disruption that occurs during HPC, which would favor astaxanthin recovery from compacts in Clusters 1 and 3. It also supports the *r* parameter results in that Cluster 2 was observed to have almost half the value in

comparison to Cluster 1 and Cluster 3. As mentioned before, parameter *r* is directly related to the availability of the extractable compounds, hence higher compression pressures favor an astaxanthin recovery independently of its microstructure.

The results of this work have validated the use of HPC for the extraction of astaxanthin from *H. pluvialis*. This type of pretreatment not only improves the volumetric extraction yield as proven before (del Valle et al, 2003b), but it can be finely controlled so as to produce microstructures that will facilitate the extraction of natural compounds such as astaxanthin. High compression pressures showed to be a crucial factor in our experiments because, besides increasing compact's density and decreasing compact's porosity, they disrupted cell increasing parameter *r*, as inferred by mathematical modeling. Hierarchical clustering analysis grouped compacts allowing us circumventing the effect of many confounding factors influencing *MF*. Our selected experimental design allowed exploring the effect of geometry on *MF* estimates. Although further research is required to elucidate the properties of the *MF*, it is reasonable concluding that *MF* values relate on inner porosity for HPC pretreatments. However, (Crossley & Aguilera, 2001) showed that *MF* for biphasic systems does not depend only on the porosity but also on the architecture of the matrix. Thus, unevaluated microstructural features of the compacts, such as pore shape and interconnection, may partly explain the variability of our results. Further studies using enhanced resolution techniques such as micro-focus X-ray (*MF*X) tomography can be used to examine the full 3D structure of the interconnected pore network in compacts (Rigby, Fletcher, & Riley, 2004).

4. ADSORBENT-ASSISTED SUPERCRITICAL CO_2 EXTRACTION OF CAROTENOIDS FROM *NEOCHLORIS OLEOABUNDANS* PASTE

Abstract

Neochloris oleoabundans emerges as alternative source of bioactives that complies with the algae-based biorefinery concept, which consists of a platform that offers a multitude of algae bioproducts. The development of an integrated extractive processes in line with the green chemistry principles have motivated the use of Supercritical CO_2 ($scCO_2$), as an alternative to toxic organic solvents, for the extraction of bioactives. However, process integration and optimization is challenging because microalgae are grown in liquid cultures, therefore is often necessary a drying step prior to $scCO_2$ extraction. Moreover, this step is usually energy intensive and risks damaging the compound's bioactivity. An alternative is the simultaneous extraction process of the microalgae paste (containing around 70-80% water), nevertheless little information is available that explores this type of extraction. This work aims to explore the direct extraction of microalgae paste and to evaluate the effect of water on carotenoid extractions of *N. oleoabundans*. To study the extraction under a batch-wise system, an indirect extraction system was developed by mixing the microalgae paste with low cost adsorbents as support medium. Two types of silica gels, two different chitosans and active carbon were tested as adsorbents; sea sand was used as inert control. All of the materials showed different adsorbent capacity, being chitosan adsorbents those with higher capacity. However, oleoresin yield and recovery was negligible in a system with only $scCO_2$ as a solvent and ethanol as co-solvent was required to improve the extraction yield. Although the overall oleoresin recoveries were low for all adsorbents (ranging from 2 to 10 %), chitosan-assisted extraction showed the highest carotenoid recoveries (60-140% g/g) surpassing acetone benchmark extraction in case of chitosan microspheres. Different carotenoid selectivity was observed within the adsorbents, which can be attributed to its polarity.

These results are interesting for the development of low energy consumption processes, since there is no need to dry the microalgal paste.

4.1. Introduction

Microalgae consist of a wide range of autotrophic organisms, which grow through photosynthesis similar to land based plants. Their unique unicellular structure allows them to easily convert solar energy into chemical energy and a broad range of high-value bioactives with important applications in food, cosmetics, pharmaceutical, and biofuels (Cuellar-Bermudez et al., 2015; Harun et al., 2010; Spolaore et al, 2006b). Particularly, recent consumer trends for natural and healthy products have shifted the food industry to develop new food products enriched with functional ingredients such as carotenoids, which have been recognized for preventing human diseases and maintaining good health (Plaza et al., 2008; A. V. Rao & Rao, 2007).

In light of the algae-based biorefinery concept, which consist in the development of a platform that offers a multitude of different algae derived bioproducts (bulk chemicals, food products and ingredients, fertilizers, biofuels, etc.), from an optimized and integrated process, the microalgae *Neochloris oleoabundans* emerges as an attractive and alternative source of bioactives (Herrero & Ibáñez, 2015). This microalgae has a high-lipid productivity, for biofuels applications, and is a potential source of the carotenoids lutein and astaxanthin, for functional food applications (Urreta et al., 2014). The development of an integrated processes in line with the Green Chemistry Principles (Anastas & Warner, 1998) poses significant challenges to researchers in the design of new extraction processes to recover high-value compounds from natural sources. These requirements have motivated the use of supercritical (sc) carbon dioxide (CO_2) as an alternative to organic solvents because it is nontoxic, sustainable, and has versatile qualities (Valderrama & Perrut, 2003).

The development of scCO_2 extraction technology of high-value compounds for commercial application is a demanding task that involves process optimization (operating conditions, co-solvent use, and scale-up), substrate optimization (mainly drying processes and particle size adjustments by grinding and optional agglomeration), economic assessment of capital cost (purchase, installation, and start-up of a pilot to industrial supercritical fluid plant) and operational cost as extensively described by de Melo et al.

(2014) and del Valle (2015). In the case of microalgae, since they are grown in liquid cultures, it is often necessary a drying step prior to $scCO_2$ extraction. This step is usually energy intensive and it can be an important economic bottleneck for further process development (Crampon et al., 2013; Reddy et al., 2014; Taher et al, 2014). Moreover, drying may also have a negative impact in the bioactivity of the compounds due to its vulnerability to medium-to-high temperature (Rawson et al., 2011).

We are interested in exploring the concept of simultaneous extraction process, as described by Machmudah et al. (2011), of microalgae paste. This concept involves the extraction and separation process, where both water and $scCO_2$ extraction flow counter-currently or only $scCO_2$ flows while the aqueous suspension is static in the extractor. Since water is a polar substance, partitioning of compounds will depend on polarity; mass transfer mechanism of bioactives to $scCO_2$ will need to consider the presence of water during extraction.

Previous experiments done in the "Extraction Laboratory of Biological Material" (LEMaB acronym from the Spanish name) of $scCO_2$ extraction of *Haematococcus pluvialis* paste showed that temperature and the interaction between temperature and pressure were significant in astaxanthin extraction. As temperature increase from 40 to 70 ºC so did the astaxanthin yield under low (35 MPa) to medium (45 MPa) pressures. However, under high pressure (55 MPa) this relationship reversed. Pressure by itself played no significant role, while during extraction of dried *H. pluvialis* powder it did (Aravena, 2011). Although water affected negatively the solubility of oleoresin and astaxanthin in $scCO_2$, it was possible to achieve higher purities (~20% more at high pressure conditions) (Aravena, 2012). Kinetic studies showed a sigmoidal extraction curve in which water was extracted from the extractor during the first 4 hours; after this time, the extraction started behaving similar to dry powder extraction. To fully understand the extraction dynamics under the presence of water it is necessary to keep the water inside the extractor chamber. Since this phenomenon was inevitable in a batch-wise direct extraction system, an alternative is to use an indirect liquid extraction system which involves mixing the microalgae paste with support media prior $scCO_2$ extraction (Ramsey et al, 1998). We

propose the use of adsorbents that show high affinity with water and other polar substances. These adsorbents could also reduce the negative effect of water observed previously and/or favor extraction purities of bioactives.

Thus, the objective of this work was to assess the use of adsorbents during $scCO_2$ extraction of bioactives from *N. oleoabundans* paste. Particularly, we are interested in extraction of carotenoids and its selectivity towards different adsorbents. In light of a potential industrial or analytical application, the adsorbent selection criteria will consider to be low cost, easily available, and non-toxic.

4.2. Materials and methods

4.2.1. Samples and pretreatment

N. oleoabundans (UTEX#1185) was obtained from the culture collection of algae at the University of Texas (Austin, TX, USA). Batch cultures were grown in 20- cm-wide glass reactors containing 35 L of modified Bold's basal medium supplemented with 6 mM of KNO_3 and subjected to continuous stirring by bubbling air through the mixture at a constant flow rate. Pure CO_2 was supplied every 30 s at 10-min intervals to the air stream to provide inorganic carbon and to maintain the pH at 8. This was achieved using an electronic gas-control valve (Wilkerson R03-C2). Reactors were maintained in a culture chamber at 25 ± 2 °C, with a 16:8 h light:dark photoperiod using fluorescent light (Philips TLD 58 W) at a photosynthetic photon flux density of 300 μmol photons per square meter per second. After the cells had reached the late exponential phase, biomass was harvested by centrifugation (7,000 rpm for 5 min at 10 °C), frozen at −20 °C and stored under dry and dark conditions until further use.

Frozen *N. oleoabundans* paste was thawed at room temperature and cryogenically ground as described by Castro-Puyana et al (2013) with minor modifications: 28 g of microalgae paste was treated with three cycles of cryogenic grinding using a Retsch CryoMill mixer mill (Haan, Germany). Each consecutive cycle consisted of a precooling step (frequency 5/s for 2 min), grinding (frequency 20/s for 3 min), and intermediate

cooling (frequency 5/s for 1 min). The sample was withdrawn and stored at -20 ºC under dry and dark conditions until further use.

4.2.2. Analytical methods

As benchmark, conventional acetone extraction was carried out to determine the total extractable compounds in *N. oleoabundans* paste. The method used was the one previously reported by Castro-Puyana et al. (2013), with minor modifications. A sample of 200 mg equivalent microalgae substrate (0.7 cm^3 of microalgae paste) was mixed with 20 cm^3 of HPLC-grade acetone (LabScan, Gliwice, Poland) containing 0.1% (w/v) butylated hydroxytoluene (Sigma-Aldrich, Saint Louis, MO, USA) in a 50-cm^3 Falcon protected from light using aluminum foil. The mixture was shaken for 24 h in an agitated thermostatic bath (Selecta, Barcelona, Spain) operating at 500 rpm and 20 ºC. After extraction, the exhausted substrate was precipitated out in a refrigerated centrifuge (Hettich, Tuttlingen Germany) operating at 10000 rpm and 4 ºC for 10 min. Following centrifugation, the supernatant was collected, and solvent was removed by a gentle blow of technical N_2 as done for the extracts in $scCO_2$ extractions. Dry acetone extracts were weighed and stored at -18 ºC until further use. Benchmark extractions were quadruplicated.

HPLC analysis were performed in an Agilent HP 1100 Series (Palo Alto, CA, USA) apparatus equipped with a diode array detector (DAD) using the method of Castro-Puyana et al. (2013). Carotenoids separation was performed in a YMC-C30 reversed-phase column 250 mm length × 4.6 mm (inner diameter), 5-µm particle size (YMC Europe, Schermbeck, Germany). The mobile phase was a mixture of methanol, methyl terc-butyl ether (MTBE) both from from LabScan (Gliwice, Poland), and water purified using a Milli-Q system (Millipore Corporation, Billerica, MA). Solvent A, which was a mixture of methanol–MTBE–water (90:7:3 v/v/v), and solvent B, a mixture of methanol–MTBE (10:90 v/v), were eluted according to the following gradient: 0 min, 0% solvent B; 20 min, 30% solvent B; 35 min, 50% solvent B; 45 min, 80% solvent B; 50 min, 100% solvent B; 52 min, 0% solvent B. The flow rate was adjusted to 0.8 cm^3/min and the injection volume was 20 µL. Detection was at 450 and 660 nm with a recorded spectra between 240 to 770 nm by diode-array detection (DAD). Calibration curves were prepared using solutions in

acetone of lutein (ranging from 2.5 x 10^{-5} to 0.1 mg/cm^3), cantaxanthin (1.25 x 10^{-3} - 0.02 mg/cm^3) from Sigma-Aldrich (Saint Louis, MO), and astaxanthin monopalmitate (9.4 x 10^{-4} - 7.5 x 10^{-3} mg/cm^3) from CaroteNature (Lupsingen, Switzerland). Concentrations of astaxanthin esters were quantified as a whole from the standard calibration curve prepared
from astaxanthin monopalmitate. All analyses were done in duplicates.

4.2.3. Adsorbents characteristics

The adsorbent's superficial area and pore size were obtained from the data sheet of the manufacturers (Table 4-1). Sea sand (SS) from Panreac Quimica S.A. (Barcelona, Spain) was used as a reference because it is often employed as an extraction support to avoid caking in the extractor and also for its poor adsorbent capacity. Activated carbon (AC), high-purity grade silica gels of 60 Å (S60) and 150 Å (S150) pore size with same particle size (200-425 mesh) were obtained from Sigma-Aldrich (Saint Louis, MO, USA).

Chitosan scaffold (CS) and chitosan microspheres (CM) were kindly provided by the group "Chemistry and Functionality of Carbohydrates and derived products" from CIAL (http://www.cial.uam-csic.es/ Madrid, Spain). Details of its characteristics and fabrication are described in Diez-Municio, et al. (2011). A low-molecular-weight chitosan (150 kDa) with a deacetylation degree of 90% was used to prepare *CS*, instead a medium-molecular-weight chitosan (350 kDa) with an 85% deacetylation degree was used to prepare *CM*.

Table 4-1: Summary of the relevant adsorbents characteristics.

Adsorbents	Paste adsorbent capacity [g/g]	Superficial area [m^2/g]	Pore size [μm]
Sea sand (*SS*)	0.32 ± 0.015	*n.d**	*n.d**
Activated carbon (*AC*)	18.00 ± 3.17	500 - 600	4 - 12
silica gels of 60 Å (*S60*)	5.56 ± 0.77	480	60
silica gels of 150 Å (*S150*)	7.91 ± 0.68	300	150
Chitosan scaffold (*CS*)	103.05 ± 20.40	4	57
Chitosan microspheres *(CM)*	45.5 ± 7.14	111	57

The microalgae paste adsorbent capacity was measured experimentally with *N. oleoabundans* paste. Triplicate samples (1 g) of adsorbent were added into a pre-weighed flask, and then drops of thawed microalgae paste were added using a volumetric pipette similar as a titration procedure. The mixture was continuously weighed and manually

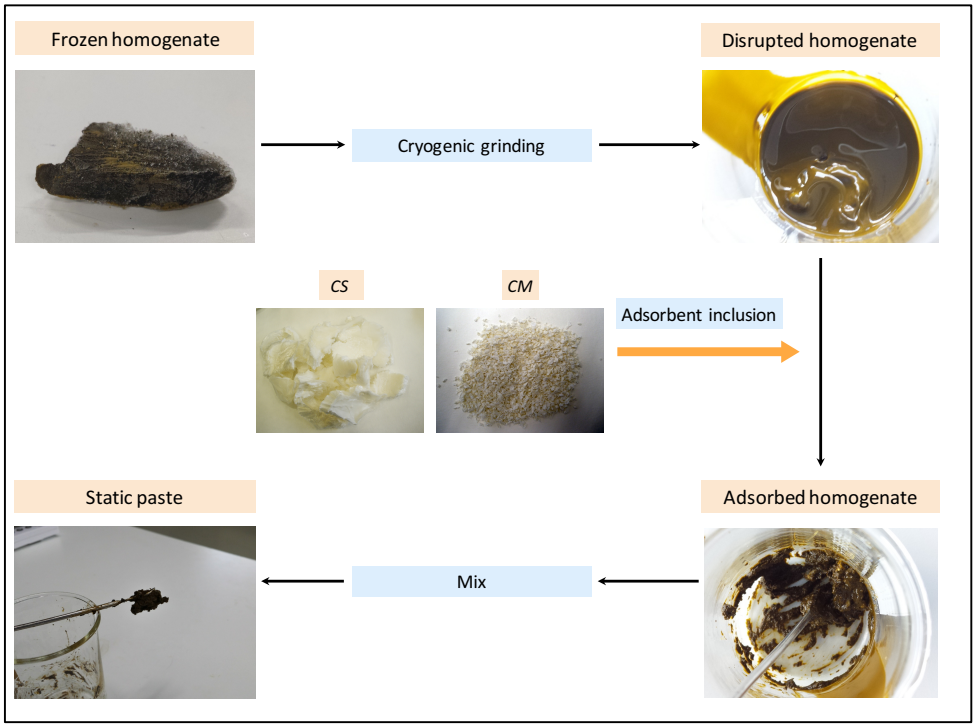

Figure 4-1: Sequential pretreatments for the production of a static microalgae paste from frozen microalgae paste. *CS* and *CM* (Chitosan Scaffold and Microspheres,

respectively) photographs are shown as examples in the adsorbent inclusion step.

stirred drop-by-drop until achieving a static paste (Figure 4-1). We assumed that the saturation of the adsorbent occurred when an increase of one drop cause the mixture to flow.

Water content was determined gravimetrically by drying in an oven WTB Binder (Tutlingen, Germany) (105 °C) to a constant final weight (24 h approximately). The moisture is expressed as a percentage in dry basis (d.b.). Solubility of water in CO_2 (S) is the weight fraction of water in CO_2 + water mixture. To analyze if the extracted water can be explained by its solubility or other phenomenon we calculated the water mass fraction (W_{H2O}) based on the consumed CO_2:

$$W_{H2O} = \frac{weight\ of\ extracted\ water}{weight\ extracted\ water + weigth\ of\ consumed\ CO_2} \quad , \qquad (4.1)$$

4.2.4. Supercritical fluid extraction

Supercritical CO_2 extractions were carried out in a PrepMaster supercritical fluid extractor from Suprex (Pittsburgh, PA). For experiments with only water and adsorbents, approximately 5 g of saturated adsorbents were added to the extraction cell. Then, extracted for 360 min at 40 MPa and 40 ºC with a constant mass flow rate (0.6 g/min) of technical quality CO_2 (Carburos Metálicos, Air Products Group, Madrid, Spain), which was adjusted at the exit of the extraction cell using two stop valves in tandem as a variable restrictor. The chosen extraction conditions correspond to the maximum allowable pressure by the equipment and a temperature which is not detrimental for carotenoids. For microalgae paste extractions, 2 g samples of *N. oleoabundans paste* were mixed with the required adsorbent to produce a static paste (Figure 4-1). The require adsorbent was calculated from the paste adsorbent capacity in Table 1, for example, 6.3 g of SS were required to produce a static paste. The mixture was then added into a 20 cm^3 stainless-steel extraction cell sandwiched between glass wool plugs at the entrance and exit of the cell to prevent plugging of tubing lines connected to the cell. Experiments using ethanol as a co-solvent (Panreac Quimica S.A., Barcelona, Spain) employed a PU2080 HPLC pump from Jasco (Tokyo, Japan) set at a volumetric flow rate of 0.06 g/min, which was equivalent to 10% (w/w).

The solvent mixture in the feed tubing was preheated to the extraction temperature in a thermostated bath. Extracts were collected in a Falcon that was cooled by immersion in dry ice. All experiments were done in duplicate and the extraction time was fixed at 120 min. Upon completion of each extraction experiment, ethanol and excess moisture were fully removed by a gentle flow of technical quality N_2 (Carburos Metálicos, Air Products Group, Madrid, Spain). Water recovery (expressed in g of extracted water/ g of total water) and Extraction yield (expressed in mg of oleoresin/g of dry extract) were determined gravimetrically by weighing the Falcon. Carotenoid content (expressed in mg carotenoids/ g dry extract) was calculated based on HPLC analysis of the extracts.

4.2.5. Statistical analysis

The statistical analysis for adsorbent-assisted extraction experiments was done by one-sided ANOVA using R software, version 3.0.3 (Team, 2014). "Boxplots" and "oneway test" functions were used to analyze data.

Table 4-2: Summary of the relevant adsorbents characteristics.

	Sea Sand extraction	Active Carbon extraction
Extraction Yield [%]	84.9 ± 7.1	28.78 ± 10.6
$Moisture_{initial}$ [%] *d.b*	23.7 ± 0.7	71.9 ± 2.1
$Moisture_{final}$ [%] *d.b*	2.5 ± 0.9	64.5 ± 1.1
W_{H2O} [g/g] *1000	7.1 ± 2.4	1.4 ± 0.49

4.3. Results and discussion

To understand the mechanisms involved in the extraction of different substances from biological matrices and its interaction with adsorbents, it is necessary to test how the system works in absence of the biological substrate; with this information it is possible to focus only on water extraction/dynamics. These preliminary results will be shown first, followed by the extraction of microalgae paste with adsorbents and its analysis.

4.3.1. Water extraction dynamics

We tested two extraction systems: water and Sea Sand (SS), and water and Active Carbon (*AC)*. In one hand, *SS* was selected because of its poor adsorbent capacity to act as a control system; on the other hand, *AC* was chosen because of its high adsorbent capacity (although significantly lower than chitosan adsorbents, *CS* and *CM).* The water extraction yield in a SS system was significantly greater than in a AC system (duplicate experiments): almost 85% water recovery was attained at 6 hours of extraction when using SS compared to 29% obtain when using AC (Table 4-2). These results correlate with the adsorbent capacity; since SS has a lower adsorbent capacity it retains less water thus yielding a greater water recovery instead of AC. When taking in account all the extracted water and the specific CO_2 consumption, the water mass fraction significantly exceeded (7.1×10^{-3} g/g) the theoretical water solubility on CO_2 at our experimental conditions (3.0×10^{-3} g/g) (value obtained by linear regression of the solubility data of water in CO_2 from Sabirzyamov et al. (2002) at 40 ºC, predicted for 40 MPa). This result implies that not only solubility is responsible for the water extraction, but that also water is dragged from the extractor due to the solvent flow. However, this is not observed in *AC* extractions system. Due to its strong adsorbent property, the small water yield could mainly be attributed to the equilibrium phenomenon, therefore to its solubility.

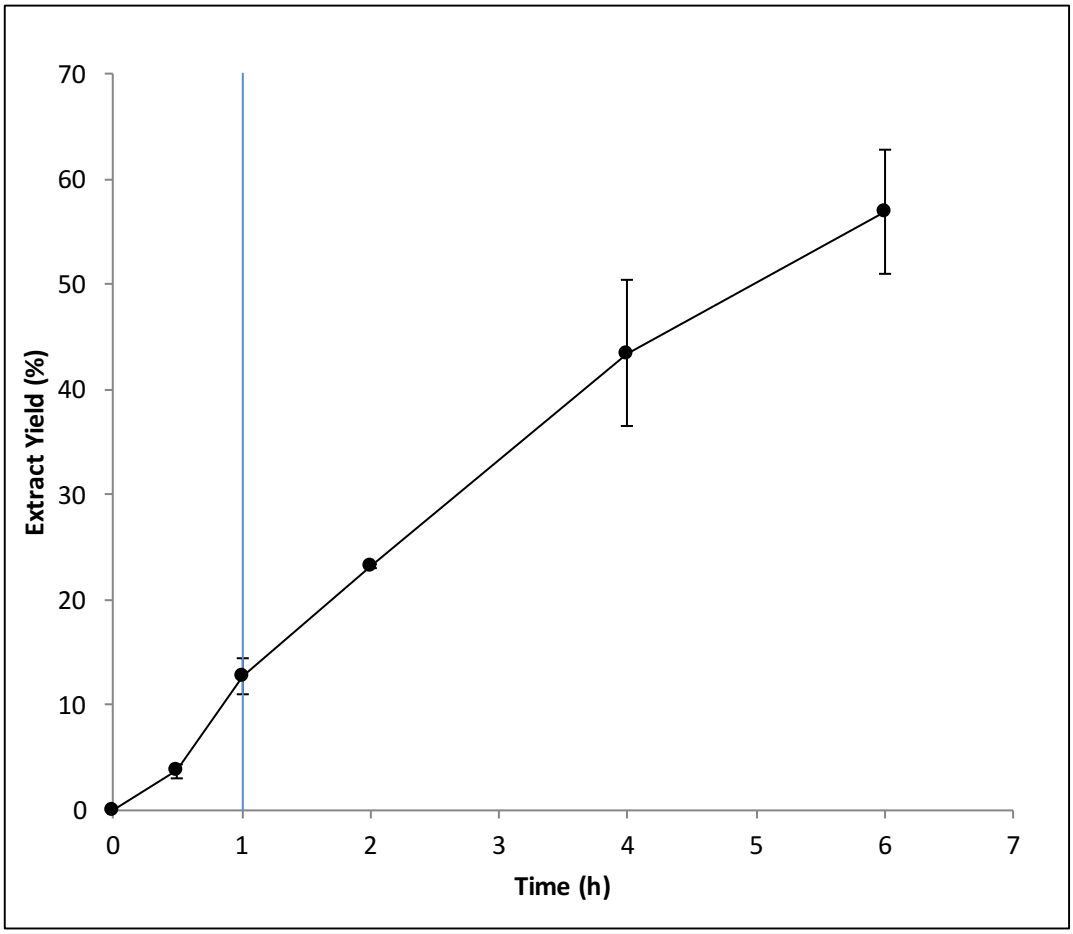

Figure 4-2: Representative extraction curve for static sea sand paste of *N. oleoabundans*. Straight line indicates the lagged portion of the extraction.

The shape of the extraction kinetics can shed light in the phenomena occurring during the extraction process. Preliminary kinetic extraction with microalgae paste *SS* extraction system showed a sigmoidal curve (Figure 4-2) similarly as describe by Aravena (2011) for *H. pluvialis* paste. This pattern was representative because it was also observed for other extraction kinetics and systems and not just for water and adsorbent. Sigmoidal curves have been described for extraction systems in which more than two phases are present, such as those including co-solvent extraction (Cocero & Garcia, 2001).

Cocero and García (2001) proposed that this initial delay (lagged portion of the curve in Figure 4-2), that consequently results in an S-shape kinetic, is strongly related to an adsorption/desorption process followed by a constant extraction rate which eventually declines as the solute is depleted. In our case, this is true for our extraction system: since water is only adsorbed, the limiting mass transfer mechanism is desorption. Moreover, water has very small solubility in CO_2 so when extracted part of it is re-adsorbed as CO_2 flows through the extractor eventually reaching equilibrium observed when entering a constant extraction rate after 1 hour of extraction. Despite Figure 4-2 kinetics involved a microalgae paste, the oleoresin fraction was not detected by our analytical weight. We concluded that virtually only water was extracted during 6 hours. Further experiments with *AC* extraction system showed again no oleoresin extract. These facts lead us to pursue a co-solvent extraction system with ethanol to increase solubility of the oleoresin fraction in $scCO_2$, thus increasing the extraction yield. Janda et al. (1996) claimed that since non-polar substances would not solubilize in water, theoretically they would be readily available for extraction by $scCO_2$. However, our substrate is hygroscopic and strongly binds water (Reyes et al, 2015b) and, in addition, microalgae paste water content is typically very high (~75 % wet basis) when fresh from a previous harvesting step (Crampon et al., 2011). Hence, water completely occludes non- polar substances hindering their extraction. Under this scenario, their extraction, on one hand, will depend on their transport from the substrate through the water phase into the $scCO_2$ phase, which would be very slow due to their marginal solubility in water. On the other hand, the extraction would be favored when sufficiently water would be extracted and/or dragged from the extraction mixture. The latter case will not be useful when extracting a continuous microalgae paste phase such as in a countercurrent solvent extraction.

4.3.2. Adsorbent assisted extraction

As described by Ramsey et al. (1998), a direct liquid-scCO$_2$ extraction has the advantage of its simplicity, but requires an equipment able of supporting fixed extraction volumes. Indirect liquid scCO$_2$ extraction is advantageous for microalgae paste samples because it can be adapted to systems typically used for dynamic extraction of solids, thus avoiding paste wring in the equipment pipeline when loading in the extraction cell. Additionally, one can choose the support medium, in our case adsorbents, that can be tailored to improve solute recovery. This is the main reason for us to explore commercially available and low cost adsorbents such as active carbon (*AC*), silica gel (*S60* and *S150*), and chitosan derivatives (*CS* and *CM*).

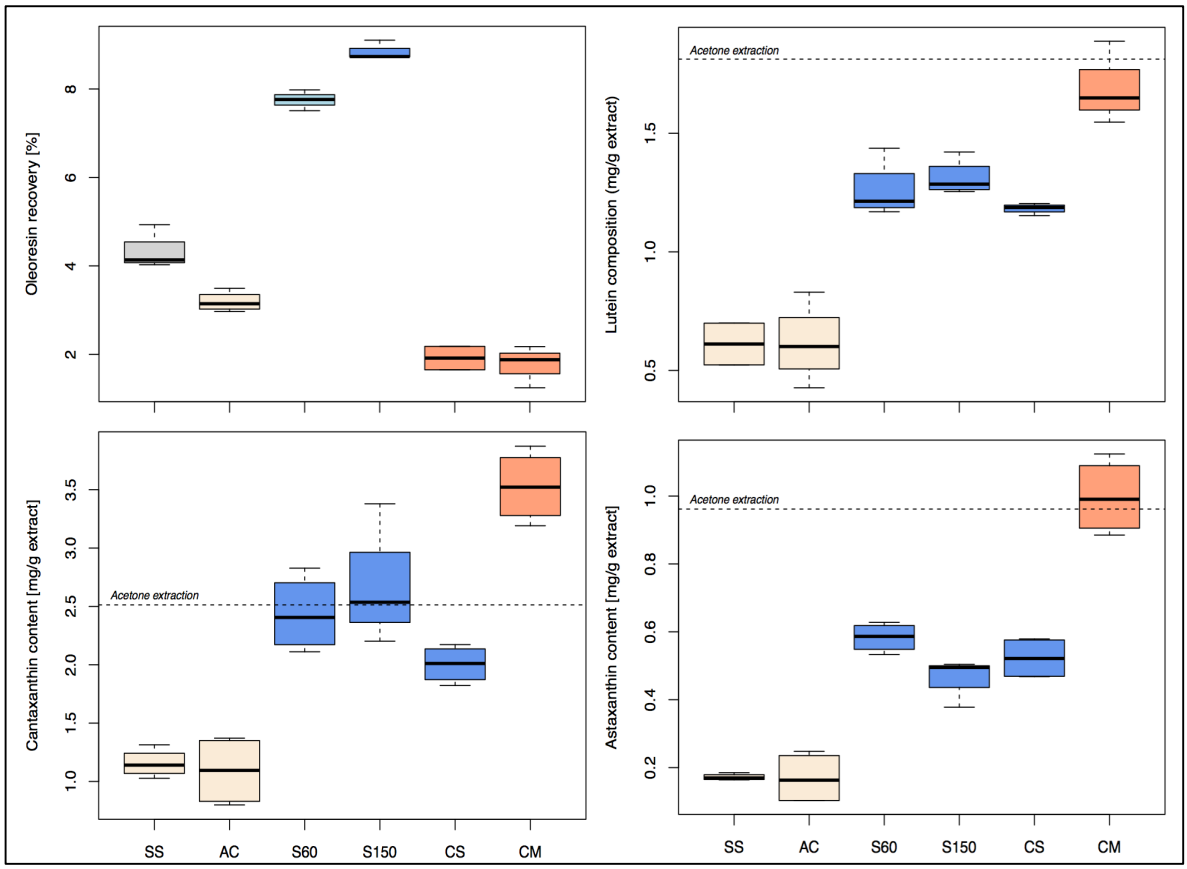

Figure 4-3: Oleoresin recovery and carotenoid content boxplots. Segmented line in carotenoids box-plots indicate the total extractable compounds by acetone extraction. Differences in colors of boxes indicate statistical significance ($p < 0.05$).

For clarity the following results and analysis are focused on the extracts of adsorbent-assisted extractions. For instance, a higher yield of adsorbent 1 with respect to adsorbent 2 means that the latter retains the extract stronger than the former.

Adsorbent assisted $scCO_2$ extraction of microalgae paste showed a small oleoresin recovery (Figure 4-3) with an average maximum of 8.85 ± 0.22 % of total oleoresin, which corresponded to an average oleoresin yield of 32.4 ± 0.79 mg/g of dry microalgae, for S150. The lowest extraction recovery was obtained when chitosan adsorbents were used with an average of 1.87 ± 0.41 % of total oleoresin (6.84± 1.52 mg/g of dry microalgae). Although chitosan adsorbents had a significant difference in their paste adsorbent capacity (Table 4-1), there was no significant difference ($p > 0.05$) between oleoresin recovery of both chitosan-assisted extractions. Differences may become apparent when analyzing the content of the extracts, which is going to be analyze in the next section. Besides the use of chitosan adsorbents, the rest of the adsorbent's oleoresin recovery showed significant difference ($p < 0.05$) between each other having an overall small standard deviation. Since *SS* is an inert material it does not truly act as an adsorbent, the small adsorbent capacity is mainly related to capillary sorption in the packed bed. Moreover, *SS*-assisted oleoresin recovery serves as a reference system in which the extraction dynamics will be dependent primarily in $scCO_2$-ethanol-water mixture. Consequently, adsorbents, which show statistically lower oleoresin recoveries, are indicative of the adsorbent effect. Indeed, this is the case of *AC* and chitosan adsorbents, which show a greater adsorbency towards oleoresin and water. Silica adsorbents, on the other hand, are an outlier of this relationship (~ 8% oleoresin recovery) thus there will be discussed separately.

Figure 4 shows representative chromatographic profile of the extract obtained by HPLC-DAD. Three mayor carotenoids were identified as indicated by their respective molecular structure: cantaxanthin, lutein, and free astaxanthin (mono- and diesters are related to their –OH radicals having decreasing polarity compared to free astaxanthin). Figure 3B-D also shows the extraction content of each of these carotenoids with respect to acetone extraction, which is considered 100%.

It is interesting to observe that *CM*-assisted extraction resulted in extracts that had the highest content for the three carotenoids, being equivalent to acetone extracts for lutein (2 mg/g) and astaxanthin (1 mg/g), but superior in cantaxanthin (1.4 times acetone cantaxanthin content). The trio S60, *S150* and *CS* followed *CM*-assisted carotenoid content and finally *AC* and *SS*, which produced extracts that had the lowest carotenoid content. On average, *CM*-assisted extraction content was 1.68 ± 0.14 mg/g, 3.53 ± 0.31 mg/g, 1.00 ± 0.11 mg/g for lutein, cantaxanthin and astaxanthin respectively. For *S60*, *S150* and *CS* assisted extractions it was 1.25 ± 0.09 mg/g, 2.37 ± 0.43 mg/g, 0.50 ± 0.09 mg/g for lutein, cantaxanthin and astaxanthin respectively and for *AC* and *SS,* 0.61 ± 0.13 mg/g, 1.12 ± 0.22 mg/g, 0.17 ± 0.05 mg/g for lutein, cantaxanthin and astaxanthin, respectively.

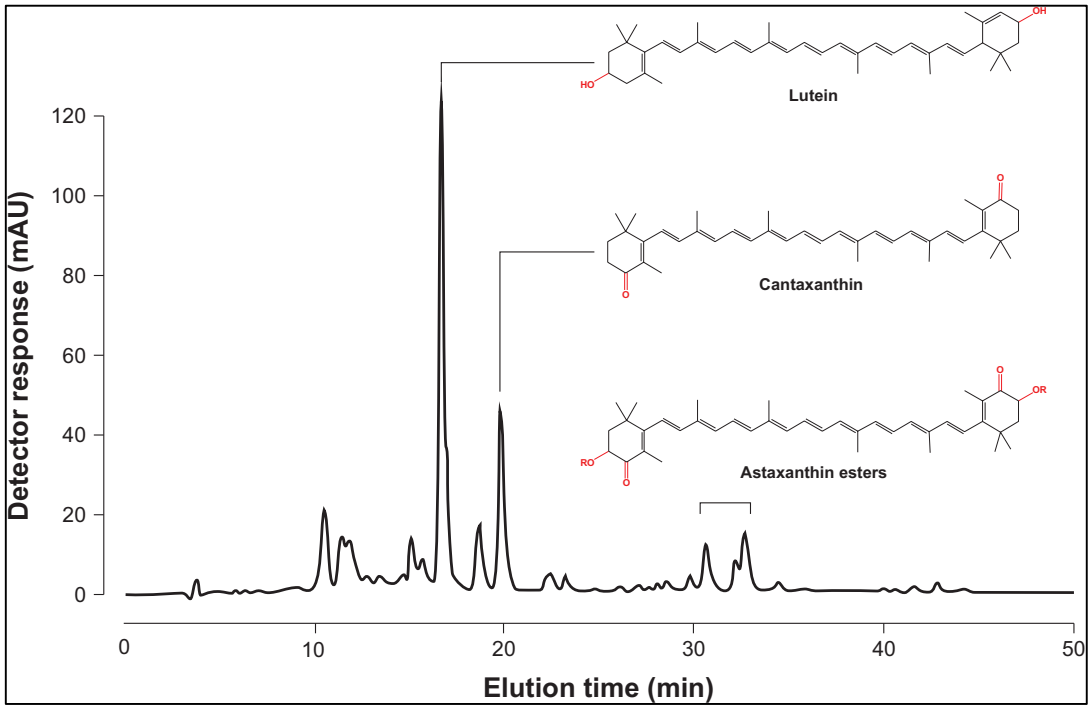

Figure 4-4: Representative HPLC-DAD chromatogram of *S60* assisted $scCO_2$ extraction of N. oleoabundans. Mayor carotenoid peaks are identified (480 nm) with their representative molecular structure from ChemSpider database (Pence & Williams, 2010)

Although *CM*-assisted extractions showed the lowest oleoresin recovery (2%), its extracts were enriched in carotenoids, similarly to acetone extracts, when compared to the rest of the adsorbents. The differences between the carotenoid content when using different adsorbents can be related to the nature of each, thus to its functional groups.

AC is a widely used adsorbent in water treatment, because of their wide spectrum adsorption on organic compounds (Pollard et al, 1992), particularly the near perfect adsorption ability for low-molecular-weight organic compounds such as phenols (Dabrowski et al, 2005). Thus, it is expected to adsorb the organic and water content present in the microalgae paste with variable ability depending on their polarity, molecular weight and size (Dabrowski et al., 2005). Functional groups that have been long identified for its adsorptive capacities are mainly carbon groups such as C-C, C-H, C=O, and possibly C-O-C (Mattson et al, 1969). It is interesting to observe that, although *AC*-assisted extraction had extracts with lower oleoresin recovery (3.7%) than when using SS (4.3%), there is no statistical difference ($p > 0.05$) in their carotenoids content (Figure 4-3). AC may adsorb other compounds, preferentially of smaller molecular weight, with greater strength instead of carotenoids. Hence, compared to *SS* the extract is enriched. On the other hand, chitosan is highly reactive because of its amine groups that confer it cationic characteristics, thus allowing an interaction with negatively charged molecules (Brugnerotto et al., 2001; Díez-Municio et al., 2011). Therefore, chitosan will be less likely to adsorb low-polar compounds such as carotenoids than *AC*, possibly explaining the higher carotenoid content (over 3 times *AC*-assisted concentration). Similarly, to *CM* but in a lower degree, *CS* shows a relatively high overall carotenoids content, when compared to *AC*-assisted extractions (over twice its content). Differences between *CS* and *CM* are related to their production methodology; *CM's* showed to be spherical with rough and compact surface, instead *CS* consisted on leafs that are uniformly distributed in layers presenting a very high porous structure (Díez-Municio et al., 2011). Scanning electron microscopy studies of the fabricated chitosan done by Díez-Municio et al. (2011) showed that although chitosan adsorbents showed the same pore size they had a substantial difference in pore morphologies. Particularly, *CM* structure allowed its functional groups easily accessible, this was confirmed by Díez-Municio et al. (2011) when $scCO_2$

impregnation studies of lactulose in these adsorbent showed to be faster in *CM* than in *CS*. Hence, a greater rejection of the polar groups towards the lipophilic carotenoids can be expected in *CM* than in *CS*. On the other hand, chitosan adsorbents change its structure in presence of water, which is not the case for the rest of the adsorbents use. Therefore, structural changes (swelling) are expected to occur during extraction that could affect the separation of compounds within the microalgae paste.

The presence of water in the microalgae paste seems to hinder significantly the extraction yield and carotenoid content as observed in *SS*-assisted extractions. However, silica-assisted extractions showed almost twice oleoresin recoveries despite having greater adsorbent capacity than *SS*. A possible explanation is that silica adsorbents bind preferentially water over oleoresin, allowing a greater availability of the oil fraction to the $scCO_2$-ethanol mixture. A greater pore size such as in *S150* (150 Å *vs* 60 Å) could allow greater access to its adsorbent surface even though having lower superficial area than *S60*. This is reflected in its adsorbent capacity (Table 1), thus a greater oleoresin recovery can correspond to this phenomenon in which an increase adsorbent capacity relates to increase oleoresin availability. Silica-assisted extractions in accordance to their oleoresin recovery have proportionally higher carotenoid content equivalent to carotenoid content obtain with *CS* (1.2, 2.5 and 0.5 mg/g for lutein, cantaxanthin and astaxanthin respectively). Nevertheless, *CS*-assisted oleoresin yield is substantially lower than silica-assisted extractions, which means that the purity of the carotenoid content when using *CS* is significantly higher than silica adsorbents. When comparing the carotenoid content of silica-assisted extractions there is no significant ($p > 0.05$) difference between them, thus differences in adsorbent capacity and pore size does not affect the carotenoid extraction directly, whereas it did when observing the oleoresin yield (4 times the oleoresin recovery of CS-assisted extractions), thus supporting the evidence towards its selectivity towards water.

4.4. Conclusion

This work has explored the use of adsorbents to improve the extraction of carotenoids from microalgae paste of *N. oleoabundans*. Preliminary works in water extraction showed that kinetic curves present an initial delay associated with desorption/adsorption process during the extraction. Water is observed in the extract and its extraction process is explained by its marginal solubility in $scCO_2$ phase, but also by its dragging with the solvent phase. Oleoresin yield and recovery was negligible in microalgae paste $scCO_2$ extraction, since water acted as a strong barrier to mass transfer when working with a high moisture substrate. Consequently, ethanol was needed as a co-solvent to improve the extraction yield by increasing the solubility of the oleoresin in ethanol and $scCO_2$.

Adsorbent assisted $scCO_2$ co-solvent extraction of microalgae paste showed low overall oleoresin recoveries with an average maximum for silica adsorbents. Interestingly, when using chitosan microspheres, the extracts showed the highest carotenoid content, equivalent to acetone extraction, whereas having the worst oleoresin recoveries. Similar selectivity was observed but in a lower extent when using chitosan scaffolds. Selectivity seems to be related to the adsorbent's functional groups. Chitosan adsorbents have higher polarity than, for example, active carbon. Thus, chitosan adsorbents are less likely to retain carotenoids favoring smaller and more polar substances' retention. Further research will be required to elucidate the interaction and partition of substances between the tested adsorbents. Although results are far from being applicable at industrial scale (low extraction yields), the knowledge of the mechanisms involved in adsorbent assisted $scCO_2$ co-solvent extraction open the door to more specific studies involving the selection of selective adsorbents for high added value compounds embedded in matrices with medium water content.

5. CONCLUSIONS AND PERSPECTIVES

Solving the issue of caking is an important step forward the development of new green separation processes from microalgae derived bioactives. This thesis proposed two technological alternatives with the objective of improving the $scCO_2$ extraction of high-value compounds, such as carotenoids from microalgae, by avoiding caking phenomenon. These two alternatives consisted in High Pressure Compaction (HPC) of the microalgae powder as a pretreatment before $scCO_2$ extraction and direct-extraction of the microalgae paste. This thesis addressed mayor constrains relating each of the alternatives. On one hand, the key constrain in HPC is how can we fabricate reproducible compacts that have a favorable microstructure for the $scCO_2$ extraction of carotenoids. On the other hand, evaluating the effect of water during the extraction of microalgae paste of carotenoids is a key aspect that can validate the use of this alternative. The conclusions of this work will be shown in accordance of the objectives ending with a global conclusion taking in consideration what was learned and its perspectives.

First, the thesis explored the problem of caking of microalgae powder using as a model *H. pluvialis* (*Paper 1*). This microalga was selected because of the relevance and potential it has in the Chilean industry. This work was a requirement before studying HPC because water not only favors caking but also affects the mechanical behavior during HPC. This thesis developed an easy, fast and simple method to characterize hygroscopic powders destined for HPC. This method took advantage of the mechanical phenomenon called pressure-induced squeeze flow, which changed in presence of different water content. By comparing these results with the water sorption isotherm and differential scanning calorimetric analysis we found out that this change in squeeze-flow behavior was strongly related to the glass transition temperature (T_g). Thus, as water content increases it decreases T_g favoring squeeze-flow behavior at lower compression pressures. Pressure-induce squeeze flow behavior sets a limit of the applied compression pressure during HPC; if water content increases the range of compression pressures gets narrower. This thesis proposed that water content for HPC of *H. pluvialis* must not be over 11.9% (d.b), to avoid stickiness problems during the loading of HPC, and to have a minimum working range of

200 MPa of compression pressures. Recommendations were also proposed to avoid the risk of caking during the $scCO_2$ extraction of *H. pluvialis* powder. The thesis proposes a 5% (d.b) or lower water content to be able to comfortably extract between 40-50ºC. This recommendation is only useful when HPC is not possible. However, to achieve lower water content it is necessary a complimentary drying, which is usually undesirable.

Findings in *Paper 1* lead to design a HPC methodology based on uniaxial compaction of the powder in a process similar to tableting. Following the recommendations of the previous work, the experiments of *Paper 2* were done at very low water content near its monolayer water content (3.67% d.b). One interesting results was that high compression pressures (100-400 MPa) compacts did not extract differently from low compression pressure compacts, even though compacts produced at high compression pressures showed low particle porosity. Further research took advantage of clustering analysis to group compacts, based on its specific surface and particle porosity, to improve the mathematical modeling of the extraction of compacts. This methodology in combination with Sovová broken-and-intact cell model proved to be crucial in elucidating confounding factors that influenced the microstructural factor (*MF*), which is a relevant parameter in $scCO_2$ extraction of bioactives. This worked showed that high compression pressures correlated with low particle porosity, and thus low *MFs*. Nevertheless, high compression pressures increased the parameter *r*, which is the fraction of broken cells in Sovová's model, inferring that a cell disruption was favored under these conditions. This finding explains the reason because high compression compacts extracted the same as low compression compacts; a higher fraction of broken cells increase the availability of the solute consequently increasing its yield. This work led to the development of a pending patent application (*Paper 4*) where it describes a novel tableting process for the production of compacts, at laboratory and pilot scale, for $scCO_2$ extraction of carotenoids from dry microalgae powder (Reyes et al., 2013). This thesis recommends the use of high compression pressures (> 100 MPa) and small size compacts (specific surface over 1500 $1/m^{-1}$) to favor the extraction of bioactives, such as astaxanthin from *H. pluvialis*, when using $scCO_2$.

Water has been shown to be a strong barrier to mass transfer of lipophilic bioactives (*i.e* carotenoids) when extracting high moisture substrate, for instance, microalgae paste. Preliminary experiments in LEMaB have confirmed this, however the results have been confounded because water is co-extracted and hence the substrate is dried during the extraction. Looking forward for a commercial production of bioactives from pastes using $scCO_2$ an excellent alternative is using continuous countercurrent extraction in columns. Under this scenario the $scCO_2$ is continuously contacted with fresh microalgae paste, therefore this thesis emphasized the need to evaluate the water effect in the extraction by avoiding its co-extraction or elimination from the extraction system. In *Paper 3* we proposed a scale-down batch-wise system were the microalgae paste is statically placed, whereas CO_2 flows upward through the extractor. To achieve this, we made use of an indirect liquid extraction system, which consisted in using adsorbents to assist in loading and extraction of the microalgae paste. Early findings showed that water hinders significantly the extraction yield of carotenoids from *N. oleoabundans* paste (a carotenoid rich microalgae). For example, extraction experiments with active carbon (*AC*) and silica gel adsorbents (*S60* and *S150*), which are known to bind water, had virtually no oleoresin extraction. Only water was extracted when using sea sand (*SS*), which was used as a reference due to its poor adsorbent capacity. In light of these results there is no evidence that supports the use of microalgae paste for the extraction of bioactives with only $scCO_2$ as a solvent. Ethanol as a co-solvent was used to increase the polarity of the solvent mixture and favor oleoresin extraction in presence of a high moisture substrate. Nevertheless, oleoresin recoveries were overall low for all adsorbents being chitosan adsorbents (*CM* and *CS*) the lowest (~ 2% recovery). Still chitosan microspheres (*CM*) show promise in the area of analytical experimentation; *CM* had a higher selectivity towards water thus increasing the oleoresin availability an its extraction. Particularly, it achieved the highest carotenoid content equivalent to the conventional acetone extraction (~5.5 mg/g of extract). To the author knowledge, this is the first work that used adsorbent-assisted system for the extraction of carotenoids from microalgae paste. This study opens the door to new types of extraction studies involving high moisture substrate for the extraction of high valued compounds. The use of adsorbents adds another dimension of

possibilities during the extraction which take advantage of the selectivity towards the compounds present within the substrate. Future work could focus in understanding the use of different types of co-solvent and adsorbents, with their respective interactions, in the extraction of bioactives from high moisture substrates.

This thesis showed that although both alternatives avoid caking phenomenon, only HPC is an improvement over the powder extraction. The process and technology developed in this thesis validated the use of HPC for the production of astaxanthin from *H. pluvialis* with promising industrial applications.

NOMENCLATURE

AC	active carbon
a_0	specific surface area per unit volume of extraction bed (m^{-1})
a_p	specific surface area per unit volume of solid (m^{-1})
a_s	specific area between the region of intact and broken cells (m^{-1})
a_w	water activity
CM	chitosan scaffold
CS	chitosan microspheres
c_u	initial solute concentration in the substrate (kg kg^{-1} solute/solid)
D_{eq}	equivalent Sauter diameter (m)
D_{12}	binary diffusion coefficient of solute in SC-CO_2 (m^2 s^{-1})
D_e	effective diffusivity of solute in the solid matrix (m^2 s^{-1})
D	compact's diameter (m)
H_b	extraction bed length (m)
H	compact's height (m)
J_f	dimensionless flux from broken cells to solvent (-)
J_s	dimensionless flux from intact cells to broken cells
k_f	fluid-phase mass transfer coefficient (m s^{-1})
k_s	solid-phase mass transfer coefficient (m s^{-1})
K	partition coefficient
MF	microstructural factor (-)

MRE mean relative error

n number of mixers in series (–)

N substrate charge in the extractor (kg)

r volumetric fraction of broken cells in the particle

SS sea sand

S60 silica gels of 60 Å

S150 silica gels of 150 Å

$(S/V)_{cyl}$ specific surface of an infinite cylinder calculated based on $X_{cylinder}$

$(S/V)_{slb}$ specific surface of an infinite plane calculated based on X_{slab}

$(S/V)_{sph}$ specific surface of a sphere calculated based on X_{sphere}

t_d dimensionless extraction time defined in Eq. (3-16) (-)

T_g glass transition temperature

t_r ($= H_b/U$) residence time of the solvent in the extraction bed (s)

U interstitial fluid velocity (m s^{-1})

V_b total volume of extraction bed (m^3)

W water content in a dry basis

x_1 concentration of solute in broken cells (kg kg^{-1})

x_{10} initial concentration of solute in broken cells (kg kg^{-1})

X_1 ($= x_1/x_{10}$) dimensionless concentration of solute in broken cells (-)

x_2 concentration of solute in intact cells (kg kg^{-1})

x_{20} initial concentration of solute in intact cells (kg kg^{-1})

X_2 (= x_2/x_{20}) dimensionless concentration of solute in intact cells (-)

X_{cyl} average distance from the compacts central axis to the surface (m)

X_{slb} average distance from the compacts central plane to the surface (m)

X_{sph} average distance from the compacts center to the surface (m)

y fluid phase concentration (kg kg^{-1} solute/CO_2)

y_0 initial fluid phase concentration (kg kg^{-1} solute/CO_2)

Y (= y/y_0) dimensionless fluid phase concentration (-)

Y^* dimensionless equilibrium fluid phase concentration (-)

Greek Letters

ε_b bed porosity (-)

ε_p compact's porosity (-)

Φ dimensionless extraction yield (-)

Γ initial solute distribution between solvent and broken cells (-)

ν geometrical factor (-)

μ viscosity of $scCO_2$ (Pa s)

Θ_e dimensionless external mass transfer parameter (-)

Θ_i dimensionless internal mass transfer parameter (-)

ρ density of $scCO_2$ (kg m^{-3})

ρ_b bulk density of $scCO_2$ (kg m^{-3})

ρ_s compact's density (kg m^{-3})

ρ_t compact's true density (kg m^{-3})

τ dimensionless time (-)

τ_p particle tortuosity (-)

REFERENCE

Acién Fernández, F. G., Fernandez-Sevilla, J. M., & Molina Grima, E. (2013). Photobioreactors for the production of microalgae. *Reviews in Environmental Science and Bio/Technology*, 12(2), 131–151.

Aguilera, J. M. (1999). Revision: Extraccion con CO_2 a alta presion. Fundamentos y aplicaciones en la industria de alimentos. *Food Science and Technology International*, 5(1), 1–24.

Aguilera, J. M., & Stanley, D. W. (1999). Microstructural principles food processing and engineering. Gaitherburg, *MD: Aspen Publishers, Inc*.

Aguilera, J. M., del Valle, J. M., & Karel, M. (1995). Caking Phenomena in Amorphous Food Powders. *Trends in Food Science & Technology*, 6(5), 149–155.

Aguilera, J. M., Levi, G., & Karel, M. (1993). Effect of water content on the glass transition and caking of fish protein hydrolyzates. *Biotechnology Progress*, 9, 651–654.

Ambati, R. R., Phang, S. M., Ravi, S., & Aswathanarayana, R. G. (2014). Astaxanthin: sources, extraction, stability, biological activities and its commercial applications--a review. *Marine Drugs*, 12(1), 128–152.

Anastas, P. T., & Warner, J. C. (1998). *Green Chemistry: Theory and Practice* (pp. 25-59). New York: Oxford University Press.

Aravena, R. (2011). Extracción de astaxantina de *Haematococcus pluvialis* usando CO_2 supercritico. M.Sc thesis, Pontificia Universidad Católica de Chile, Santiago. Chile.

Bank, D. D. (2011). Dortmund Data Bank Software and Separation Technology. Oldenburg.

Barredo, J. L. (2012). Microbial carotenoids from bacteria and microalgae. Methods Molecular Biology, 892, 133-141.

Blahovec, J., & Yanniotis, S. (2008). GAB Generalized Equation for Sorption Phenomena. *Food and Bioprocess Technology*, 1(1), 82–90.

Blanken, W., Cuaresma, M., Wijffels, R. H., & Janssen, M. (2013). Cultivation of microalgae on artificial light comes at a cost. *Algal Research-Biomass Biofuels and Bioproducts*, 2(4), 333–340.

Boonyai, P., Bhandari, B., & Howes, T. (2004). Stickiness measurement techniques for food powders: a review. *Powder Technology*, 145, 34–46.

Boonyai, P., Howes, T., & Bhandari, B. (2007). Instrumentation and testing of a thermal mechanical compression test for glass–rubber transition analysis of food powders. J*ournal of Food Engineering,* 78, 1333–1342.

Borowitzka, M. A. (1999). Commercial production of microalgae: ponds, tanks, and fermenters. *Progress in Industrial Microbiology*, 35, 313–321.

Borowitzka, M. A. (2013). High-value products from microalgae-their development and commercialisation. *Journal of Applied Phycology*, 25(3), 743–756.

Brennan, L., & Owende, P. (2010). Biofuels from microalgae—a review of technologies for production, processing, and extractions of biofuels and co-products. *Renewable and sustainable energy reviews*, *14*(2), 557-577.

Brugnerotto, J., Lizardi, J., Goycoolea, F. M., Arguelles-Monal, W., Desbrieres, J., & Rinaudo, M. (2001). An infrared investigation in relation with chitin and chitosan characterization. *Polymer*, 42(8), 3569–3580.

Brunauer, S., Deming, L. S., & Deming, W. E. (1940). On a theory of the van der Waals adsorption of gases. *Journal of the American Society*, 62, 1723–1732.

Campanella, O. H., & Peleg, M. (2002). Squeezing flow viscometry for nonelastic semiliquid foods—theory and applications. *Critical Reviews in Food Science and Nutrition*, 42, 241–264.

Bowles, D. (2007). Micro-and macro-algae: utility for industrial applications. *Outputs from the EPOBIO project*.

Carniglia, S. C. (1986). Construction of the tortuosity factor from porosimetry. *Journal of Catalysis*, 102(2), 401–418.

Castro-Puyana, M., Herrero, M., Urreta, I., Mendiola, J. A., Cifuentes, A., Ibáñez, E., & Suárez-Alvarez, S. (2013). Optimization of clean extraction methods to isolate carotenoids from the microalga *Neochloris oleoabundans* and subsequent chemical characterization using liquid chromatography tandem mass spectrometry. *Analytical and Bioanalytical Chemistry*, 405(13), 4607–4616.

Catchpole, O. J., & King, M. B. (1994). Measurement and correlation of binary diffusion coefficients in near critical fluids. *Industrial & Engineering Chemistry Research*, *33*(7), 1828-1837.

Chacón Lee, T. L., & González Mariño, G. E. (2010). Microalgae for "Healthy" Foods—Possibilities and Challenges. *Comprehensive Reviews in Food Science and Food Safety*, 9(6), 655–675.

Chen, H., Qiu, T., Rong, J., He, C., & Wang, Q. (2015). Microalgal biofuel revisited: An informatics-based analysis of developments to date and future prospects. *Applied Energy*, 155(C), 585–598.

Chen, X. D., & Özkan, N. (2007). Stickiness, Functionality, and Microstructure of Food Powders. *Drying Technology,* 25(6), 959–969.

Chordia, L., & Martinez, J. L. (2006). *U.S. Patent No. 7,091,366*. Washington, DC: U.S. Patent and Trademark Office.

Christaki, E., Bonos, E., Giannenas, I., & Florou-Paneri, P. (2012). Functional properties of carotenoids originating from algae. *Journal of the Science of Food and Agriculture*, 93, 5–11.

Cocero, M. J., & Garcia, J. (2001). Mathematical model of supercritical extraction applied to oil seed extraction by CO2 plus saturated alcohol - I. Desorption model. *The Journal of Supercritical Fluids*, 20(3), 229–243.

Crampon, C., Boutin, O., & Badens, E. (2011). Supercritical carbon dioxide extraction of molecules of interest from microalgae and seaweeds. *Industrial Engineering and Chemistry Research*, 50, 8941–8953.

Crampon, C., Mouahid, A., Toudji, S., & Lépine, O. (2013). Influence of pretreatment on supercritical CO 2 extraction from Nannochloropsis oculata. *The Journal of Supercritical Fluids*, 79, 337–334.

Crossley, J. I., & Aguilera, J. M. (2001). Modeling the effect of microstructure on food extraction. *Journal of Food Process Engineering*, 24(3), 161–177.

Cuellar-Bermudez, S. P., Aguilar-Hernandez, I., Cardenas-Chavez, D. L., Ornelas-Soto, N., Romero-Ogawa, M. A., & Parra-Saldivar, R. (2015). Extraction and purification of high-value metabolites from microalgae: essential lipids, astaxanthin and phycobiliproteins. *Microbial Biotechnology*, 8(2), 190–209.

Dabrowski, A., Podkoscielny, P., Hubicki, Z., & Barczak, M. (2005). Adsorption of phenolic compounds by activated carbon - a critical review. *Chemosphere*, 58(8), 1049–1070.

Dandge, D. K., Heller, J. P., & Wilson, K. V. (1985). Structure solubility correlations: organic compounds and dense carbon dioxide binary systems. Industrial & Engineering *Chemistry Product Research and Development*, 24(1), 162–166.

de Melo, M. M. R., Silvestre, A. J. D., & Silva, C. M. (2014). Supercritical fluid extraction of vegetable matrices: Applications, trends and future perspectives of a convincing green technology. *The Journal of Supercritical Fluids,* 92, 115–176.

de Oliveira, M. A. C. L., Monteiro, M. P. C., Robbs, P. G., & Leite, S. G. F. (1999). Growth and Chemical Composition of *Spirulina Maxima* and *Spirulina Platensis* Biomass at Different Temperatures. *Aquaculture International*, 7(4), 261–275.

del Valle, J. M. (2015). Extraction of natural compounds using supercritical CO_2: Going from the laboratory to the industrial application. *The Journal of Supercritical Fluids*, 96, 180–199.

del Valle, J. M., & la Fuente, de, J. C. (2006). Supercritical CO_2 extraction of oilseeds: review of kinetic and equilibrium models. *Critical Reviews in Food Science and Nutrition*, 46(2), 131–160.

del Valle, J. M., Germain, J. C., Uquiche, E., Zetzl, C., & Brunner, G. (2006). Microstructural effects on internal mass transfer of lipids in prepressed and flaked vegetable substrates. *The Journal of Supercritical Fluids*, 37(2), 178–190.

del Valle, J. M., Jimenez, M., & la Fuente, de, J. C. (2003a). Extraction kinetics of pre-pelletized Jalapeño peppers with supercritical CO_2. *The Journal of Supercritical Fluids*, 25(1), 33–44.

del Valle, J. M., Jimenez, M., Napolitano, P., Zetzl, C., & Brunner, G. (2003b). Supercritical carbon dioxide extraction of pelletized Jalapeño peppers. *Journal of the Science of Food and Agriculture*, (83), 550–556.

Descamps, N., Palzer, S., & Roos, Y. H. (2013). Glass transition and flowability/caking behaviour of maltodextrin DE 21. *Journal of Food Engineering,* 119, 809–813.

Dhankhar, J., Kadian, S. S., & Sharma, A. (2012). Astaxanthin: A potential carotenoid. *International Journal of Pharmaceutical Sciences and Research*, 3, 1246–1259.

Díaz-Reinoso, B., Moure, A., Domínguez, H., & Parajó, J. C. (2006). Supercritical CO_2 Extraction and Purification of Compounds with Antioxidant Activity. *Journal of Agricultural and Food Chemistry*, 54(7), 2441–2469.

Díez-Municio, M., Montilla, A., Herrero, M., & Olano, A. (2011). Supercritical CO_2 impregnation of lactulose on chitosan: A comparison between scaffolds and microspheres form. *The Journal of Supercritical Fluids*, 57, 73–79.

Dufossé, L., Galaup, P., Yaron, A., Arad, S. M., & Blanc, P. (2005). Microorganisms and microalgae as sources of pigments for food use: a scientific oddity or an industrial reality? *Trends in Food Science & Technology*, 16, 389–406.

Dunahay, T., Benemann, J., & Roessler, P. (1998). *A look back at the US Department of Energy's aquatic species program: biodiesel from algae* (Vol. 328). Golden: National Renewable Energy Laboratory. Sinka, I. C. (2007). Modelling powder compaction. Kona, 25, 4–22.

Dutcher, C. S., Ge, X., Wexler, A. S., & Clegg, S. L. (2011). Statistical Mechanics of Multilayer Sorption: Extension of the Brunauer–Emmett–Teller (BET) and Guggenheim–Anderson–de Boer (GAB) Adsorption Isotherms. *The Journal of Physical Chemistry C*, 115(33), 16474–16487.

Foster, K. D., Bronlund, J. E., & Paterson, A. (2006). Glass transition related cohesion of amorphous sugar powders. *Journal of Food Engineering*, 77, 997–1006.

Glatzel, V., & Martínez, J. L. (2012a). Supercritical CO_2 extraction of allicin from garlic flakes: Screening and kinetic studies. *Food Research International*, 45, 216–224.

Glatzel, V., & Martínez, J. L. (2012b). Supercritical CO_2 extraction of allicin from garlic flakes: Screening and kinetic studies. *Food Research International,* 45, 216–224.

Gordon, M., & Taylor, J. S. (1952). Ideal copolymers and the second-order transitions of synthetic rubbers. i. non-crystalline copolymers. *Journal of Applied Chemistry*, 2, 493–500.

Goswami, G., Chaudhuri, S., & Dutta, D. (2010). The present perspective of astaxanthin with reference to biosynthesis and pharmacological importance. *World Journal of Microbiology and Biotechnology*, 26(11), 1925–1939.

Goula, A. M., Karapantsios, T. D., & Achilias, D. S. (2008). Water sorption isotherms and glass transition temperature of spray dried tomato pulp. *Journal of Food Engineering*, 85, 73–83.

Guedes, A. C., Amaro, H. M., & Malcata, F. X. (2011). Microalgae as sources of carotenoids. *Marine Drugs,* 9(4), 625–644.

Guerin, M., Huntley, M. E., & Olaizola, M. (2003). *Haematococcus* astaxanthin: applications for human health and nutrition. *Trends in Biotechnology*, 21(5), 210–216.

Halim, R., Danquah, M. K., & Webley, P. A. (2012). Extraction of oil from microalgae for biodiesel production: A review. *Biotechnology Advances*, 30(3), 709–732.

Hallberg, W., Jekat, H., Schutz, E., Stork, K., & Vollbrecht, H. R. (1989). *U.S. Patent No. 4,828,867*. Washington, DC: U.S. Patent and Trademark Office.

Han, D., Li, Y., & Hu, Q. (2013). Astaxanthin in microalgae: pathways, functions and biotechnological implications. *Algae*, 28, 131–147.

Haque, M. K., & Roos, Y. H. (2004). Water plasticization and crystallization of lactose in spray-dried lactose/protein mixtures. *Journal of Food Science*, 69(1), E23–E29.

Hartmann, M., & Palzer, S. (2011). Caking of amorphous powders—Material aspects, modelling and applications. *Powder Technology*, 206, 112–121.

Harun, R., Singh, M., Forde, G. M., & Danquah, M. K. (2010). Bioprocess engineering of microalgae to produce a variety of consumer products. *Renewable and Sustainable Energy Reviews*, 14, 1037–1047.

Henriksen, U. B., Holm, J. K., Simonsen, P., Berg, M., Posselt, D., Nikolaisen, L., et al. (2008). Fundamental Understanding of Pelletization. *EFP-2005 Project*, 1–51.

Herrero, M., & Ibáñez, E. (2015). Green processes and sustainability: An overview on the extraction of high added-value products from seaweeds and microalgae. *The Journal of Supercritical Fluids*, 96, 211–216.

Herrero, M., Castro-Puyana, M., Mendiola, J. A., & Ibañez, E. (2013). Compressed fluids for the extraction of bioactive compounds. *TrAC Trends in Analytical Chemistry*, *43*, 67-83.

Higuera-Ciapara, I., Felix-Valenzuela, L., & Goycoolea, F. M. (2006). Astaxanthin: A review of its chemistry and applications. *Critical Reviews in Food Science and Nutrition*, 46(2), 185–196.

Hussein, G., Sankawa, U., Goto, H., Matsumoto, K., & Watanabe, H. (2006). Astaxanthin, a carotenoid with potential in human health and nutrition. *Journal of Natural Products*, 69(3), 443–449.

Ibáñez, E., & Cifuentes, A. (2013). Benefits of using algae as natural sources of functional ingredients. *Journal of the Science of Food and Agriculture*, 93(4), 703–709.

Im, H., Lee, H., Park, M. S., Yang, J.-W., & Lee, J. W. (2014). Concurrent extraction and reaction for the production of biodiesel from wet microalgae. *Bioresource Technology*, 152, 534–537.

Industry-Experts. (2015). Global Astaxanthin Market - Sources, Technologies and Application. Retrieved from http://www.researchandmarkets.com/research/t4crxd/global

Jaime, L., RodrIguez-Meizoso, I., Cifuentes, A., Santoyo, S., Suarez, S., Ibáñez, E., & SeNorans, F. J. (2010). Pressurized liquids as an alternative process to antioxidant carotenoids□ extraction from *Haematococcus pluvialis* microalgae. *Lebensmittel-Wissenschaft Und-Technologie*, 43(1), 105–112.

Janda, V., Mikesova, M., & Vejrosta, J. (1996). Direct supercritical fluid extraction of water-based matrices. *Journal of Chromatography* A, 733(1-2), 35–40.

Jaren-Galan, M., Nienaber, U., & Schwartz, S. J. (1999). Paprika (*Capsicum annuum*) oleoresin extraction with supercritical carbon dioxide. *Journal of Agricultural and Food Chemistry*, 47(9), 3558–3564.

Johari, G. P., Hallbrucker, A., & Mayer, E. (1987). The glass–liquid transition of hyperquenched water. *Nature*, 330, 552–553.

Kadam, S. U., Tiwari, B. K., & O'Donnell, C. P. (2013). Application of Novel Extraction Technologies for Bioactives from Marine Algae. *Journal of Agricultural and Food Chemistry*, 61(20), 4667–4675.

Karel, M., Anglea, s.,Buera, p., Karmas, r., Levi, g., & roos, Y. H. (1994). Stability-Related Transitions of Amorphous Foods. *Thermochimica Acta*, 246(2), 249–269.

Kidd, P. (2011). Astaxanthin, Cell Membrane Nutrient with Diverse Clinical Benefits and Anti-Aging Potential. *Alternative Medicine Review*, 16(4), 355–364.

Kitada, K., Machmudah, S., Sasaki, M., Goto, M., Nakashima, Y., Kumamoto, S., & Hasegawa, T. (2009). Supercritical CO_2 extraction of pigment components with pharmaceutical importance from Chlorella vulgaris. *Journal of Chemical Technology and Biotechnology*, *84*(5), 657-661.

Krichnavaruk, S., Shotipruk, A., Goto, M., & Pavasant, P. (2008). Supercritical carbon dioxide extraction of astaxanthin from *Haematococcus pluvialis* with vegetable oils as co-solvent. *Bioresource Technology*, 99(13), 5556–5560.

la Fuente, de, J. C., & Cardarelli, D. A. (2005). Contributions to supercritical extraction of vegetable substrates in Latin America. *Journal of Food Engineering,* 67, 35–57.

Labuza, T. P. (2000). Creation of moisture sorption isotherms for hygroscopic materials. *Water Activity and Glass Transition, University of Minnesota, Department of Food Science and Nutrition*.

Lam, M. K., & Lee, K. T. (2012). Microalgae biofuels: A critical review of issues, problems and the way forward. *Biotechnology Advances*, 30(3), 673–690.

Lannutti, J. J. (1997). Characterization and control of compact microstructure. *MRS Bulletin*, *22*(12), 38-44.

Lemmon, E. W., Huber, M. L., & McLinden, M. O. (2012). NIST Standard Reference Database 23. *Reference Fluid Thermodynamic and Transport Properties (REFPROP)*.

Lomauro, C. J., Bakshi, A. S., & Labuza, T. P. (1985). Evaluation of food moisture sorption isotherm equations. Part I: Fruit, vegetable and meat products. *Lebensmittel-Wissenschaft und-Technologie*, *18*(2), 111-117.

Lorenz, R. T. (1999). A technical review of *Haematococcus* algae. *Naturose Technical Bulletin*.

Lorenz, R. T., & Cysewski, G. R. (2000). Commercial potential for *Haematococcus* microalgae as a natural source of astaxanthin. *Trends in Biotechnology*, 18(4), 160–167.

Ma, Y. H., & Evans, L. B. (1968). Transient diffusion from a well-stirred reservoir to a body of arbitrary shape. *AIChE Journal*, 14(6), 956–961.

Machmudah, S., Kitada, K., Kitada, K., Sasaki, M., Goto, M., Munemasa, J., et al. (2011). Simultaneous extraction and separation process for coffee beans with supercritical CO_2 and water. *Industrial & Engineering Chemistry Research*, 50(4), 2227–2235.

Machmudah, S., Shotipruk, A., & Goto, M. (2006). Extraction of Astaxanthin from Haematococcus p luvialis Using Supercritical CO_2 and Ethanol as Entrainer. *Industrial Engineering Chemical Research*, 45, 3652–3657.

Macías-Sánchez, M. D., Mantell Serrano, C., Rodríguez Rodríguez, M., Martínez de la Ossa, E., Lubián, L. M., & Montero, O. (2008). Extraction of carotenoids and chlorophyll from microalgae with supercritical carbon dioxide and ethanol as cosolvent. *Journal of Separation Science*, 31(8), 1352–1362.

Macías-Sánchez, M. D., Mantell, C., Rodriguez, M., Martínez de la Ossa, E., Lubián, L. M., & Montero, O. (2009). Comparison of supercritical fluid and ultrasound-assisted extraction of carotenoids and chlorophyll a from *Dunaliella salina*. Talanta, 77(3), 948–952.

Mattson, J. S., Mark, H. B., & Weber, W. J. (1969). Identification of surface functional groups on active carbon by infrared internal-reflection spectrometry. *Analytical Chemistry*, 41(2), 355–358.

Mendes, R. L., Fernandes, H. L., Coelho, J. P., Reis, E. C., Cabral, J., Novais, J. M., & Palavra, A. F. (1995). Supercritical CO_2 Extraction of Carotenoids and Other Lipids From *Chlorella Vulgaris*. *Food Chemistry*, 53(1), 99–103.

Mendes, R. L., Nobre, B. P., Cardoso, M. T., Pereira, A. P., & Palavra, A. F. (2003). Supercritical carbon dioxide extraction of compounds with pharmaceutical importance from microalgae. *Inorganica Chimica Acta,* 356, 328–334.

Mendes, R. L., Reis, A. D., & Palavra, A. F. (2006). Supercritical CO_2 extraction of γ-linolenic acid and other lipids from *Arthrospira* (*Spirulina*) *maxima*: Comparison with organic solvent extraction. *Food Chemistry*, 99(1), 57–63.

Mendes-Pinto, M. M., Raposo, M., & Bowen, J. (2001). Evaluation of different cell disruption processes on encysted cells of *Haematococcus pluvialis*: effects on astaxanthin recovery and implications for bio-availability. *Journal of Applied Phycology* 13, 19–24.

Mendiola, J. A., Jaime, L., Santoyo, S., & Reglero, G. (2007). Screening of functional compounds in supercritical fluid extracts from *Spirulina platensis*. *Food Chemistry*.

Mercer, P., & Armenta, R. E. (2011). Developments in oil extraction from microalgae. *European Journal of Lipid Science and Technology*, 113(5), 539–547.

Nagy, B., & Simándi, B. (2008). Effects of particle size distribution, moisture content, and initial oil content on the supercritical fluid extraction of paprika. *The Journal of Supercritical Fluids*, 46, 293–298.

Nijdam, J. J., & Langrish, T. A. G. (2006). The effect of surface composition on the functional properties of milk powders. *Journal of Food Engineering*, 77(4), 919–925.

Nobre, B., Marcelo, F., Passos, R., Beirao, L., Palavra, A., Gouveia, L., & Mendes, R. (2006). Supercritical carbon dioxide extraction of astaxanthin and other carotenoids from the microalga *Haematococcus pluvialis*. *European Food Research and Technology*, 223(6), 787–790.

Oliveira, E. G., Rosa, G. S., Moraes, M. A., & Pinto, L. A. A. (2009). Characterization of thin layer drying of Spirulina platensis utilizing perpendicular air flow. *Bioresource Technology*, 100(3), 1297–1303.

Palou, E., LopezMalo, A., & Argaiz, A. (1997). Effect of temperature on the moisture sorption isotherms of some cookies and corn snacks. *Journal of Food Engineering*, 31(1), 85–93.

Palzer, S. (2005). The effect of glass transition on the desired and undesired agglomeration of amorphous food powders. *Chemical Engineering Science*, 60, 3959–3968.

Palzer, S. (2011). Agglomeration of pharmaceutical, detergent, chemical and food powders—similarities and differences of materials and processes. *Powder technology*, *206*(1), 2-17.

Pan, J.-L., Wang, H.-M., Chen, C.-Y., & Chang, J.-S. (2012). Extraction of astaxanthin from *Haematococcus pluvialis* by supercritical carbon dioxide fluid with ethanol modifier. *Engineering in Life Sciences,* 12(6), 638–647.

Peleg, M. (1992). On the use of the WLF model in polymers and foods. *Critical Reviews in Food Science and Nutrition*, 32(1), 59–66.

Peleg, M. (1993). "Glass transition and the physical stability of food powders" *The Glassy State in Foods*. Ed. J.M.V. Blanshard P.J. Lilliford. 435-451

Pence, H. E., & Williams, A. (2010). ChemSpider: An Online Chemical Information Resource. *Journal of Chemical Education*, 87(11), 1123–1124.

Pereira, C. G., & Meireles, M. A. A. (2009). Supercritical Fluid Extraction of Bioactive Compounds: Fundamentals, Applications and Economic Perspectives. *Food and Bioprocess Technology*, 3(3), 340–372.

Perrut, M. (2000). Supercritical Fluid Applications: Industrial Developments and Economic Issues. *Industrial & Engineering Chemistry Research*, 39(12), 4531–4535.

Plaza, M., Cifuentes, A., & Ibáñez, E. (2008). In the search of new functional food ingredients from algae. *Trends in Food Science & Technology*, 19, 31–39.

Plaza, M., Herrero, M., Cifuentes, A., & Ibáñez, E. (2009). Innovative natural functional ingredients from microalgae. *Journal of Agricultural and Food Chemistry,* 57(16), 7159–

Pollard, S., Fowler, G. D., Sollars, C. J., & Perry, R. (1992). Low-cost adsorbents for waste and waste-water treatment - a review. *Science of the Total Environment*, 116(1-2), 31–52.

Puiggené, J., Larrayoz, M. A., & Recasens, F. (1997). Free liquid-to-supercritical fluid mass transfer in packed beds. *Chemical Engineering Science*, *52*(2), 195-212.

Ramsey, E. D., Minty, B., & Babecki, R. (1998). Supercritical fluid extraction strategies of liquid-based matrices. *In Analytical Supercritical Fluid Extraction Techniques* (pp. 109–157). Dordrecht: Springer Netherlands.

Rao, A. V., & Rao, L. G. (2007). Carotenoids and human health. *Pharmacological Research,* 55(3), 207–216.

Raposo, Maria, de Morais, A., & de Morais, R. (2015). Carotenoids from Marine Microalgae: A Valuable Natural Source for the Prevention of Chronic Diseases. *Marine Drugs*, 13(8), 5128–5155.

Rawson, A., Patras, A., Tiwari, B. K., Noci, F., Koutchma, T., & Brunton, N. (2011). Effect of thermal and non thermal processing technologies on the bioactive content of

exotic fruits and their products: Review of recent advances. *Food Research International*, 44(7), 1875–1887.

Reddy, H. K., Muppaneni, T., Patil, P. D., Ponnusamy, S., Cooke, P., Schaub, T., & Deng, S. (2014). Direct conversion of wet algae to crude biodiesel under supercritical ethanol conditions. *Fuel*, 115, 720–726.

Reverchon, E. (1996). Mathematical modeling of supercritical extraction of sage oil. *AIChE Journal*, 42(6), 1765–1771.

Reverchon, E., & De Marco, I. (2006). Supercritical fluid extraction and fractionation of natural matter. *The Journal of Supercritical Fluids*, 38, 146–166.

Reyes, F. A., Mendiola, J. A., & Ibáñez, E. (2014). Astaxanthin extraction from *Haematococcus pluvialis* using CO_2-expanded ethanol. *The Journal of Supercritical Fluids*, 92, 75–83.

Reyes, F. A., Muñoz, L. A., & A, H. (2015a). Water relationships in *Haematoccoccus pluvialis* and their effect in pretreatment for supercritical CO_2 extraction. *Journal of Food Engineering*, 1–25.

Reyes, F. A., Muñoz, L. A., Hansen, A., & del Valle, J. M. (2015b). Water relationships in *Haematoccoccus pluvialis* and their effect in high-pressure agglomeration for supercritical CO2 extraction. *Journal of Food Engineering*. (*submitted*)

Reyes, F.A., Núñez, G.A., del Valle, J.M., 2013. Métodos para la obtención de compuestos carotenoides a partir de un sustrato de microalgas que comprende proveer un sustrato de polvo de microalgas, comprimirlo y realizar extracción mediante CO_2 supercrítico. *Chilean Patent Application*, 2013–03813

Rhén, C., Gref, R., Sjöström, M., & Wästerlund, I. (2005). Effects of raw material moisture content, densification pressure and temperature on some properties of Norway spruce pellets. *Fuel Processing Technology*, 87, 11–16.

Richmond, A. (Ed.). (2008). *Handbook of microalgal culture: biotechnology and applied phycology*. John Wiley & Sons.

Rigby, S. P., Fletcher, R. S., & Riley, S. N. (2004). Characterisation of porous solids using integrated nitrogen sorption and mercury porosimetry. *Chemical Engineering Science*, 59(1), 41–51.

Roney, D., Waibel, B., & Marentis, R. (2008). *U.S. Patent Application 12/026,802*.

Roos, Y. H. (2010). Glass transition temperature and its relevance in food processing. *Annual Review of Food Science and Technology*, 1, 469–496.

Roos, Y., & Karel, M. (1991). Applying state diagrams to food processing and development. *Food Technology*, 45(12), 66–68–71– 107.

Ruen ngam, D., Shotipruk, A., Pavasant, P., Machmudah, S., & Goto, M. (2012). Selective Extraction of Lutein from Alcohol Treated Chlorella vulgaris by Supercritical CO_2. *Chemical Engineering & Technology*, 35(2), 255–260.

Sabirzyanov, A. N., Il'in, A. P., Akhunov, A. R., & Gumerov, F. M. (2002). Solubility of water in Supercritical carbon dioxide. *High Temperature*, 40(2), 203–206.

Sablani, S. S., Syamaladevi, R. M., & Swanson, B. G. (2010). A review of methods, data and applications of state diagrams of food systems. *Food Engineering Reviews*, 2, 168–203.

Sajilata, M. G., Singhal, R. S., & Kamat, M. Y. (2008). Supercritical CO_2 extraction of γ-linolenic acid (GLA) from *Spirulina platensis* ARM 740 using response surface methodology. *Journal of Food Engineering*, 84(2), 321–326.

Santoyo, S., Rodríguez-Meizoso, I., Cifuentes, A., Jaime, L., García-Blairsy Reina, G., Señoráns, F. J., & Ibáñez, E. (2009). Green processes based on the extraction with pressurized fluids to obtain potent antimicrobials from *Haematococcus pluvialis* microalgae. *Lebensmittel-Wissenschaft Und-Technologie*, 42(7), 1213–1218.

Sarada, R., Vidhyavathi, R., Usha, D., & Ravishankar, G. A. (2006). An efficient method for extraction of astaxanthin from green alga *Haematococcus pluvialis*. *Journal of Agricultural and Food Chemistry*, 54(20), 7585–7588.

Satyanarayana, K. G., Mariano, A. B., & Vargas, J. V. C. (2011). A review on microalgae, a versatile source for sustainable energy and materials. *International Journal of energy research*, *35*(4), 291-311.

Sovová, H. (2005). Mathematical model for supercritical fluid extraction of natural products and extraction curve evaluation. *The Journal of Supercritical Fluids*, 33(1), 35–52.

Sovová, H., & Stateva, R. P. (2011). Supercritical fluid extraction from vegetable materials. *Reviews in Chemical Engineering*, 27(3-4), 1–78.

Spolaore, P., Joannis-Cassan, C., Duran, E., & Isambert, A. (2006a). Commercial applications of microalgae. *Journal of Bioscience and Bioengineering*, 101(2), 87–96.

Spolaore, P., Joannis-Cassan, C., Duran, E., & Isambert, A. (2006b). Commercial applications of microalgae. *Journal of Bioscience and Bioengineering*, 101(2), 87–96.

Sun, A., & Gunasekaran, S. (2009). Yield stress in foods: measurements and applications. *International Journal of Food Properties*, 12, 70–101.

Taher, H., Al-Zuhair, S., Al-Marzouqi, A. H., Haik, Y., & Farid, M. (2014). Effective extraction of microalgae lipids from wet biomass for biodiesel production. *Biomass and Bioenergy*, 66, 159–167.

Team, R. C. (2014). R: a language and environment for statistical computing. Vienna, Austria: *R Foundation for Statistical Computing*. Open access available at: http://cran. r-project. org.

Thana, P., Thana, P., Machmudah, S., Goto, M., Sasaki, M., Pavasant, P., & Shotipruk, A. (2008). Response surface methodology to supercritical carbon dioxide extraction of astaxanthin from *Haematococcus pluvialis*. *Bioresource Technology*, 99(8), 3110–3115.

Timmermann, E. O., Chirife, J., & Iglesias, H. A. (2001). Water sorption isotherms of foods and foodstuffs: BET or GAB parameters? *Journal of Food Engineering*, 48(1), 19–31.

Ugwu, C. U., Aoyagi, H., & Uchiyama, H. (2008). Photobioreactors for mass cultivation of algae. *Bioresource Technology*, 99(10), 4021–4028.

Uquiche, E., & Ortiz, J. (2004). Supercritical carbon dioxide extraction of red pepper (*Capsicum annuum L.*) oleoresin. *Journal of Food Engineering*, 65, 55–66.

Uquiche, E., Uquiche, E., Valle, J. M., Valle, J. M., Ihl, M., & Ihl, M. (2006). Microstructure-Extractability Relationships in the Extraction of Prepelletized Jalapeño Peppers with Supercritical Carbon Dioxide. *Journal of Food Science*, 70(6), e379–e386.

Urrego, F. A., Núñez, G. A., Donaire, Y. D., & del Valle, J. M. (2015). Equilibrium partition of rapeseed oil between supercritical CO_2 and prepressed rapeseed. *The Journal of Supercritical Fluids,* 102, 80–91

Urreta, I., Ikaran, Z., Janices, I., Ibáñez, E., Castro-Puyana, M., Castanon, S., & Suarez-Alvarez, S. (2014). Revalorization of *Neochloris oleoabundans* biomass as source of biodiesel by concurrent production of lipids and carotenoids. *Algal Research-Biomass Biofuels and Bioproducts*, 5, 16–22.

Valderrama, J. O., & Perrut, M. (2003). Extraction of astaxantine and phycocyanine from microalgae with supercritical carbon dioxide. *Journal of Chemical Engineering Data*, 48, 827–830.

Valle, J. M., & Aguilera, J. M. (1989). Effects of substrate densification and CO_2 conditions on supercritical extraction of mushroom oleoresins. *Journal of Food Science*, 54, 135–141.

Van den Berg, C. (1984). Description of water activity of foods for engineering purposes by means of the GAB model of sorption. In: McKenna, B.M. (Ed.), *Engineering and Food*, 1. Elsevier, London, UK, pp. 311–321.

Villermaux, J. (1987). Chemical engineering approach to dynamic modelling of linear chromatography: A flexible method for representing complex phenomena from simple concepts. *Journal of Chromatography* A, 406, 11–26.

Wahl, M., Bröckel, U., Brendel, L., Feise, H. J., Weigl, B., Röck, M., & Schwedes, J. (2008). Understanding powder caking: Predicting caking strength from individual particle contacts. *Powder Technology,* 188(2), 147–152.

Wakao, N., & Smith, J. M. (1962). Diffusion in catalyst pellets. *Chemical Engineering Science*, *17*(11), 825-834.

Wang, H., Liu, Y., Wei, S., & Yan, Z. (2012a). Application of response surface methodology to optimise supercritical carbon dioxide extraction of essential oil from Cyperus rotundus Linn. *Food Chemistry*, 132(1), 582–587.

Wang, L., Yang, B., Yan, B., & Yao, X. (2012b). Supercritical fluid extraction of astaxanthin from Haematococcus pluvialis and its antioxidant potential in sunflower oil. *Innovative Food Science and Emerging Technologies*, 13(C), 120–127.

Williams, M. L., Landel, R. F., & Ferry, J. D. (1955). The temperature dependence of relaxation mechanisms in amorphous polymers and other glass-forming liquids. *Journal of the American Society*, 77(14), 3701–3707.

Wright, S. W., Jeffrey, S. W., & Mantoura, R. F. C. (Eds.). (2005). *Phytoplankton pigments in oceanography: guidelines to modern methods*. Unesco Pub.

Yanfen, L., Zehao, H., & Xiaoqian, M. (2012). Energy analysis and environmental impacts of microalgal biodiesel in China. *Energy Policy*, 45, 142–151.

Yang, Y., Kim, B., & Lee, J. Y. (2013). Astaxanthin structure, metabolism, and health benefits. *Journal of Human Nutrition & Food Science*, 1, 1003.

Yen, H.-W., Yang, S.-C., Chen, C.-H., Jesisca, & Chang, J.-S. (2015). Supercritical fluid extraction of valuable compounds from microalgal biomass. *Bioresource Technology*, 184, 291–296.

Yuan, J.-P., Peng, J., Yin, K., & Wang, J.-H. (2011). Potential health-promoting effects of astaxanthin: a high-value carotenoid mostly from microalgae. *Molecular Nutrition & Food Research,* 55(1), 150–165.

APPENDIX A: DETAIL CALCULATIONS FOR GEOMETRIC RELATED CHARACTERISTICS

Figure A1 describes the geometry of a typical compact, having two spherical caps of radius R and limited by an angle θ_{max} with the axis, and a cylindrical section of diameter D. Natoli (St. Charles, MO) defines the magnitude Δz (height of the spherical cap) as a function of D (die diameter) for their punch tooling elements (0.43, 0.66, and 0.84 mm for the 3, 5, and 7 mm punch elements, respectively). The following relationships hold:

$$\cos\left(\theta_{max}\right) = \frac{R - \Delta z}{R}$$, from which

$$\frac{\Delta z}{R} = 1 - \cos\left(\theta_{max}\right) \qquad \text{(A1)}$$

$$\sin\left(\theta_{max}\right) = \frac{D/2}{R} = \frac{D}{2\,R} \qquad \text{(A2)}$$

Dividing Eq. (A1) by Eq. (A2) the following fundamental equation results, from which angle θ_{max} can be estimated:

$$\frac{1 - \cos\left(\theta_{max}\right)}{\sin\left(\theta_{max}\right)} = \frac{\Delta z}{D/2} = \frac{2\,\Delta z}{D} \qquad \text{(A3)}$$

Values of θ_{max} for all punch tooling elements were about 29.5º. From known values of Δz and θ_{max}, the value of R for each punching element can be estimated using Eq. (A4):

$$R = \frac{\Delta z}{1 - \cos\left(\theta_{max}\right)} \qquad \text{(A4)}$$

The characteristic dimensions X_{slb}, X_{cyl}, and X_{sph} of each compact were calculated based on the following general equation:

$$X = \frac{1}{S}\int_{S}\left(\text{distance from center or symmetry plane / axis}\right) dS \qquad \text{(A5)}$$

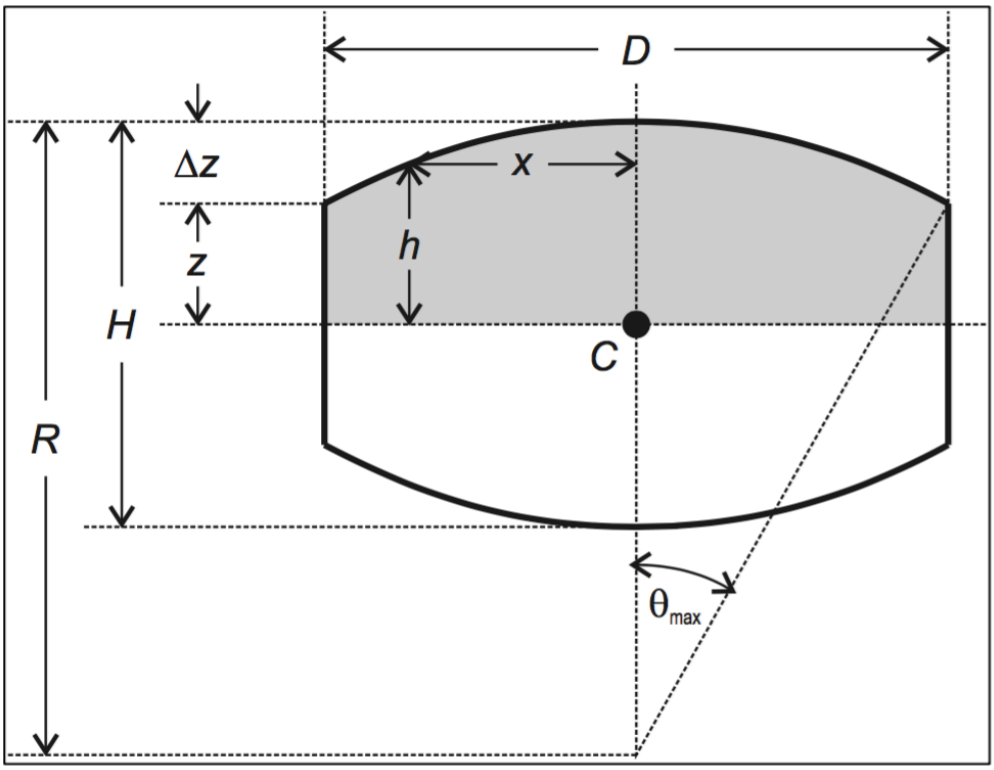

Figure A-1: Representative geometrical diagram of a compact fabricated from *H. pluvialis* that is characterize by two spherical caps of diameter *R* and a cylindrical section of diameter *D*. By knowing *D* and the height of the spherical cap (Δz) (provided by the manufacturer), and measuring the cylindrical length (2*z*) one can calculate all of its geometric characteristics

For the spherical section of the compact, the element of surface and surface are defined as follows:

$$dS_s = 2\pi R^2 \sin(\theta) d\theta, \quad \text{(A6)}$$

$$S_s = 2\pi R^2 \left[1 - \cos(\theta_{max})\right], \text{ and, } \quad \text{(A7)}$$

whereas for its upper cylindrical section, the element of surface and surface are defined as follows:

$$dS_c = \pi D\, dz, \text{ and, } \quad \text{(A8)}$$

$$S_c = \pi D \frac{H - 2\,\Delta z}{2}. \qquad \text{(A9)}$$

The distance from the plane to the surface in the spherical section is defined as follows:

$$h = R\cos(\theta) - \left(R - \frac{H}{2}\right) = \frac{H}{2} - R\left[1 - \cos(\theta)\right]. \qquad \text{(A10)}$$

The distance from the central axis to the surface in the spherical section is defined as:

$$x = R\sin(\theta), \qquad \text{(A11)}$$

whereas that from the central axis to the surface in the cylindrical section is given by:

$$x = \frac{D}{2}. \qquad \text{(A12)}$$

The distance from the center to the surface in the spherical section is defined as follows:

$$l_c = \sqrt{h^2 + x^2}, \qquad \text{(A13)}$$

whereas that from the center to the surface in the cylindrical section is given by:

$$l_c = \sqrt{z^2 + \left(\frac{D}{2}\right)^2}. \qquad \text{(A14)}$$

Based on the previous definitions, X_{slb} was calculated using Eq. (A15):

$$X_{slb} = \frac{1}{S_s}\int_0^{\theta_{max}} h\, dS_s = \frac{1}{4}\left[\frac{1 - \cos(2\,\theta_{max})}{1 - \cos(\theta_{max})}\right] - \left(R - \frac{H}{2}\right), \qquad \text{(A15)}$$

X_{cyl} using Eq. (A16):

$$X_{\text{cyl}} = \frac{1}{S_{\text{s}} + S_{\text{c}}}\left[\int_0^{\theta_{\max}} x\, dS_{\text{s}} + \frac{D}{2}\left(\pi\, D\frac{H - 2\,\Delta z}{2}\right)\right], \text{ from which:}$$

$$X_{\text{cyl}} = \frac{D}{2}\left\{\frac{D\left(0.5H - \Delta z\right) + 4\,R^3\left[1 - \cos\left(\theta_{\max}\right)\right]/D}{D\left(0.5H - \Delta z\right) + 2\,R^2}\right\}, \quad \text{(A16)}$$

and X_{sph} using Eq. (A17):

$$X_{\text{sph}} = \frac{1}{S_{\text{s}} + S_{\text{c}}}\left(\int_0^{\theta_{\max}} l_{\text{s}} dS_{\text{s}} + \int_0^{0.5H - \Delta z} l_{\text{c}} dS_{\text{c}}\right), \text{ from which:}$$

$$X_{\text{sph}} = \frac{4\sqrt{2}\;\pi}{3}\sqrt{\frac{H}{2} - R}\left\{\left[\frac{\left(0.5H/R\right)^2}{H/\left(R - 0.5\right)}\right]^{1.5} - \left[\frac{\left(0.5H/R\right)^2}{H/\left(R - 0.5\right)} - 1 + \cos\left(\theta_{\max}\right)\right]^{1.5}\right\},$$

if $H/2 > R$ (A17a)

or

$$X_{\text{sph}} = \frac{4\sqrt{2}\;\pi}{3}\sqrt{R - \frac{H}{2}}\left\{\left[1 - \cos\left(\theta_{\max}\right) - \frac{\left(0.5H/R\right)^2}{H/\left(R - 0.5\right)}\right]^{1.5} - \left[\frac{\left(0.5H/R\right)^2}{H/\left(0.5 - R\right)}\right]^{1.5}\right\},$$

if $R > H/2$ (A17b)

The surface-to-volume ratio of a finite cylinder (radius X_{cyl} and half-height X_{slb}) and sphere (radius X_{sph}) are defined as follows:

$$\left(S/V\right)_{\text{finite cylinder}} = \frac{2\left(\pi\, X_{\text{cyl}}^2\right) + 2\pi\, X_{\text{cyl}}\left(2X_{\text{slb}}\right)}{\pi X_{\text{cyl}}^2\left(2X_{\text{slb}}\right)} = \frac{1}{X_{\text{slb}}} + \frac{2}{X_{\text{cyl}}}, \text{ and (A18)}$$

$$\left(S/V\right)_{\text{sph}} = \frac{4\pi\, X_{\text{sph}}^2}{4\pi\, X_{\text{sph}}^3/3} = \frac{3}{X_{\text{sph}}}. \quad \text{(A19)}$$

The surface-to-volume ratio of an infinite slab is defined by Eq. (A18) when X_{cyl} tends to infinity:

$$\left(S/V\right)_{slb} = \left(S/V\right)_{\substack{\text{finite cylinder} \\ X_{cyl}\to\infty}} = \frac{1}{X_{slb}} + \left(\frac{2}{X_{cyl}}\right)_{X_{cyl}\to\infty}, \qquad \text{(A18a)}$$

whereas that of an infinite cylinder is defined by Eq. (A18) when X_{slb} tends to infinity:

$$\left(S/V\right)_{cyl} = \left(S/V\right)_{\substack{\text{finite cylinder} \\ X_{slb}\to\infty}} = \left(\frac{1}{X_{slb}}\right)_{X_{slb}\to\infty} + \frac{2}{X_{cyl}}. \qquad \text{(A18b)}$$

Considering that $\left(\frac{1}{X_{slb}}\right)_{X_{slb}\to\infty} \approx \left(\frac{2}{X_{cyl}}\right)_{X_{slb}\to\infty} \approx 0$, then Eqs. (A18a) and (A18b) simplify to the following:

$$\left(S/V\right)_{slb} \approx \frac{1}{X_{slb}}, \text{ and} \qquad \text{(A20)}$$

$$\left(S/V\right)_{cyl} \approx \frac{2}{X_{cyl}}. \qquad \text{(A21)}$$